Atlantic Climate Adaptation Solutions Association

Solutions d'adaptation aux changements climatiques pour l'Atlantique

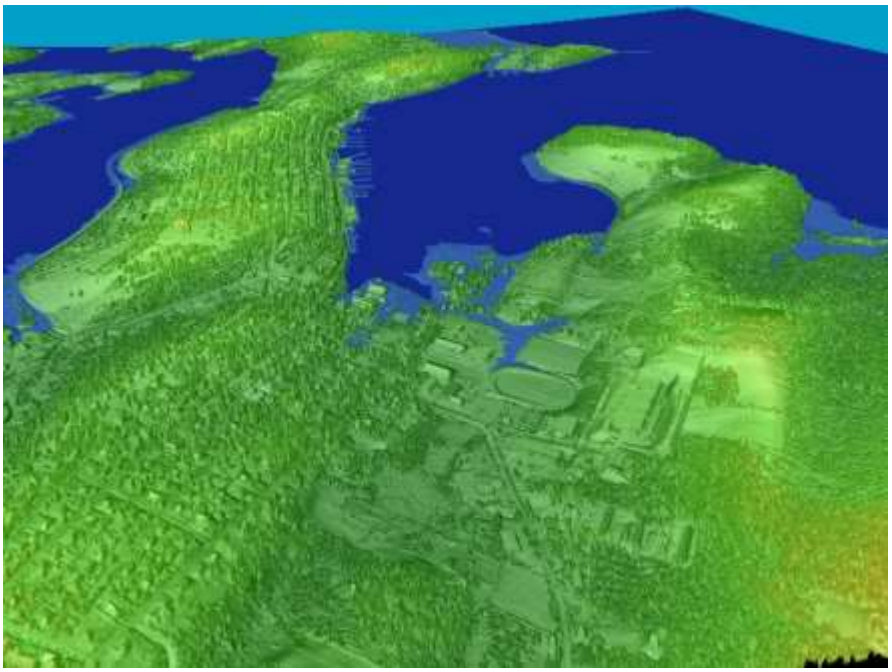

Lidar processing and Flood Risk Mapping for the Communities of the District of Lunenburg, Oxford-Port Howe, Town and District of Yarmouth, Chignecto Isthmus and Minas Basin

By
Tim Webster, Kevin McGuigan and Candace MacDonald
Applied Geomatics Research Group
Centre of Geographic Sciences
Nova Scotia Community College, Middleton
Tel. 902 825 5475
email: timothy.webster@nscc.ca

May 2012

NOVA SCOTIA · New Nouveau Brunswick · Prince Edward Island CANADA · Newfoundland Labrador · Natural Resources Canada · Ressources naturelles Canada · Canada

Report commissioned by the Atlantic Climate Solutions Association (ACASA), a non-profit organization formed to coordinate project management and planning for climate change adaptation initiatives in Nova Scotia, New Brunswick, Prince Edward Island and Newfoundland and Labrador and supported through the Regional Adaptation Collaborative, a joint undertaking between the Atlantic provinces, Natural Resources Canada and regional municipalities and other partners.

Project management: Climate Change Directorate, Nova Scotia Department of the Environment, P O Box 442, Halifax, NS B3J 2P8

This report is also available for download from the ACASA website at:
www.atlanticadaptation.ca

Acknowledgements

We would like to thank several individuals for their assistance during this project; Lyly Ngo, Chris Webster, Charity Mouland, Nathan Crowell, Chris Hopkinson, and Allyson Fox from the Applied Geomatics Research Group. Roger Mosher for assistance with the Time Series Modeler and GeoNet technologies Inc. for use of the program. Will Green of NS Environment for funding the project and Danny Walmsley, ACAS coordinator for logistics. As always at AGRG, thanks to Bob Maher, Debby Hebb and Brenda Veinot, for assisting in the financial administration of this project. We thank the members of the various municipalities who we interacted with.

Executive Summary

The Canadian coastlines have been assessed for sensitivity to future sea-level change and it has been determined that the east coast of Canada is highly vulnerable to erosion and flooding. (Shaw et al., 1998). The Atlantic Climate Adaptation Solutions (ACAS) project aims to address some of these issues. This report deals with the construction of flood risk maps to support communities that are vulnerable to coastal flooding from storm surges and long term sea-level rise. Our coasts are presently at risk to the occurrence of storm surges during high tide which results in flooding and erosion. For future planning we need to identify the current areas, then look to future sea-level predictions and determine the areas at long term risk. The latest Intergovernmental Panel on Climate Change (IPCC) Assessment Report 4 (AR4) has projected global mean seal-level to rise between 0.18 and 0.59 m from 1990 to 2095 (Meehl et al. 2007). However as Forbes et al. (2009) point out, these projections do not account for the large ice sheets melting and that measurements of actual global sea-level rise (SLR) are higher than the previous predictions of the third assessment report. Rhamstorf et al. (2007) compared observed global sea-level rise to that projected and found it exceeded the IPCC AR3 projections and have suggested a rise between 0.5 and 1.4 m from 1990 to 2100. Forbes et al. (2009) used an upper limit of 1.3 m of SLR over 100 years as a precautionary approach to SLR projections in the Halifax region. The selection of an upper limit of flooding is dependent on realistic projections of SLR. However, because of the variations in SLR projections we have generated flood risk maps to a maximum level of 5 and12 m depending on the study site and tidal range. The tidal range from mean sea-level varies from 2 m on the Northumberland Straight and Atlantic to 7 m in the upper Bay of Fundy communities thus requiring the different flood level ranges. The number of flood level GIS layers ensures that the flood extent information is available whatever the water level used in the projections in the future.

In order to generate accurate flood inundation maps along the coastal communities we developed elevation models using an airborne laser scanning technique, lidar, to acquire a new generation of maps during the project. The ACAS communities have the benefit of having the detailed 1-2 m bare earth elevation model accurate to 15 cm in the vertical, they also have the surface model which incorporates the tops of the trees and buildings. These two types of maps can provide a wealth of information to various engineering or resource based projects that require GIS analysis. The bare earth map was used to increase the ocean sea-level and determine

the inundation area every 10 cm of flooding. Hydraulic pathways, as represented by culverts and bridges, have been applied to the bare earth model connecting the ocean to inland low lying areas. For the areas protected by dykes we have generated a set of flood layers that represent dyke overtopping. These layers highlight the areas at risk of flooding if the ocean water level were to exceed the dyke elevation. We have also implemented a set of flood layers associated with dyke breaching, where we have simulated a break in the dyke and allowed the water to flood immediately behind the dyke. We have used benchmark storms for each of the ACAS communities to highlight past flooding events. This was done to show decision makers and citizens that these coastal areas have been vulnerable to storm surges in the past and allows people to better understand the potential implications of climate change and sea-level rise in the future.

We have used the water level time series data from available tide gauges (Halifax, Yarmouth and Saint John, NB) and no-longer operating (Pictou) to estimate the return periods of high water events and the benchmark storms. These events represent storm surges where the atmospheric pressure and wind have caused the water level to exceed that of a normal predicted tide. We have calculated the return period of such events based on current relative sea-level (RSL) rise as well imposed higher rates of sea-level rise (73 cm/century and 146 cm/century) from climate change. We have also used the time series data to calculate the water level of the 100 year storm events at a 95% probability of occurrence under these different RSL conditions. Under current RSL conditions the 100 year water level (CGVD28) for the Lunenburg area is 2.2 m, for the Port Howe area is 2.4 m and for Yarmouth is 3.5 m. These levels increase under different RSL predictions with climate change. The benchmark storms for these areas approach the 100 year events, Hurricane Juan in Sept. 2003 water level in Halifax was 2.1 m and along the Northumberland Strait in Dec. 1993 and more recently in Dec. 2010 water levels reached 2.3 and 2.2 m respectively. The Groundhog Day storm in Yarmouth in Feb. 1976 reached a level of 3.4 m.

Each ACAS municipality has taken delivery of various GIS layers lidar derived surface model and elevation model as well as the different flood layers. Presentations have been made to each of the municipalities to transfer the results and technology and provide the scientific explanation of how these maps were generated and how to use them. This report is the summary document to be used in association with those GIS data files.

Table of Contents

List of Figures

List of Tables

1. Introduction

Many coastal communities in Nova Scotia are at risk to flooding from storm-surge events. A storm-surge is an increase in the ocean water level above what is expected from the normal tidal level that can be predicted from astronomical observations. Storm surges are caused by the winds and low atmospheric pressure of storms. The global climate is changing due to the increase of greenhouse gas emissions, the resulting warming trends will result in an increase of global sea level (Titus et al. 1991). Future projections of sea-level change depend on estimated future greenhouse gas emissions and are predicted based on a number of scenarios (Raper et al. 2006). Global sea-level rise, as predicted by climate change models, will increase the problem of flooding and erosion making more coastal areas vulnerable. The third assessment of the Intergovernmental Panel on Climate Change (IPCC) indicates that there will be an increase in mean global sea-level from 1990 to 2100 between 0.09 m and 0.88 m (Church et al. 2001). The latest IPCC Assessment Report 4 (AR4) has projected global mean seal-level to rise between 0.18 and 0.59 m from 1990 to 2095 (Meehl et al. 2007). However as Forbes et al. (2009) point out, these projections do not account for the large ice sheets melting and measurements of actual global sea-level rise are higher than the previous predictions of the third assessment report. Rhamstorf et al. (2007) compared observed global sea-level rise (SLR) to that projected in the third assessment report and found it exceeded the projections. They have suggested a rise between 0.5 and 1.4 m from 1990 to 2100. This projected increase in global mean sea level and the fact that many coastal areas of Maritime Canada have been deemed highly susceptible to sea-level rise (Shaw et al. 1998) has led to various studies to produce detailed flood-risk maps of coastal communities in PEI, NB, and NS (Webster et al. 2004; Webster and Forbes, 2005; Webster et al. 2006; Webster et al. 2008; Webster 2010). The Atlantic Climate Adaptation Solutions (ACAS) project objectives are to provide five coastal communities within Nova Scotia better information about which areas are vulnerable to coastal flooding today, and in the future considering projected SLR conditions under climate change scenarios. The results of this ACAS project will provide information to support coastal planners and decision makers with details of which areas are at risk of coastal flooding. Similar methods that were employed in the previous Maritime flood-risk studies mentioned were used in this project. A set of spatial analysis tools were applied within a Geographic Information System (GIS) to assist coastal municipalities in identifying areas at risk to coastal flooding and long-term sea-level rise from climate change.

Metadata for the GIS layers delivered for this project can be found in Appendix 1. The main deliverables of this project were a set of flood inundation levels at 10 cm increments to show the extent of the ocean level rising, and an analysis of long term ocean water level records (tide gauges) to determine the probability of a water level occurring or risk. These two datasets can be used together, the GIS will tell you the spatial extent of a water level and the tables can tell you the probability of that level being reached. The water levels in the risk analysis are referenced to local chart datum for each harbor and the GIS flood maps are referenced to a land datum so offsets (Table 2, CGVD28_Chart datum offset) must be applied when combining these data.

The current detail of elevation information available from the province of Nova Scotia along the coastal zone is not sufficient to make accurate predictions of areas at risk to coastal flooding from storms and long term sea-level rise. For much of the Nova Scotia coast the best available terrain information is based on the Nova Scotia Topographic Database at a scale of 1:10,000 with a vertical accuracy of 2.5 m. Importantly, for predicting the abovementioned impacts of climate change, the maps define the 5 or 10 m contour as their lowest elevation inland from the shoreline. While it is noted that terrain information is available at larger scales (1:2,000 and 1:4,000) and finer elevation resolution (2 m contour intervals), these data are for small sections of the Nova Scotia coast. A 2 m contour interval remains an inadequate base for detailed coastal risk assessments. The application of lidar (Light Detection and Ranging) was used to construct high-resolution digital elevation models (DEM) and digital surface models (DSM) which incorporate the trees and buildings into the model for all of the ACAS communities. Lidar is a remote sensing technique that involves an aircraft equipped with a laser rangefinder that shoots pulses of light towards the earth, and by measuring the two-way travel time, determines the distance or range from the aircraft to the earth's surface very accurately. By knowing the precise location of the aircraft by GPS and the distance to the earth's surface, land elevations can be determined. The lidar measures the earth's surface every 1-2 m on the ground with vertical accuracies within 15 cm. Under this ACAS project, the lidar data were collected for three case study communities, while three others have had lidar previously collected either by private data providers under contract to or by the Applied Geomatics Research Group (AGRG), NSCC Middleton. The case study communities all have pressing coastal management issues sensitive to climate change predictions for elevated sea levels. Three of the communities did not have adequate lidar coverage and additional data had to be acquired for:

- **The Municipality of the District of Lunenburg**
- **Oxford to Port Howe**
- **Chignecto Isthmus – Amherst and Fundy shore**

The two case study communities where lidar coverage exists and was provided by researchers at the AGRG-NSCC include:

- **Town and District of Yarmouth**
- **Minas Basin - Municipalities of the County of Kings, Towns of Wolfville, Kentville, Windsor, Hantsport and the District of West Hants.**

The purpose of this project was to determine the extent of various coastal flood levels for the five ACAS case study communities around the province (Fig. 1). In addition to producing the flood inundation maps from the lidar DEMs, benchmark storms were researched for each community and used to demonstrate their vulnerability to coastal flooding. The return periods of the water levels estimated for these benchmark storms were calculated for the present day and future sea-level rise conditions from climate change. In this study we utilized a new program, Time Series Modeler that analyzes a time-series of water levels from tide gauge records to calculate return periods (Webster et al. 2008).

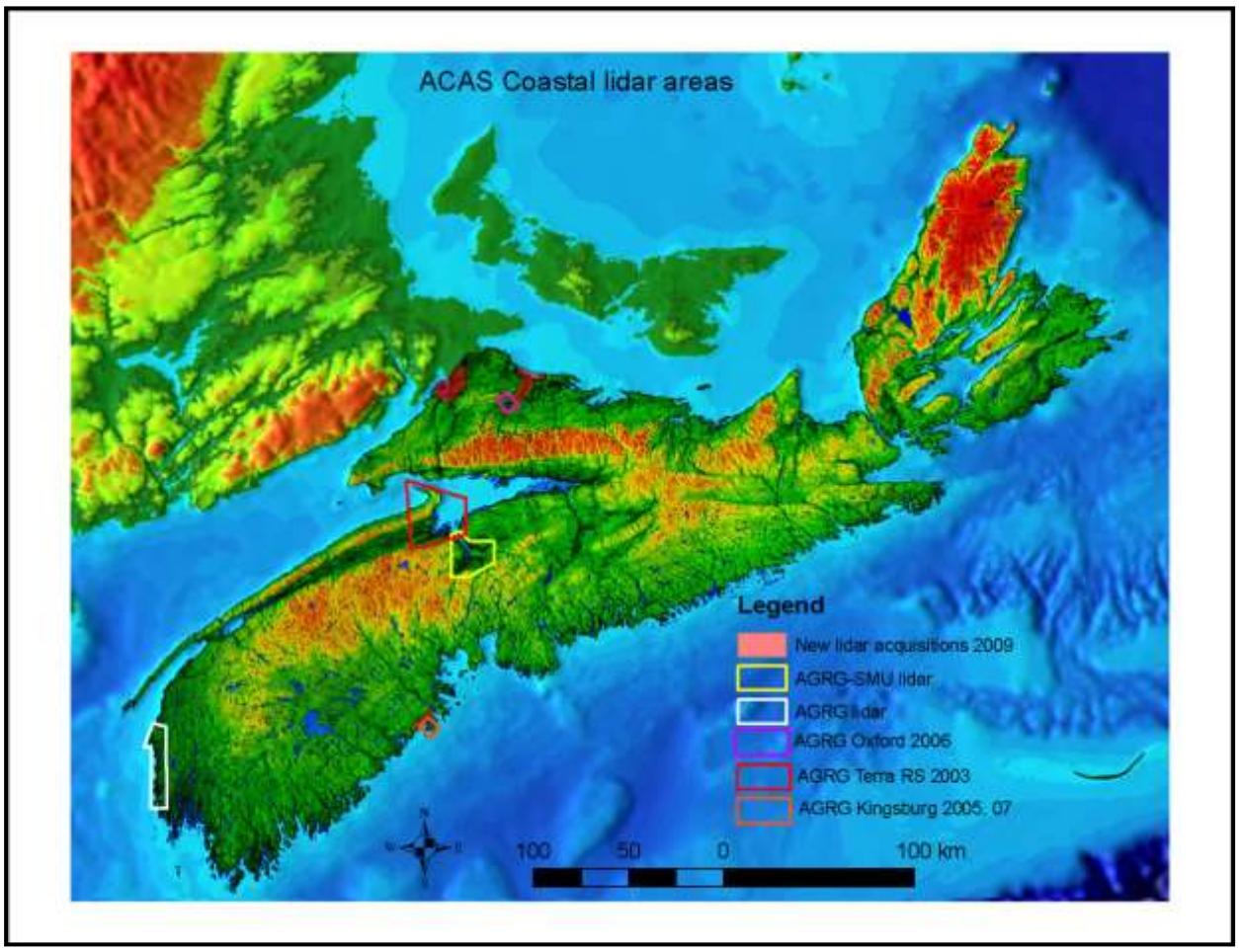

Figure 1: Overview of study areas where lidar DEMs have been constructed and used to generate flood-risk maps.

2. Methods

2.1.Lidar Acquisition

Airborne lidar is a remote sensing technology that is used to acquire elevation information about the Earth's surface. A lidar system is comprised of three technologies: GPS (Global Positioning System); an IMU (Inertial Measurement Unit); and a laser ranging system (Flood & Gutelius, 1997; Liu, 2008) (Fig 2.).

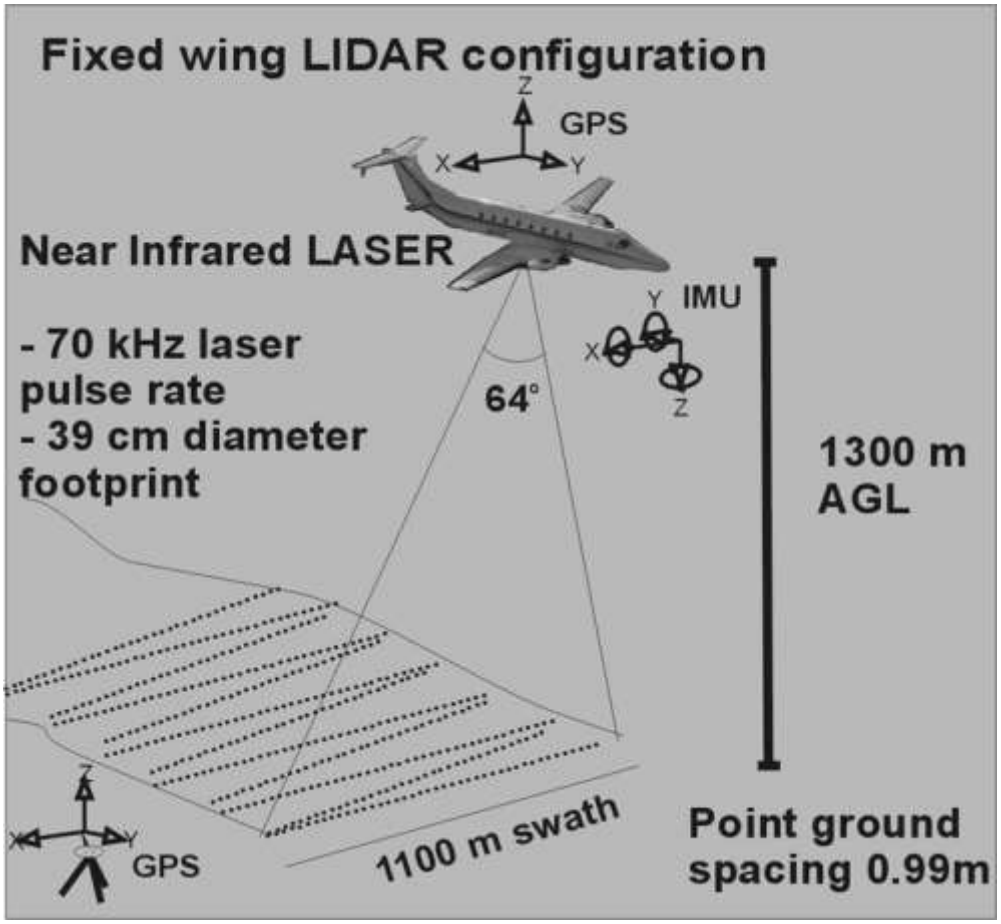

Figure 2 Typical lidar configuration used by AGRG for the coastal surveys. Although the ground point spacing is approximately 1 m, the surveys were flown with 50% overlap, effectively providing a point spacing of 0.5 m.

The GPS is used to determine the 3-D geographic position and elevation of the aircraft. The IMU was used to measure the attitude of the aircraft (roll, pitch and heading) (Liu, 2008). The roll, pitch, and heading were accurately measured to allow for the correction of the motion of the aircraft by computer software (Flood & Gutelius, 1997). The laser ranging system transmitts a laser pulse towards the Earth's surface, and records the time delay between the transmission of the laser pulse and its return. Each laser pulse was capable of recording up to four returns encoded with the GPS, IMU and range data (Liu, 2008). The laser pulses are directed across a swath with an oscillating mirror. Researchers such as Flood & Gutelius (1997) and Wehr & Lohr (1999) provide a general description and overview concerning airborne lidar technology and the principles behind it. In Maritime Canada, previous topographic maps derived

from aerial photo surveys were hampered in forested areas where the ground was obscured by the trees and accurate measurements of the terrain were difficult. The benefit of lidar is that a narrow laser beam is directed from the aircraft towards the earth's surface is reflected back in order to measure the range or distance from the aircraft to the surface. The beam divergence is typically very small (0.3 mrad), resulting in a laser footprint diameter of 20-30 cm on the ground, depending on flying height. Only a portion of that beam has to make it through the gaps in the forest canopy and hit the ground in order for it to be reflected back to the aircraft. Thus in the forest, if one can see patches of the sky above them, there is a good chance the laser beam will make it through a gap and reflect off of the ground or near ground features such as dense shrubs. The lidar sensor records a series of points that represent what the laser pulse was reflected off of including vegetation, buildings, and the ground. The points are processed in the computer and classified into 'ground' and 'non-ground' targets. Since the lidar sensor can acquire more 'ground' measurements in the forest and in open areas than traditional methods such as photogrammetry, the resultant high-resolution DEM provides new images never seen before of the earth's surface.

The ACAS communities were surveyed with lidar as far back as 2003 in addition to a lidar campaign conducted in 2009 to complete the study areas. The dates of acquisition and lidar sensors used for the different surveys are provided in Table 1. The details of the lidar processing and corrections applied to the data are supplied in the Appendices 2-6.

Table 1 Lidar study areas, acquisition dates, provider and sensor used. CFI – Canada Foundation for Innovation, SMU – Saint Mary's University, NSDOE – Nova Scotia Department of Environment, AIF – Atlantic Innovation Fund.

Funding-Partner	**Study Area**	**Date(s)**	**Lidar Provider & System**
AGRG-NSDOE AGRG-AIF AGRG-AIF AGRG-AIF	District of Lunenburg Atlantic coast	Oct. 27, 2009 Nov. 21, 2007 Aug. 4, 2006 Oct. 4, 2005	AGRG, ALTM3100 AGRG, ALTM3100 AGRG, ALTM3100 AGRG, ALTM3100
AGRG- NSDOE AGRG-Oxford Frozen Foods	Oxford-Port Howe Northumberland Strait coast	Oct. 28, 29, 2009 May 12, 2006	AGRG, ALTM3100 AGRG, ALTM3100
AGRG	Town and District of Yarmouth Gulf of Maine coast	Sept. 16, 2008	AGRG, ALTM3100
AGRG- NSDOE	Chignecto Isthmus Fundy coast	Oct. 29, 2009	AGRG, ALTM3100
AGRG-CFI AGRG-SMU	Minas Basin Fundy coast	May, 2003 April, 2007	Terra Remote Sensing Inc., Mark 1 AGRG, ALTM3100

The District of Lunenburg area represents a contiguous section of mainland coastline along Lunenburg County. Previous work by AGRG (R. Mosher) has acquired lidar for the Kingsburg area (Webster, Mosher and Pearson, 2008). The new lidar areas overlap with the existing lidar DEM provided by AGRG (Fig. 3).

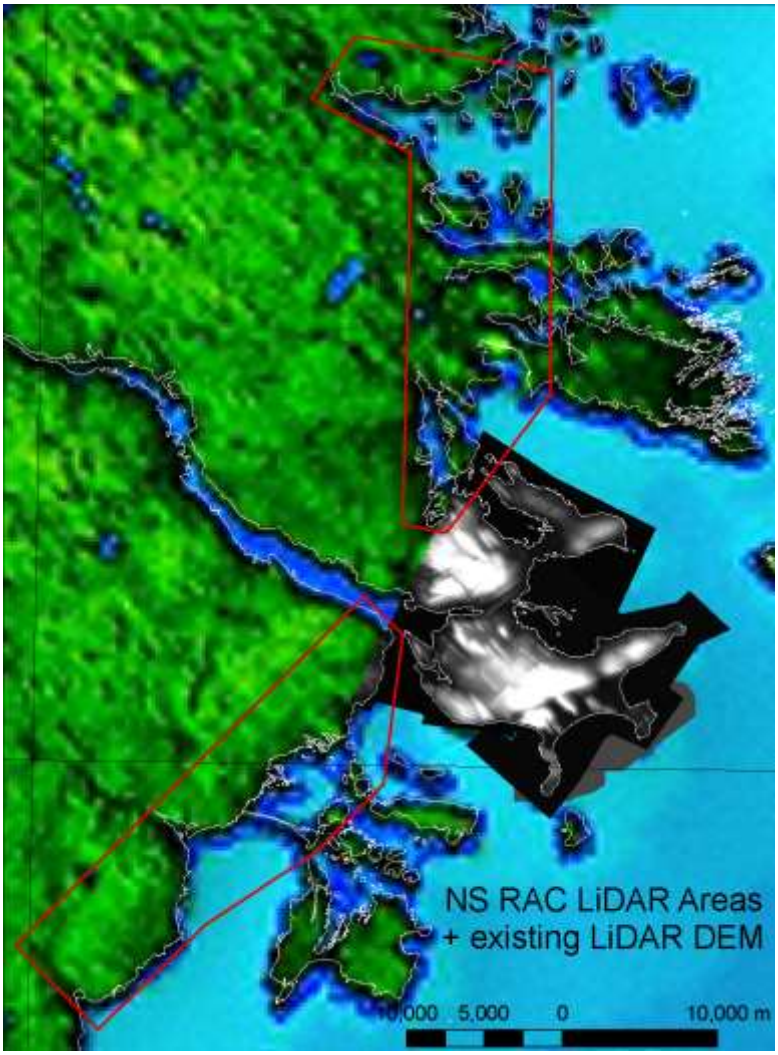

Figure 3 District of Lunenburg, red polygons represent the new lidar acquisition with the existing Lidar DEM (greyscale).

The Oxford-Port Howe area represents the seaward connection of the town of Oxford which is vulnerable to flooding and has been the subject of a previous study using lidar by AGRG & Acadia University (D. Stiff, MSc project). The new lidar coverage overlap the existing coverage for the town of Oxford (Fig. 4).

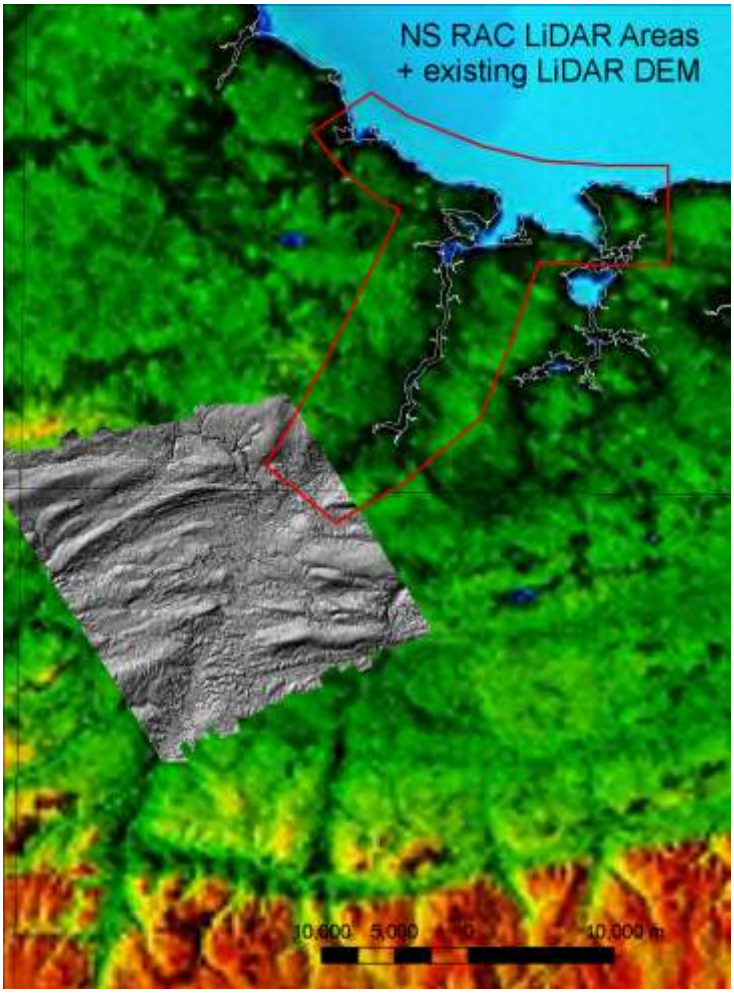

Figure 4 New lidar coverage (red polygon) connecting Port Howe with the existing lidar DEM for the town of Oxford (grey scale).

The Chignecto Isthmus area represents the upper Bay of Fundy, including the Town of Amherst and portion of the County of Cumberland and the border with New Brunswick. Previous lidar had been acquired for a small section of the coast for a study related to salt marsh restoration, a MSc joint project between AGRG & Acadia University (K. Millard, MSc project) (Fig. 5).

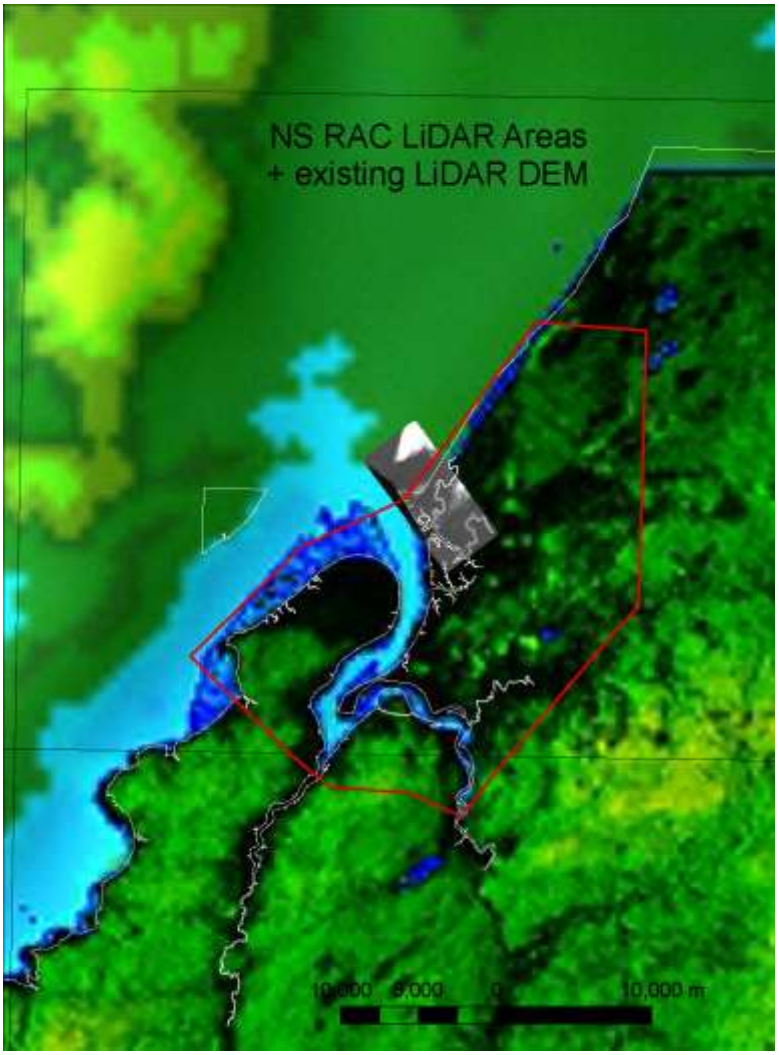

Figure 5 Chignecto Isthmus new lidar acquisition area in red polygon, existing lidar DEM in greyscale.

2.2.Lidar Processing

After the lidar flights the GPS and IMU data were processed to determine the trajectory of the aircraft and the laser points were geocoded and their position on the earth determined. The Lidar point clouds were then exported as binary LAS format files for each flight line of the study area. These files are very large and contained billions of points and were processed in specialized Lidar software, Terrascan™ from TerraSolid. A Terrascan project was defined for each area and the lidar data divided into blocks measuring 1040 m by 1040 m, with 40 m overlap between blocks. The blocks were used to process and adjust the data into manageable file sizes. For

example, the Lunenburg surveys consisted of approximately 50 flight lines which were separated into 317 blocks (Fig. 6).

Figure 6 District of Lunenburg, example of the flight lines and 317 blocks (red squares). Each red block is 1040 m by 1040 m.

The lidar point clouds for each block were then processed separately. The initial processing involves removing erroneous points that are either too high or too low. The high points are typically birds or aerosols and the low points are caused by the laser pulse experiencing multi-path reflections, thus being projected below the earth surface when the scan angle and range are used to compute their position. The next step in the processing involves inspecting the relative position of lidar points between flight lines. A common issue with airborne lidar is the slight misalignment of points between flight lines, both in the horizontal and vertical plane. This is usually caused by a calibration problem which relates the alignment and offset of the GPS and attitude sensor (IMU for pitch, heading and roll) with the lidar sensor. These calibration errors can be resolved to a certain degree by post processing the data and applying rotations and offsets to the points in each flight line. Upon visual inspection of the point clouds for each flight line differences in the spatial locations of objects were observed. Various corrections were applied using Terra-Match to align the point clouds for each flight line (Appendices 2-6). Once the point cloud data were sufficiently aligned, the next stage of the processing involved classifying ground points. A standard set of parameters were used to classify points as ground versus non ground objects. Coastal areas with abrupt changes in relief, either natural geomorphic features or anthropogenic structures such as wharfs or shoreline armouring often cause classification errors using the standard techniques. Since an accurate classification of the ground is critical for the accurate construction of the Digital Elevation Model (DEM), which is then the basis for the flood risk modeling & mapping, the coastal areas were critically examined. The lidar point clouds were visually examined along the coast and erroneous points were manually classified to ensure we produced the most accurate elevation model of that area as possible.

Once the ground classification was assessed and deemed acceptable based on a visual assessment, surface models were constructed from the lidar point cloud for each block. Two

surface models were constructed; a DEM which was based only on classified ground points, and a digital surface model (DSM) which incorporated the ground and non-ground points. The horizontal lidar point clouds are projected into a standard map projection, in this case UTM Zone 20 NAD83, however the elevations are referenced to the GRS80 ellipsoid, since they are derived from laser ranges and position from GPS observation. Most land-based topographic maps contain elevations relative to a geodetic vertical datum. In Canada, this is known as the Canadian Geodetic Vertical Datum of 1928 (CGVD28). In order to have height measurements related to sea level and other terrestrial surveys a transformation was applied to convert the heights from referencing the ellipsoid to the geoid. This was done using the HT2 geoid-ellipsoid separation model, available from Natural Resources Canada, and is described in Webster et al. (2004, 2006, 2008). The resultant DEM and DSM elevations are now referenced to (CGVD28) and are considered to be orthometric heights. The term orthometric is used because the elevations are measured orthogonal to the geoid surface.

2.3.Lidar DEM validation

The lidar points and surfaces were expected to have an absolute vertical error less than 30 cm, and typically less than 15 cm. To ensure that the LIDAR DEMs had accurate elevation values, the models were compared to RTK (real time kinematic) GPS surveys that were conducted along roads and other hard surfaces. The GPS checkpoint surveys consisted of setting up a GPS base station and radio over a HPN (high precision network) monument of known precise location and using a GPS rover on the pole or mounted to a vehicle to collect the checkpoints. The GPS surveys were conducted using a Leica GPS System 500 and 1200, where baselines were kept below 15 km in length, allowing the RTK GPS rover to achieve a vertical precision of 3 cm or better. The vehicle mounted checkpoints were collected along the roads and

the pole was used for limited transects and checking the vehicles heights (e.g. Fig. 7). Elevations were transformed from ellipsoidal to orthometric and compared to the lidar DEM following procedures outlined by Webster (2005).

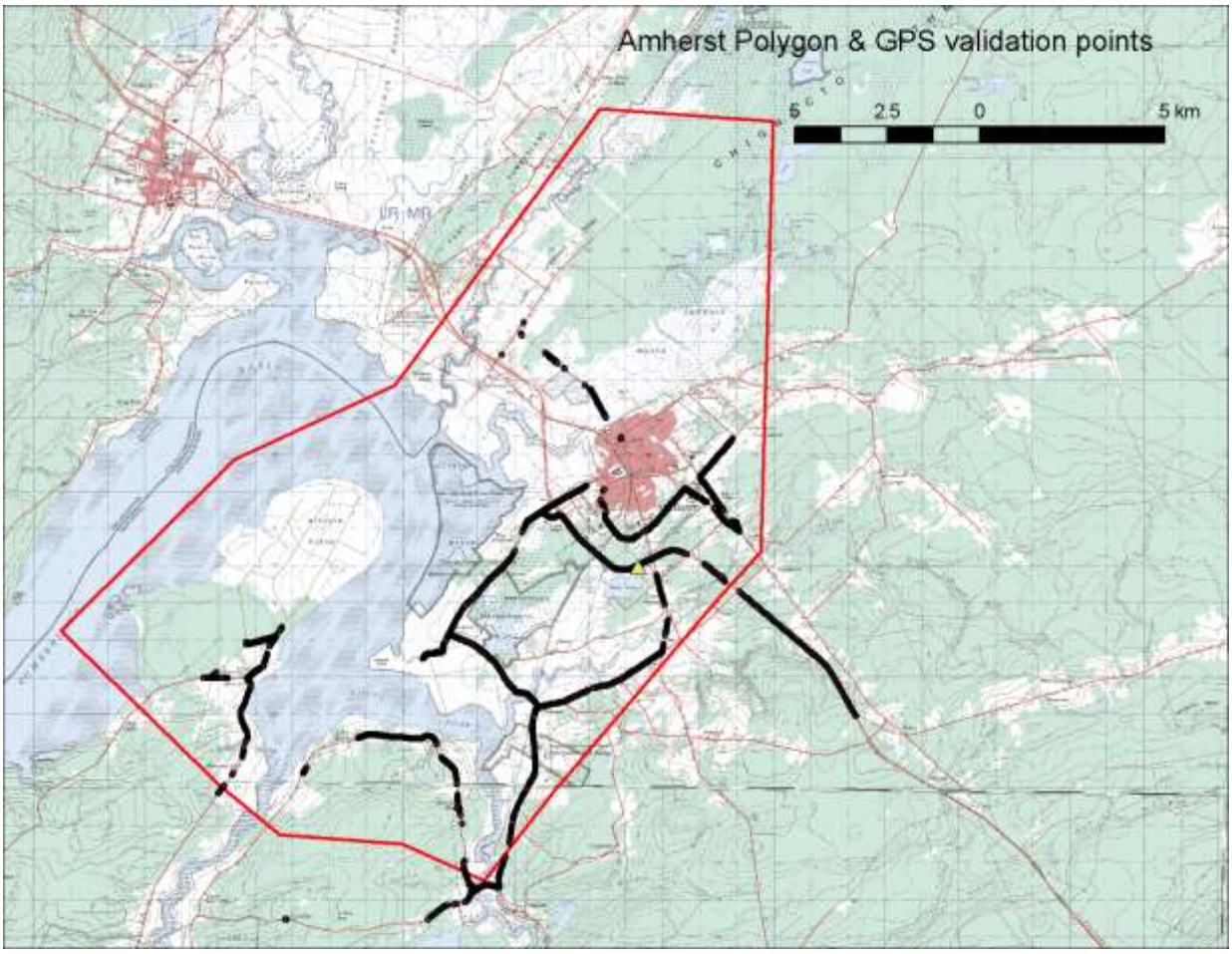

Figure 7 Chignecto Isthmus area GPS checkpoints (black dots) and the high precision network monument used for a GPS base station (yellow triangle) near Amherst. The lidar extent is defined by the red outline.

2.4. Lidar Map products: Colour shaded relief models

The lidar surface models DSM (all points including ground, buildings and vegetation canopy) and the DEM (ground only) can be used to derive a variety of other map layers including slope, aspect (land facing orientation), as well as maps that can be used to improve our interpretation of the landscape morphology. Shaded relief maps have been constructed from the lidar surface models where the terrain was illuminated from the northwest at a 45 degree angle. In order to enhance the subtle relief present in the study areas, a 5 times vertical exaggeration has been applied to the terrain. The shaded relief maps are viewed and interpreted as greyscale maps which highlight the local relief, but do not depict the actual elevation (ie. A slope in the valley will look the same as a slope at the top of a hill). Another series of map products that have been constructed consist of colour shade relief (CSR) maps. Colours have been assigned to the elevations based on the lidar surface models and merged with the shaded relief maps. The colour ramp was selected to optimize the Chroma stereoscopy, which is a technique of using colour to visualize maps in 3-D when using glasses from Chromatech^{TM}. The glasses utilize a diffraction grating that splits the light into a diffraction pattern that is proportional to the wavelength of the light, thus if the terrain is coloured from low elevations with short wavelength blue to high elevations with longer wavelength red, the map appears in 3-D. Two colour schemes were used; a “standard - S” colour scheme which allows DEMs from around the province to be displayed using a common palette or colour scheme. A “personalized” – P colour scheme was optimized for the local relief to use the entire spectrum (rainbow) from blue to red. The colourized elevation is then merged with the shaded relief that gives the terrain texture and enhances the information that can be interpreted from the map. CSR maps have been built for both the DSM and DEM datasets for both colour ranges, standard and personalized (Figs. 8, 9). These maps are

qualitative and are designed for use as a backdrop to other information within the GIS. These CSR images have been converted into a compressed georeferenced format, JPEG 2000, this is compatible with most GIS systems.

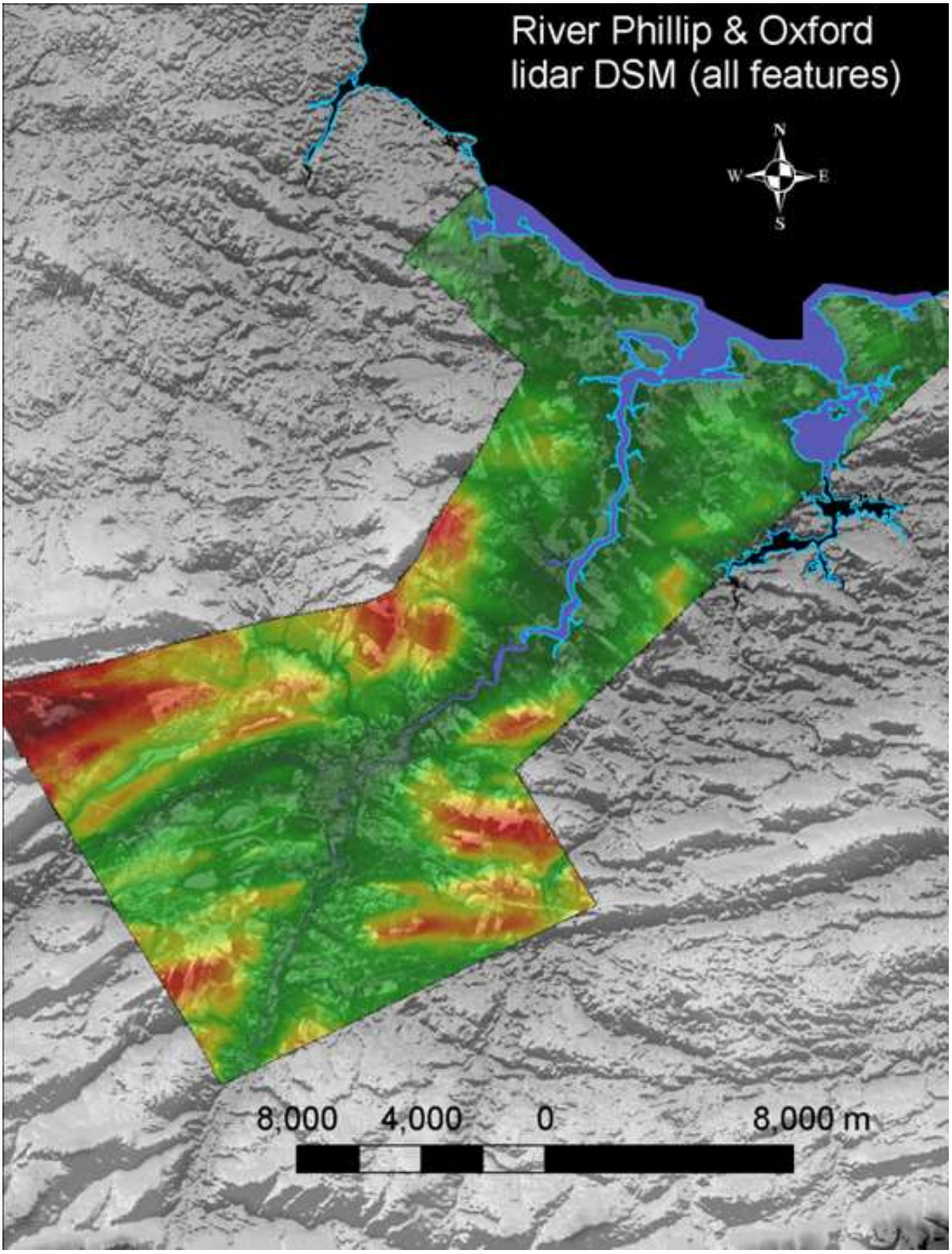

Figure 8 Lidar Digital Surface Model (DSM) personalized colour shaded relief (CSR) map of Oxford-Port Howe area. Grey background image is based on the NS 1:10,000 topographic data. Blue represents elevation below 0 m, green lowest land through red highest land elevations.

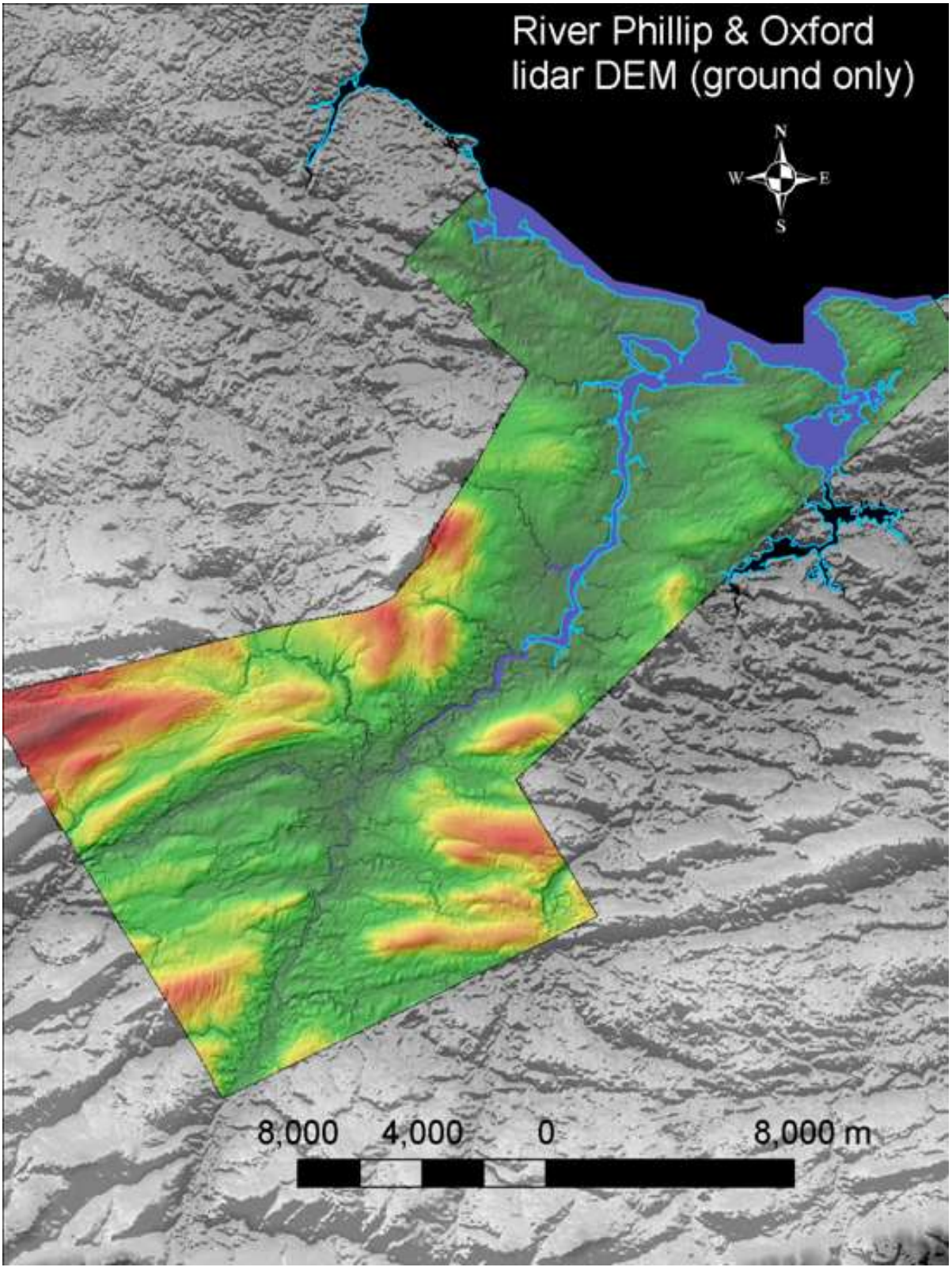

Figure 9 Lidar Digital Elevation Model (DEM) personalized colour shaded relief (CSR) map of Oxford-Port Howe area. Grey background image is based on the NS 1:10,000 topographic data. Blue represents elevation below 0 m, green lowest land through red highest land elevations.

2.5. Flood Inundation Mapping

The last processing step required for the DEM prior to flood inundation mapping was to ensure hydraulic connectivity along water ways. Roads that have streams running under them usually contain a culvert or bridge to allow for the flow of water. However, lidar point elevations only detect the surface of the road. Therefore, when determining the flow path of water to or from the ocean along low lying areas, the road in the unedited DEM would act as a dam or barrier. To ensure that low-lying areas are properly flooded if they are connected to the ocean, the DEM was modified in areas of culverts or bridges to allow for hydraulic connection. We follow a similar method as outlined in Webster et al. (2006) for this procedure.

Flood inundation maps were generated in the ArcGIS ArcMap™ environment using an Arc script developed by the AGRG (Webster and Stiff, 2008). The script generated flood levels from a set lower limit which was dependent on the state of the tide up to an upper elevation limit relative to CGVD28 at 0.1 m increments. We use a "still water" method which assumes the ocean is a flat plane, appropriate for large scale storm surge events that cover 10s of km in area, as we raise the water level to determine areas on land the will be inundated. This method does not take into account the action of wave run-up or the travel time water takes to cross a land surface. However, for the generation of static flood inundation maps that predict the extend of flooding from the total sea level (including tide, surge and wave run-up) the still water method has been found to produce results suitable for planning purposes (Webster et al. 2006). In the case of low tide coastal lidar acquisitions we would begin flood inundation at negative elevations and increase them to positive values while ensuring only areas connected to the ocean were flooded. We have supplied all flood inundation layers (denoted N – negative flood elevations and P – positive flood elevations relative to CGVD28) that have been generated for each, ACAS case

study community. We used a benchmark storm for each study area to depict the past flooding event and to impose future sea-level rise conditions for future possible flooding. As a result of the uncertainty in global sea-level rise predictions and the expected continual revision of them in the future and as we have new data becoming available for local crustal subsidence rates having all the flood levels at 10 cm increments available allows local officials to access the appropriate flood layer as new predictions come along. For each study area, the water level of the benchmark storm was used to depict the flooded areas. For the storms that we have tide gauge records for we have extracted the maximum sea-level and compared it to the predicted tide in order to calculate the residual (difference between observed and predicted) to determine the magnitude of the storm surge. These storms were then simulated in the future under different sea-level rise conditions depending on the location. In all areas we report the worst case scenario of the highest possible predicted tide or higher high water large tide (HHWLT) plus a 1-2 m storm surge to predict possible flooded areas if no benchmark storm records exist. In order to use the tide gauge records or the predicted HHWLT elevations, which are referenced to chart datum, a transformation must be applied to convert the water level elevations to the land and DEM datum, CGVD28. The values for these conversions between chart datum (CD) and CGVD28 were supplied by the Canadian Hydrographic Service and are presented in section 2.6, Table 2. The same conversion is required when examining the risk or probability of a water level occurring (Appendices 7-10) or the return period of a specific storm (Results Section – Flood Risk) from data derived from the tide gauge with the GIS flood layers or DEM.

2.5.1. Dyke Overtopping Inundation Mapping

For some of the case study communities, Minas Basin and the Chignecto Isthmus, dykes protect low-lying areas from the ocean. Streams and ditches landward of a dyke are often drained

by a one-way culvert, aboiteau, thus not allowing the ocean to flood the land at high water levels. We have generated flood inundation maps that represent over topping of the dykes. In this case the sea level of the ocean is raised until it overtops the dyke. The resultant flood layer extent will cover the area of the low lying land behind the dyke starting at the overtopping elevation. We appreciate that our current GIS based flooding method does not adequately depict the situation where water will spread behind the dyke at the location it is overtopped or breached. To provide better information on where the water will be distributed immediately behind the dyke we have introduced a dyke breach into our methodology.

2.5.2. Dyke Breaching Inundation Mapping

In many instances in the past, dykes have breached and allowed water from the ocean to flood the low-lying area behind the dyke. Although the GIS techniques for flood inundation mapping used in this study do not take into account the time it takes for water to cross a surface, they do predict the extent the water will eventually reach. In the case of dyke breaching, we have notched the dykes to the level of the terrain landward of the dyke at the locations of drainage channels on the seaward side of the dyke, considering they may be more vulnerable to erosion (e.g. Fig. 10). We have generated a new set of inundation flood layers with the source at the breach location. This allows static maps to be constructed that depict the potential extent of such an event. For example, the map output would consist of 2 water levels; a higher ocean level at the top of the dyke with an extent seaward, and a lower water level at the landward side of the breached dyke. This lower value will increment by 10 cm steps until it has filled the areas behind the dyke. In the case of the example used in figures 10 and 11, the initial water level in the ocean would be less than 7.9 m prior to dyke overtopping. Then, as a dyke fails and the breach begins,

the first inundation level would be the lowest elevation behind the dyke, in this case 6 m (Fig. 11).

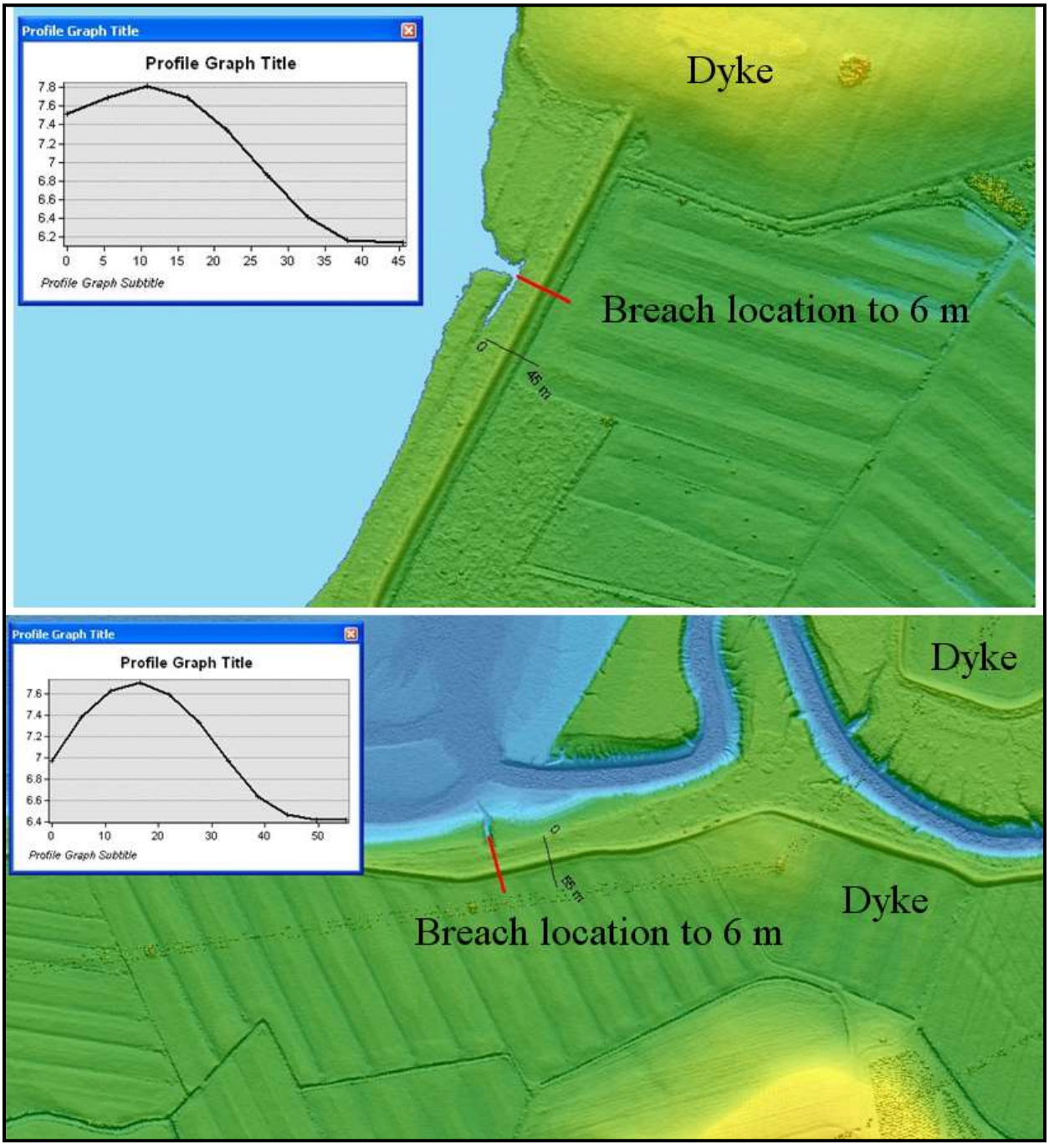

Figure 10 Examples of dyke elevation profiles near Nappan (Chignecto Isthmus). Profiles indicate the land seaward of the dyke is higher than what is landward. The location of the breach simulations points are in red.

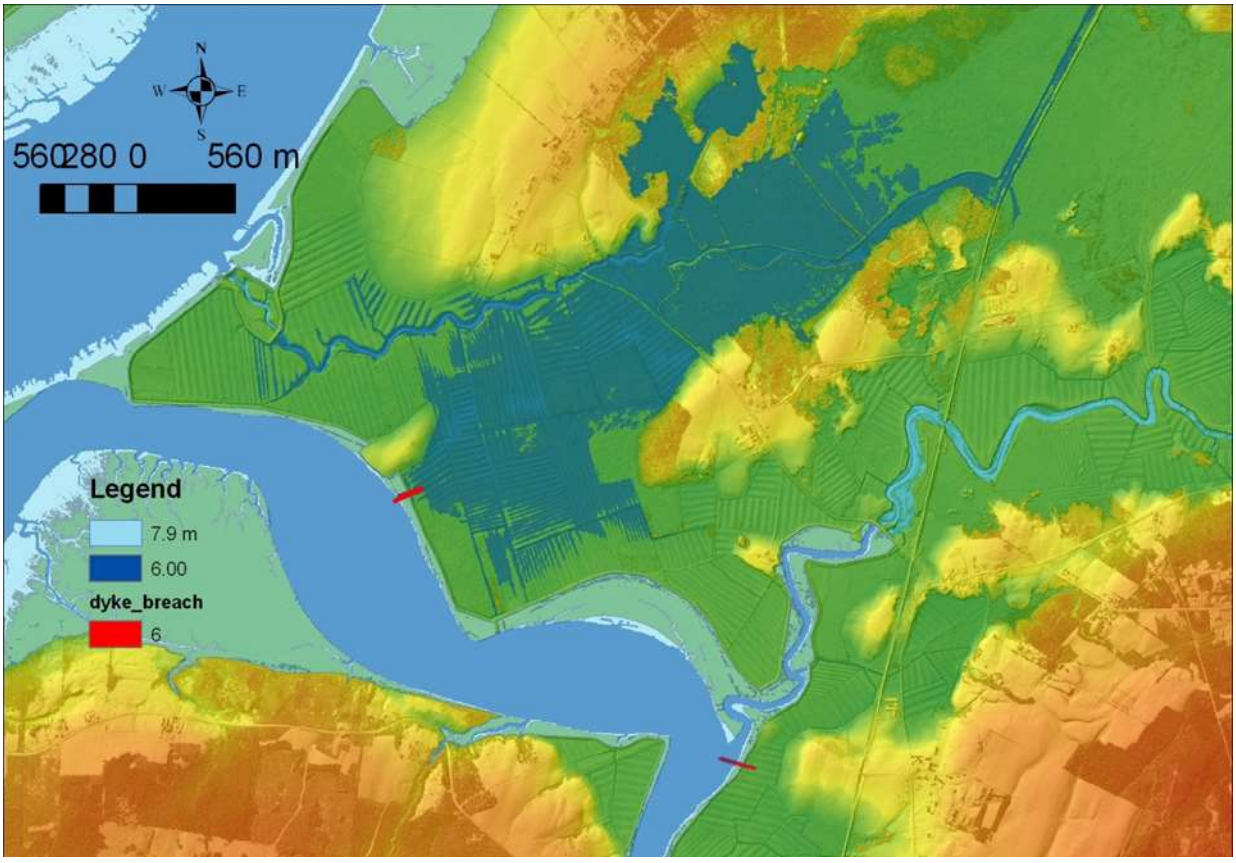

Figure 11 Example of flood inundation of a breached dyke. Ocean water level set at 7.9 m, before the dyke overtopping elevation. After the dykes are breached (red lines across dykes), the initial area flooded at the 6 m elevation landward of the dyke. The area is part of the Chignecto Isthmus with the Nappan River in the lower right.

2.6. Sea-level rise predictions

In addition to global sea-level rise, local crustal dynamics also affect relative sea-level. The major influence on crustal motion for this region is related to the last glaciation that ended ca. 10,000 years ago (Shaw et al., 1994; McCullough et al. 2002; Peltier, 2004). The areas where the ice was thickest were depressed the most and peripheral regions where uplifted, termed the "peripheral bulge". The ice was thickest over Hudson Bay in central Canada, where the crust was most depressed, however today this area is still rebounding from the removal of the ice load and continues to uplift. The Maritimes represent part of the peripheral bulge and southern New Brunswick and Nova Scotia are subsiding (Peltier, 2004). Subsidence rates vary across the

region with Nova Scotia having a rate of ~ 15 cm per century (Forbes et al., 2009). The subsidence of the crust is important for coastal communities in that it compounds the problem of local sea-level rise and must be considered when projecting future flood risk.

The Bay of Fundy tidal range is expected to increase by ca. 10-30 cm in the future with an increase in sea-level (Godin, 1992; Greenburg et al., in review). All of these factors must be combined, global sea-level rise, crustal subsidence, and tidal amplitude, to produce a potential increase in relative sea-level in the next century. This does not include the possibility of increased storm intensity or frequency.

One of the areas of the largest uncertainty is the prediction of the rise in the mean global sea-level. The third assessment report from the Intergovernmental Panel on Climate Change (IPCC) indicated that there will be an increase in mean global sea-level from 1990 to 2100 between 0.09 m and 0.88 m (Church et al., 2001). Previous coastal flood risk mapping in the region have used the central value of 0.5 m/century to project global sea-level rise into the future (Webster et al. 2006, 2006A). The latest IPCC Assessment Report 4 (AR4) has projected global mean sea-level to rise between 0.18 and 0.59 m from 1990 to 2095 (Meehl et al., 2007). However, as Forbes et al., 2009 pointed out in the Halifax Harbour study, these projections do not account for the large ice sheets melting as not enough literature on the subject was available at the time of the AR4 report. Recent sea-level observations were compared with the IPCC projections from 2001 (Rhamstorf et al., 2007). The results indicated that sea-level may be responding quicker to increased atmospheric temperature than the climate models predicted. Observations were based on tide gauge measurements and satellite altimetry. The satellite data show a linear trend (1993–2006) of 33 cm/century. The effects of fresh melt water from ice sheets on the thermohaline circulation (THC) pattern, changes sea-levels regionally and modeling results indicate the North American Atlantic coast could see an increase in sea-level between 0.5 and 1 m as the THC shuts

off (Levermann et al., 2009). Comparison of altimetry data from the Topex-Poseidon satellite between 1993 and 2003 with tide gauge measurements is consistent with a weakening of the THC (Levermann et al., 2009). Sea-level changes cannot yet be predicted with confidence using models based on physical processes, because the dynamics of ice sheets and glaciers and, to a lesser extent, that of oceanic heat uptake is not sufficiently understood. The correlation between sea-level and temperature is >0.99 for observations from 1880 to 2000 (Vermeer and Rhamstorf, 2009). Climate models predict global mean temperature with confidence and these results were used to estimate sea-levels (Vermeer and Rhamstorf, 2005; Rhamstorf, 2007). The future global temperature scenarios based on the PICC AR4 report were used to estimate global sea-level rise between 75 and 190 cm for the period of 1990–2100 (Vermeer and Rhamstorf, 2009). Due to the uncertainty in the global sea-level predictions, (Forbes et al., 2009) used 1.3 m as the upper limit for a precautionary approach to sea-level rise projections in the Halifax region.

We have adopted the value of 1.3 m for global sea-level rise by 2100 and used in the flood risk analysis. This number has been used as the global mean sea-level rise in the future in addition to crustal subsidence to determine the water level of storms, such as the Groundhog Day storm of 1976, if they occur in the future. If one considers the estimates by Vermeer and Rhamstorf (2009) global sea-level could rise by as much as 190 cm over the next century, thus decreasing the return periods of any given water level. With the high level of uncertainty involved in the estimates of global sea-level rise over the next century, flood inundation levels were mapped at every 10 cm up to an upper limit of 5 m along the Atlantic shore and Northumberland Strait and up to 12 m CGVD28 within the upper Bay of Fundy.

We have selected a conservative (0.57 m) and a higher rate of global sea-level (1.3 m) to illustrate the impacts of past storms into the future. For the District of Lunenburg, and the Oxford-Port Howe study areas we use global mean sea-level projections from the IPCC AR4

report (0.57 cm) and from Rhamstorf (2007) following the method of Forbes et al. (2009) (1.30 m). Assuming a crustal subsidence rate of 0.16 m, the upper limit of relative sea-level rise projections for 2100 are IPCC-AR 4 A1FI scenario (global 0.57 m + subsidence 0.16 m = 0.73 m) and from Rhamstorf (2007) (global 1.30 m + subsidence 0.16 m = 1.46 m). For the Bay of Fundy study areas; Town and District of Yarmouth, Chignecto Isthmus and Minas Basin areas we use projections from Greenburg et al. (in review) who estimate that Yarmouth could experience a RSL rise between 0.71 – 1.27 m by 2100 with a central value of 1.01 m and a margin of error of approximately 0.25 m. The tidal amplitude is predicted to increase by 0.10 m for this region. For the Upper Bay of Fundy (Chignetico Isthmus) the tidal amplitude will increase even more with increased RSL. They estimate RSL in Cobequid Bay (Minas Basin) to increase between 0.79 m – 1.40 m by 2100 with a central value of 1.12 m with a margin of error of approximately 0.25 m. The tidal amplitude is predicted to increase by over 0.2 m for this region. The contribution from the mean global sea-level for these predictions was approximately 0.40 m which appears to be a lower estimate than used by Forbes et al. (2009) who used a range of 0.57 m to 1.30 m (Halifax study) and Daigle (2011) who used 0.85 m for Sackville NB. Thus we have increased the RSL for Yarmouth to be between 1.00 and 1.73 m and for the Upper Bay of Fundy communities (Chignecto Isthmus and Minas Basin) to be between 1.20 and 1.93 m.

Table 2 Study site communities with the nearest tide gauge record. The chart datum – CGVD28 relationship for the tide gauge and the predicted highest possible tide level (HHWLT). The benchmark storm name and date along with the maximum water level obtained from tide gauge records or GPS on a wrack line. The relative sea-level rise projections used in this study.

Community	Tide Gauge location	Chart Datum – CGVD28 (lidar) relationship	Predicted Higher High Water Large Tide (HHWLT) m CGVD28	Benchmark Storm & water level CGVD28 From tide gauge (TG) or GPS	Projected Relative Sea-Level Rise by 2100 (min., max) cm
District of Lunenburg	Halifax	0.80	1.36	Juan 2003 2.1 m (TG)	73 cm, 146 cm
Oxford-Port Howe	Pictou	0.92	1.19	Dec 1993 2.27 m (TG) Dec 2010 2.21 m (TG) 2.6 m (GPS)	73 cm, 146 cm
Town and District of Yarmouth	Yarmouth	2.31	2.85	Groundhog Day Feb. 2 1976 3.36 m (TG) 4.81 m (GPS)	100 cm, 173 cm
Chignecto Isthmus Amherst	Fort Lawrence	7.26	6.90 *	Saxby Gale Oct 1869	120 cm, 193 cm
Minas Basin	Hantsport	7.23	8.15	April 6 1977 7.67 m (TG) 8.6 m (GPS) Saxby Gale Oct 1869	120 cm, 193 cm

- **Not available for Fort Lawrence, used Joggins with CGVD28-CD = 6.50 m**

2.7. Flood Risk Calculation

To determine the risk or probability of a given water level occurring, a software tool, Time-Series Modeler produced by AGRG and GeoNet Technologies Inc., was used to calculate the return period statistics. The software uses a time series of water level records (tide gauge data) to determine the risk or probability associated with any given water level occurring (Webster et al. 2008). The return period of a given water level or the probability of occurrence can be calculated using current relative sea-level rise conditions or one can use projected sea-level rise conditions predicted from climate change as described in the previous section.

To illustrate how the flood risk is determined from a time series, we have used the Pictou tide gauge record that spans the 1960s through to 1996 before it was decommissioned by the Canadian Hydrographic Service (CHS). Water level records are available for hourly or sometimes 15 minute sampling intervals and are referenced to the local chart datum (CD) for that harbour. The observed hourly water levels were acquired from the Integrated Science Data Management website (http://www.meds-sdmm.dfo-mpo.gc.ca) which is part of the Department of Fisheries and Oceans. The time series can be plotted to identify gaps in the record and the typical tidal range (Fig. 12).

Webster et al. (2008) describe the background and statistics used within the tool to calculate return periods if more details are desired. The next step in the process involves calculating the annual mean and maximum water levels (Fig. 13). The time series is then de-trended based on the mean sea-level, effectively removing the past RSL trend. The highest water level recorded at Pictou is 3.2 m CD and occurred on Dec. 31, 1993. This storm produced a water level 1.5 m (storm surge) higher than the predicted tide and caused coastal flooding and erosion along the Northumberland Strait. There is a significant gap in the data record from the late 1950s to 1965.

From 1965 to 1996 there are only small gaps and the record is of sufficient length (ca. 30 years) to generate return period statistics (Webster et al. 2008).

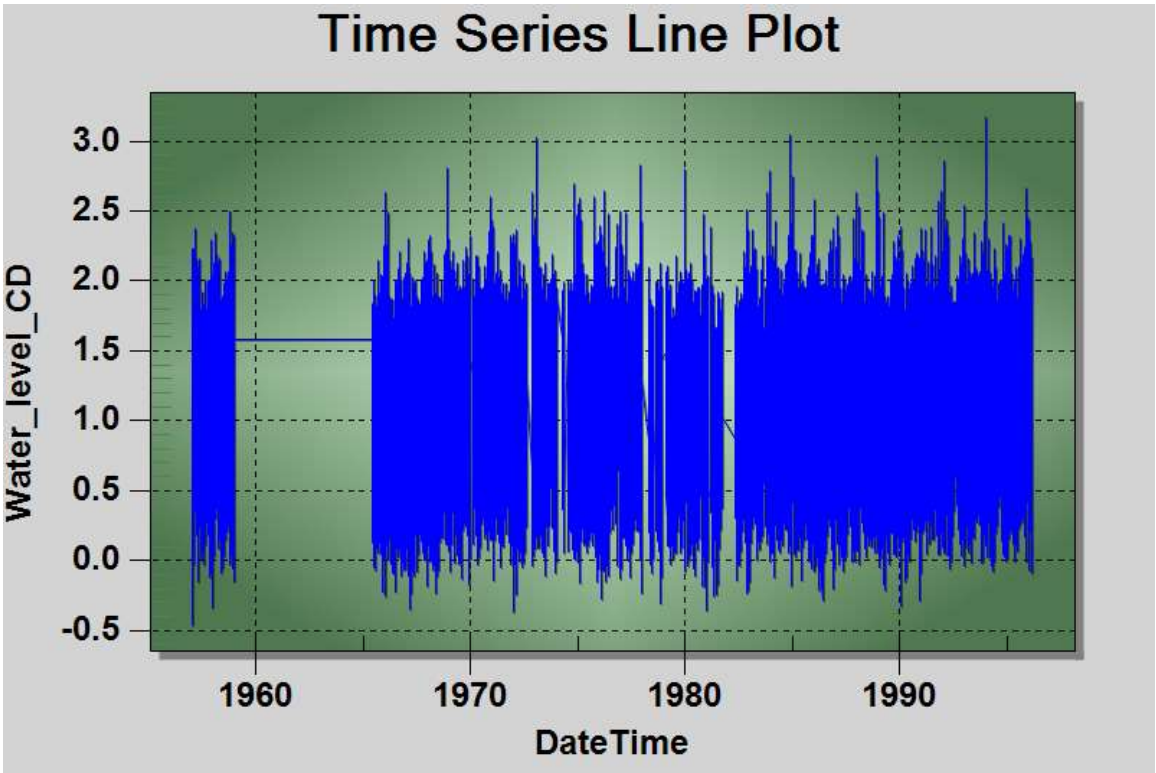

Figure 12 Tide gauge record for Pictou, water level above chart datum.

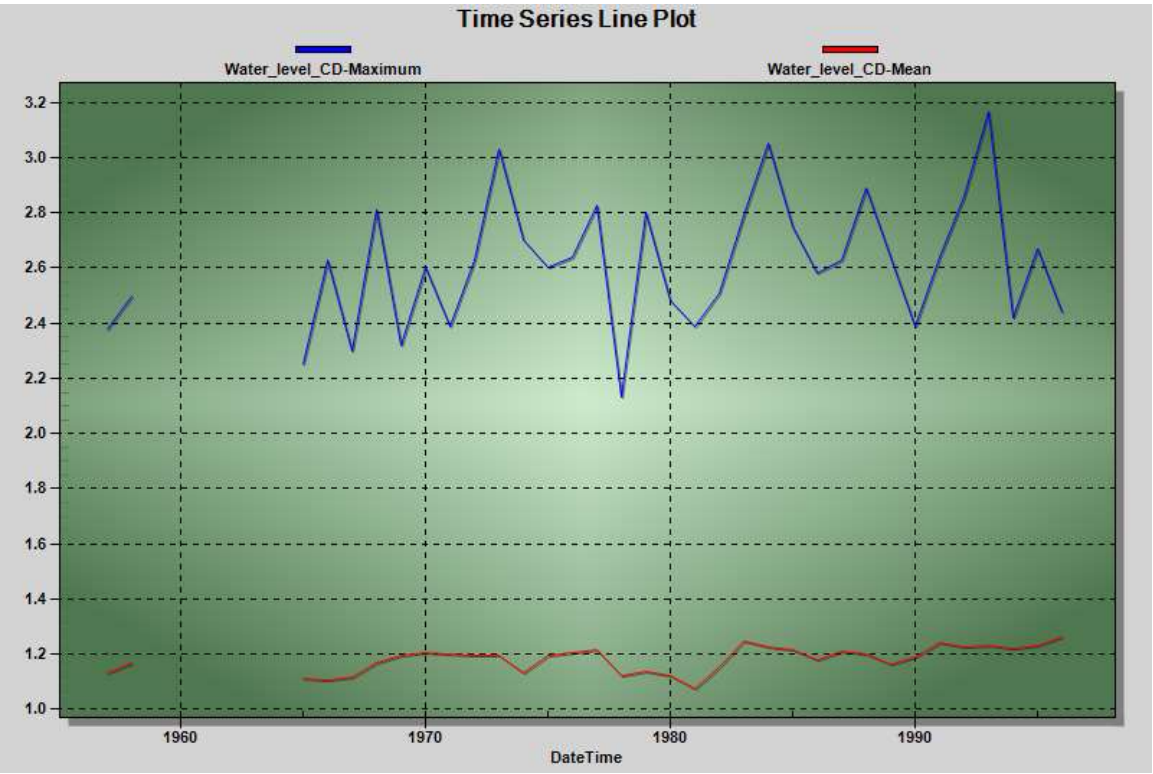

Figure 13 Pictou annual maxima (blue) and mean (red) water levels .

Several extreme value probabilities models are supported by the software and can be tested to determine which one is best suited for the time-series. The most commonly used models that are applied to the annual maximum water levels include: Gumbel, Weibull, and Logistic models. The empirical (tide gauge maxima) is plotted against the model value to assess the fit (Fig. 14). In addition to this, statistics such as the correlation and Root Mean Square (RMS) of the differences between the model and empirical data are generated (Table 3). The lower and upper model limit represent the 95% confidence interval and are achieved by a jack-knife technique of holding back some of the empirical data and generating the model (Fig. 14). The different models (Gumbel, Weibull and Logistic) fit the data differently and have different degrees of variance (Figs. 14, 15, 16). When comparing the different models, we focused our attention on how well the model fit the higher water levels, since these represent the extreme events which we are most interested in and are trying to model. The Gumbel distribution has been applied in

many applications of time series data from tide gauges (Bernier 2005, Thompson and Bernier 2009) and appears to fit the extreme water level values the best although it has the poorest overall statistics in terms of correlation and RMS (Fig. 14-16, Table 3).

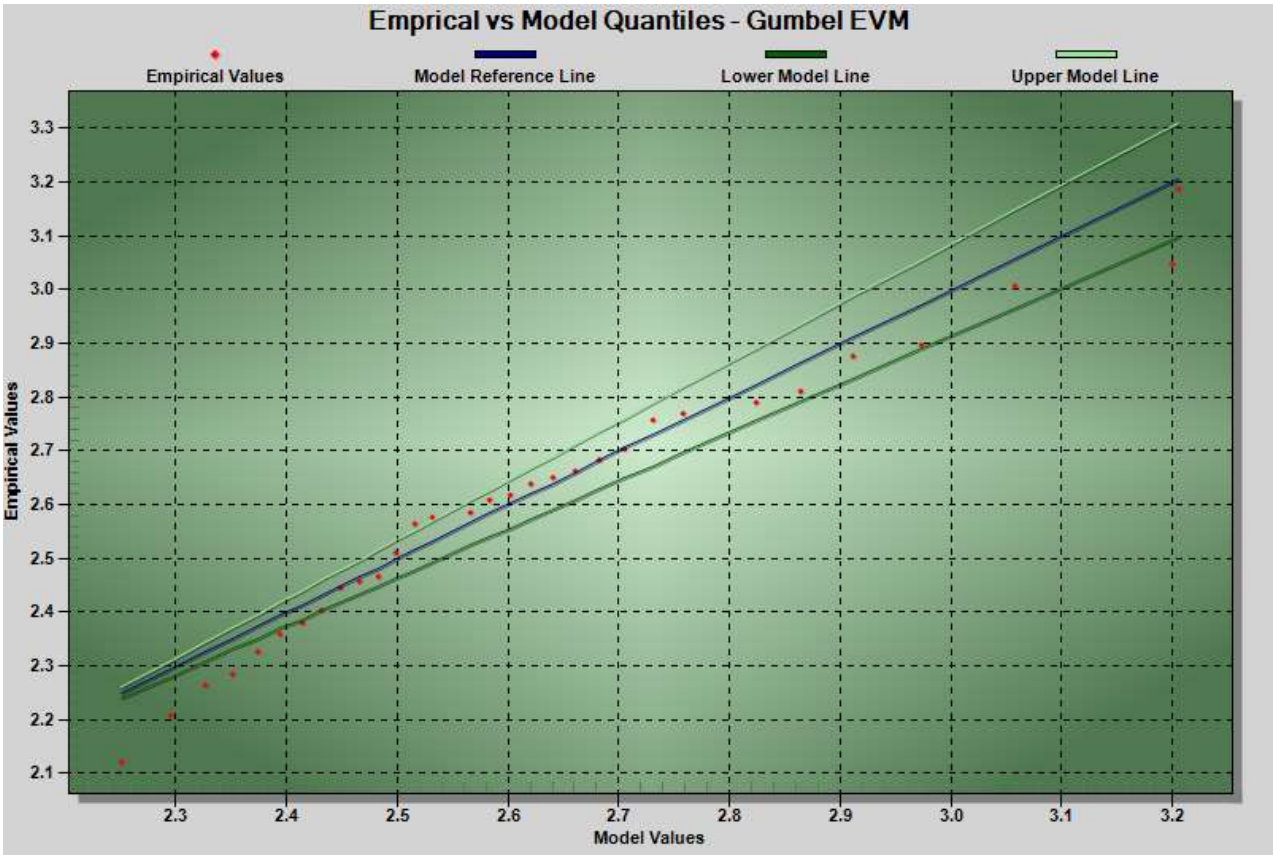

Figure 14 Gumbel extreme value model (line) fit to annual maximum water levels (red dots), with 95% confidence interval (green lines) for Pictou.

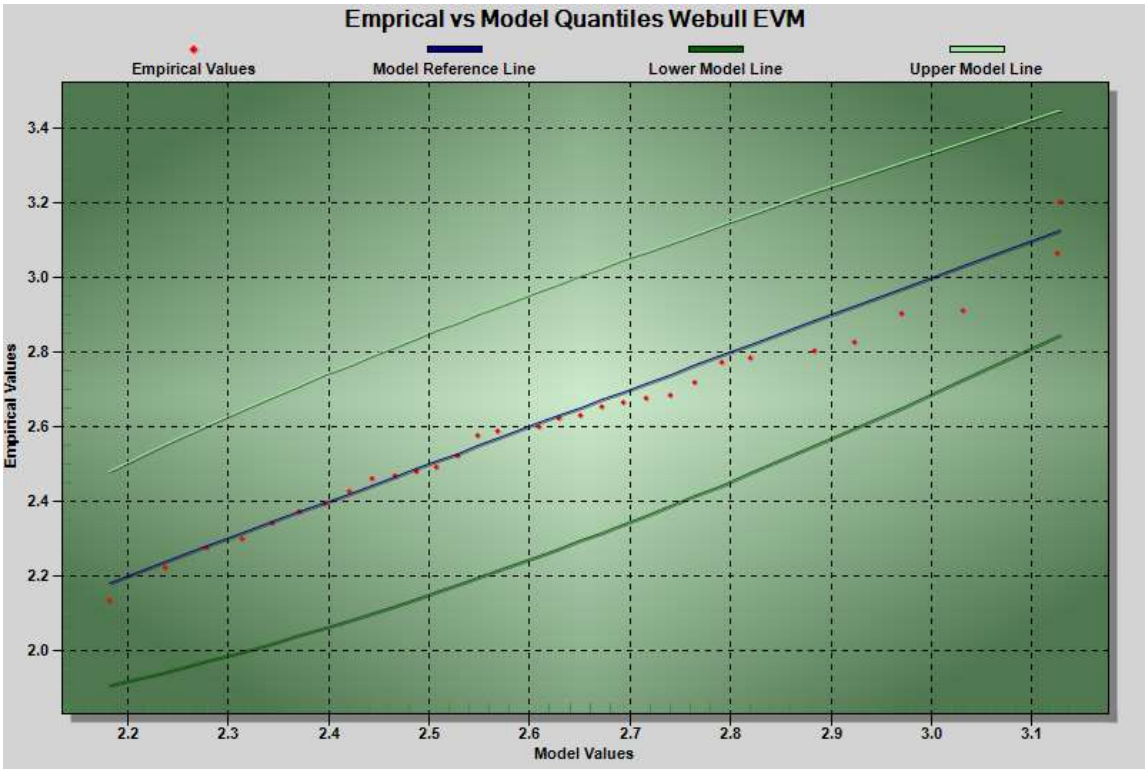

Figure 15 Weibull extreme value model (line) fit to annual maximum water levels (red dots), with 95% confidence interval (green lines) for Pictou.

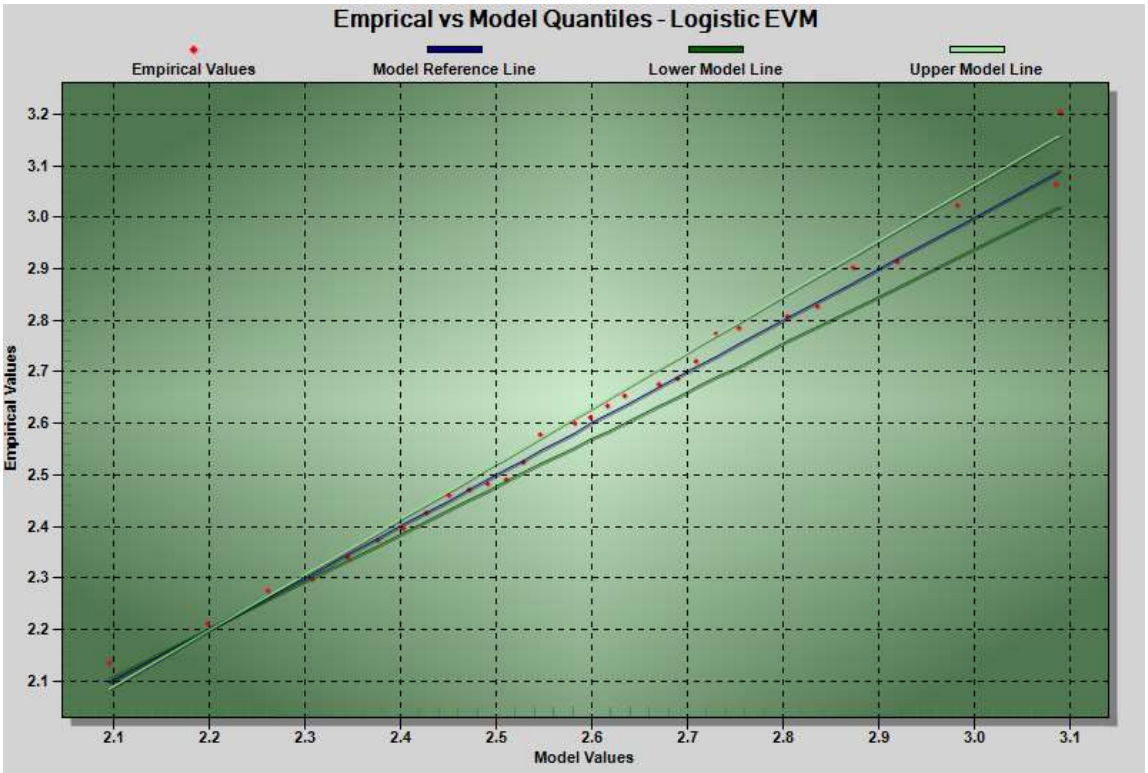

Figure 16 Logistic extreme value model (line) fit to annual maximum water levels (red dots), with 95% confidence interval (green lines) for Pictou.

Table 3 Extreme value models over all measure of how they fit the empirical data.

Model	RMS m of fit	Correlation fit
Gumbel	0.066	0.98
Webull	0.030	0.99
Logistic	0.026	0.99

The probability of occurrence of water levels can be predicted and compared between the extreme value models (EVM) (Fig. 17). Alternatively, the return period of when at least one occurrence of a given annual water level is expected can be calculated for the EVMs (Fig 18).

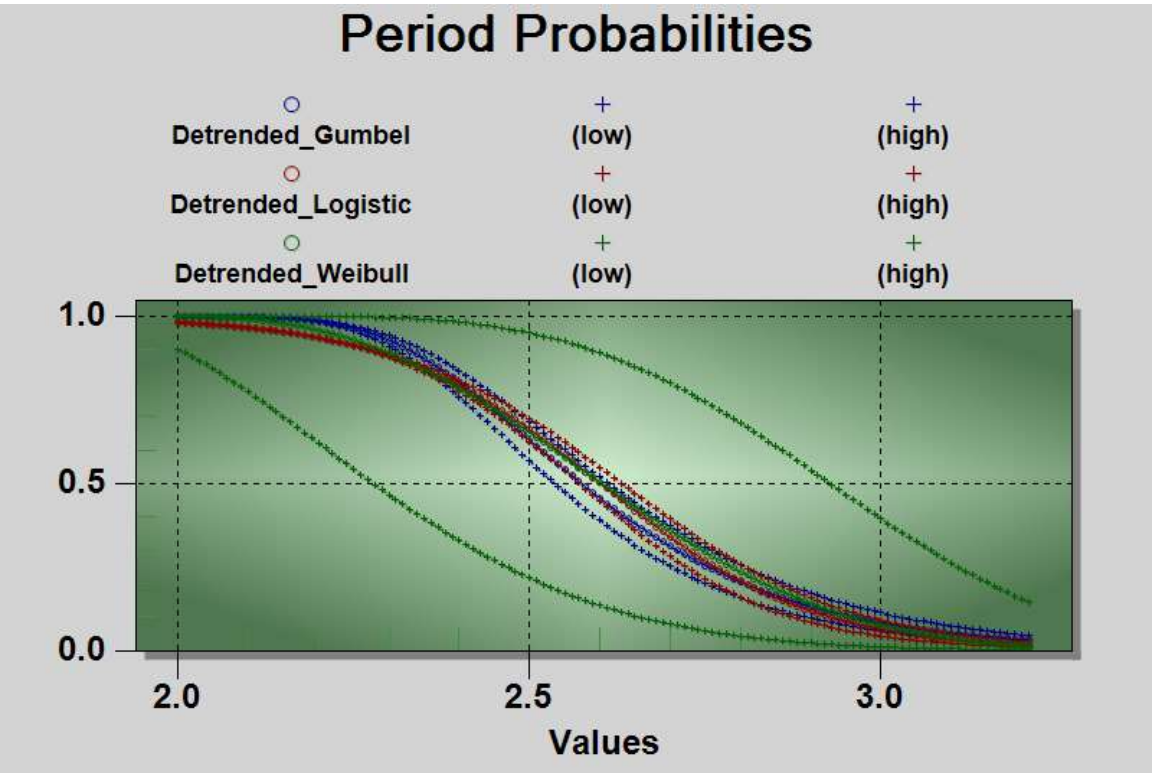

Figure 17 Comparison of EVM (95% confidence) probability of occurrence models (0-1) of a given water level (values) for Pictou.

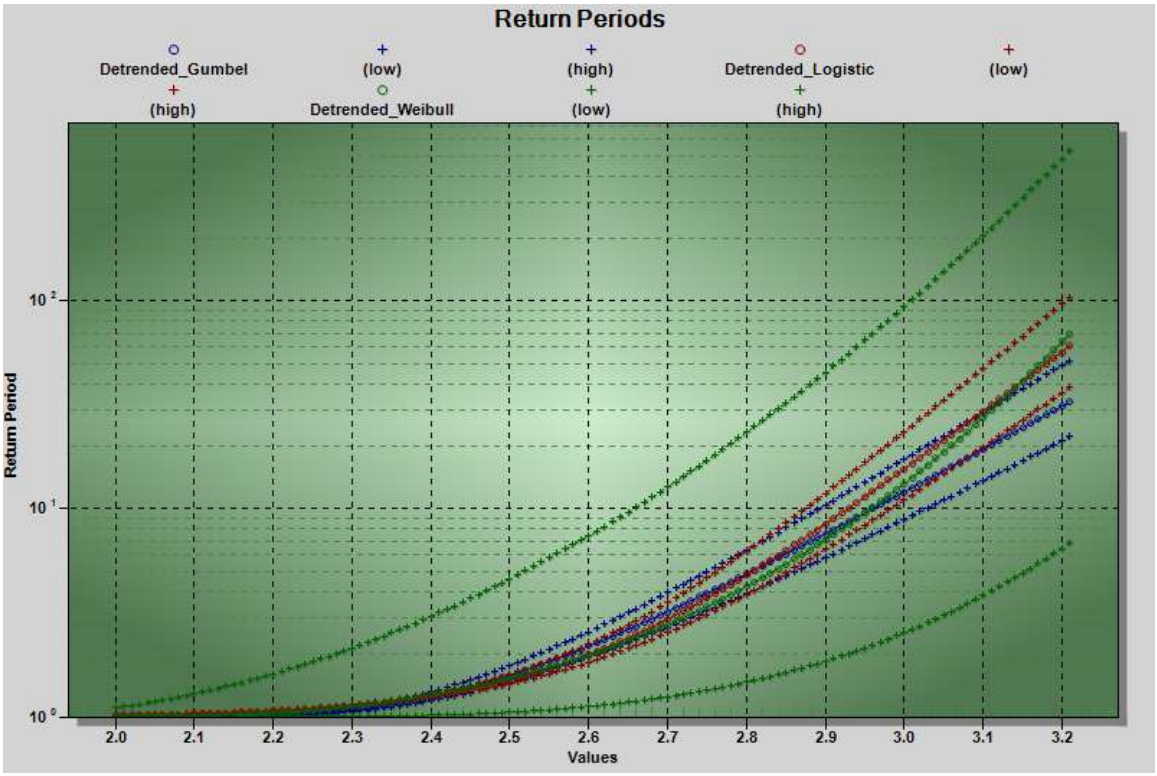

Figure 18 Comparison of EVM (with 95% confidence interval) return period in years (Log scale Y) of a given water level (values) for Pictou.

The return periods for the different EVMs are similar, with the Gumbel having the shortest return period for a water level of 3.2 m. The spread of the 95% confidence interval is similar between the Gumbel and Logistic EVM and overlap for the 3.2 m level (Fig. 18). In contrast, the spread of the 95% confidence interval for the Weibel EVM is much larger (Fig. 18). The Gumbel EVM was selected to model the tide gauge time series data and generate the statistics. The probability of occurrence (0-1) for the Gumbel model is calculated for a given water level (Fig. 19). The return periods for the Gumbel model are plotted using a Log scale (Fig. 20) and a normal scale (Fig.21).

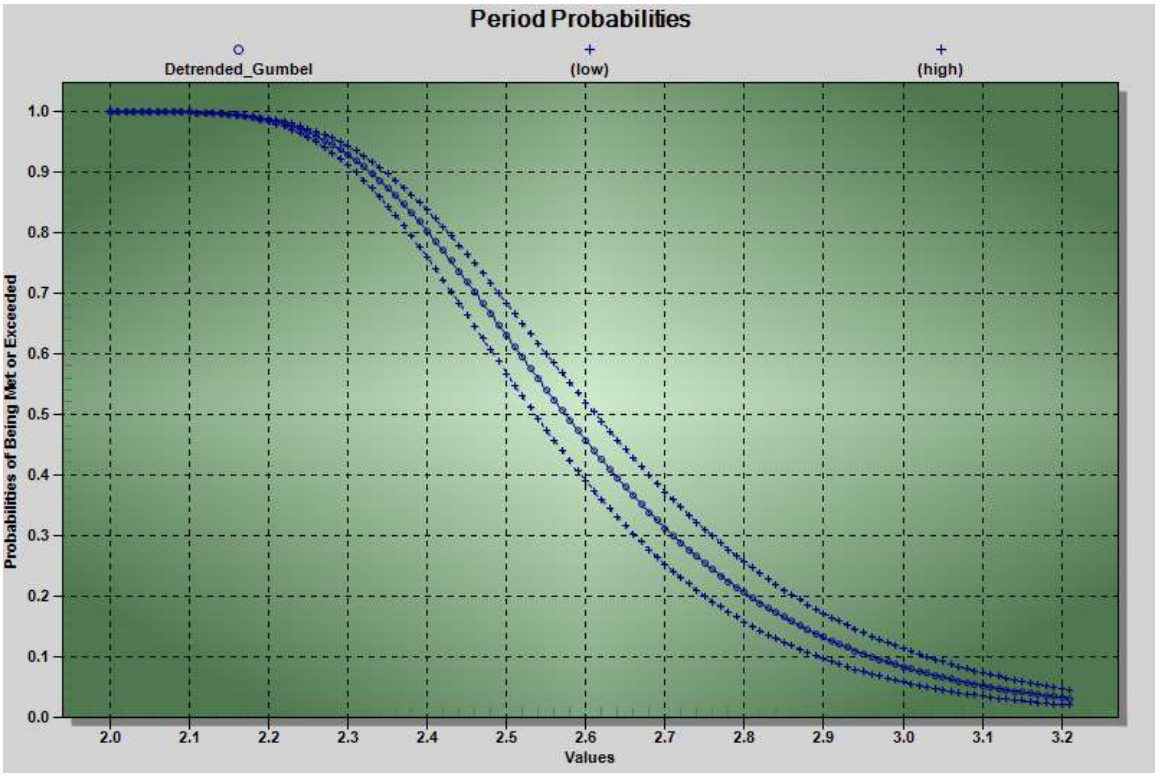

Figure 19 Gumbel model of the probability of occurrence (0-1) of a given water level (Values X-axis), with 95% confidence intervals for Pictou.

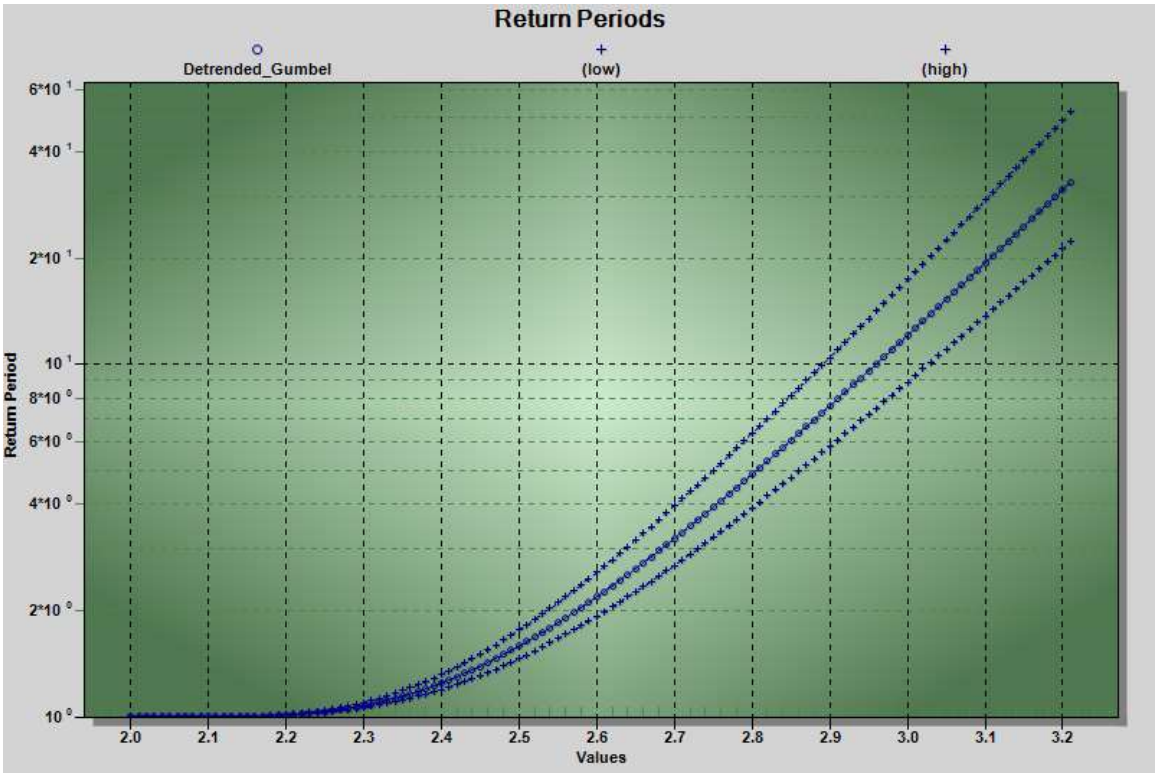

Figure 20 Return period in years (Log scale) of water level (Value) for Pictou, in this case the 3.2 m event will return in ~32 years.

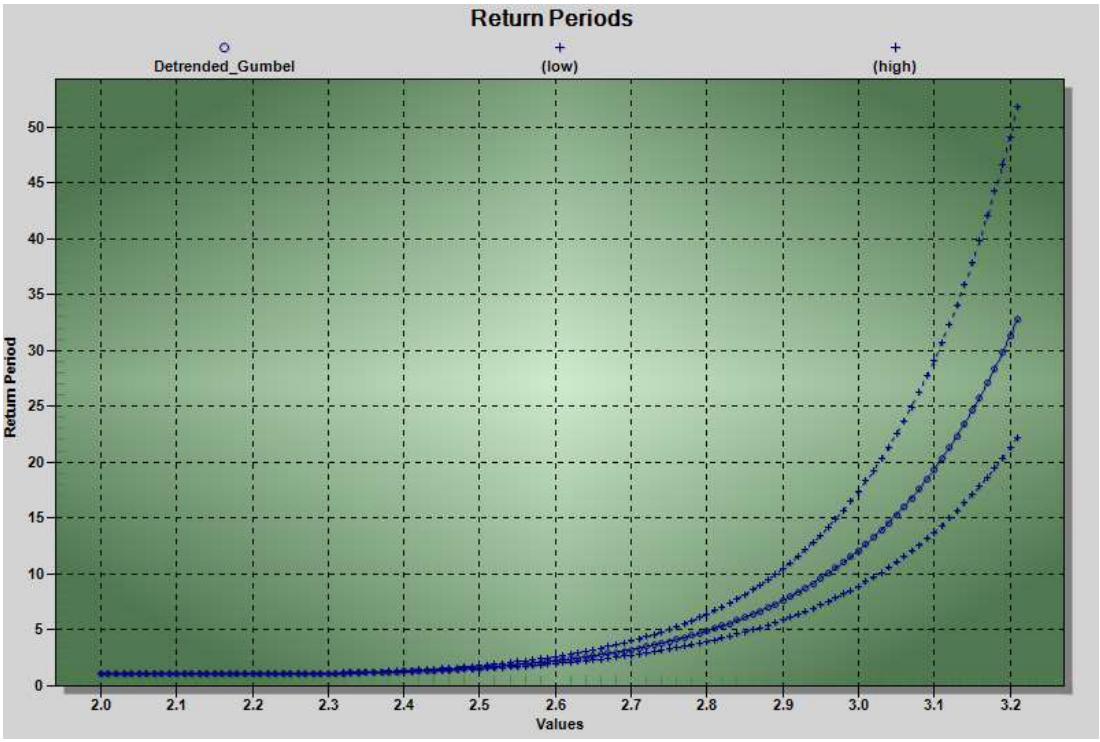

Figure 21 Return period in years (Normal scale) of water level (Value) for Pictou, in this case the 3.2 m event will return in ~32 years.

The projected relative sea-level rise in the future can be implemented using the EVM to calculate the statistics for the water level return periods. Three RSL rates were used when calculating the probabilities of occurrence and return periods (32 current rate, 73 IPCC based, 146 Rhamstorf based cm/century). The cumulative probability of a given water level occurring (3.2 m CD, the maximum level on Dec 1993) and the expected number of occurrences is plotted using the three different RSL values and termed the "Design Risk" (Fig. 22). In addition to plotting the cumulative probabilities that a given water level will occur over time, the design risk plot also calculates the expected number of occurrences which is denoted with a vertical line when this value equals 1 and is usually associated with a probability of 65%, known as the average probability (Fig. 22). The date can be read off the design risk plot indicating when this probability will be reached and at least one occurrence of that water level is expected by that date (Fig. 22). The software produces graphs as well as text files that can be used to analyze and plot the data in other software (Figs. 23, 24).

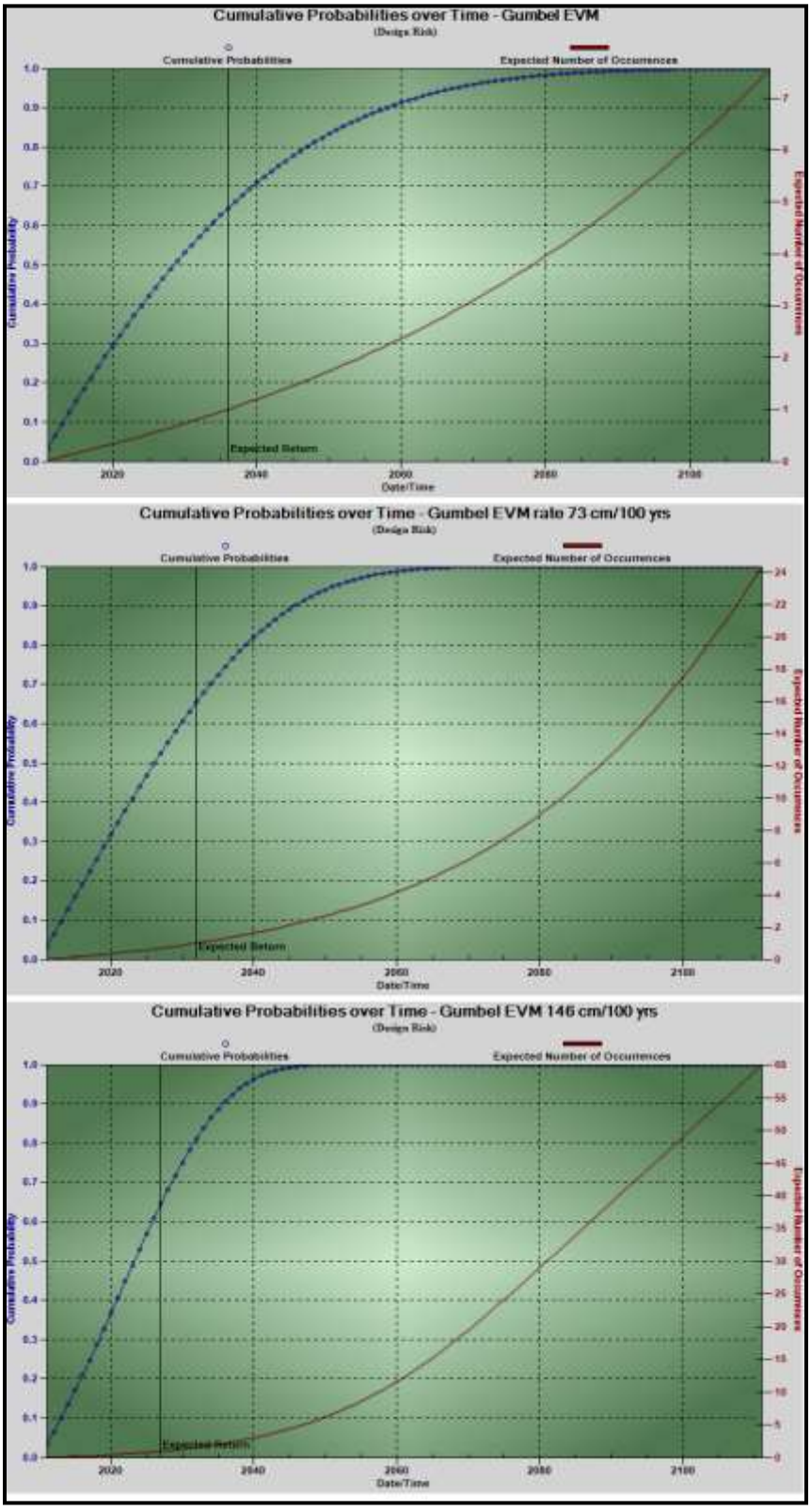

Figure 22 Design risk curves of 3.2 m CD water level with relative sea-level rise rates of 32 cm/100 years expect by 2036 (top), 73 cm/100 years expect by 2032 (middle), 146 cm/100 years expect by 2027 (bottom). Note the right Y-axis changes scale in the charts.

The effect of the different RSL rates on the probability of occurrence and the number of occurrences by a certain year can be seen on Figures 23, 24.

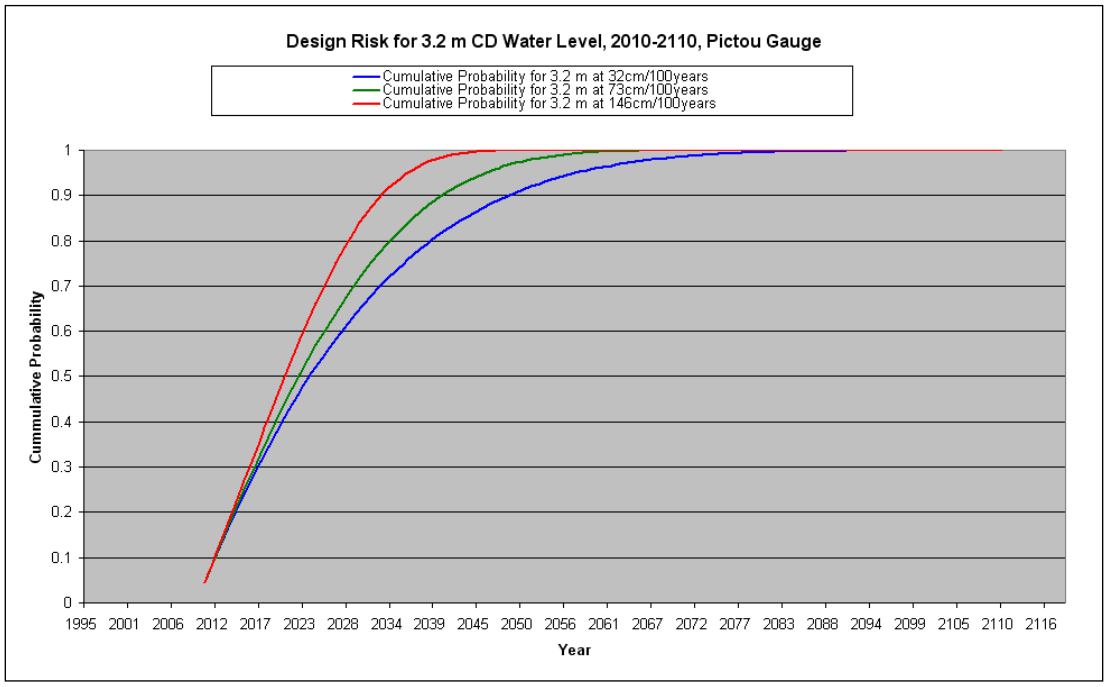

Figure 23 Combined cumulative probabilities of water level 3.2 m CD occurring at different relative sea-level rise rates for Pictou.

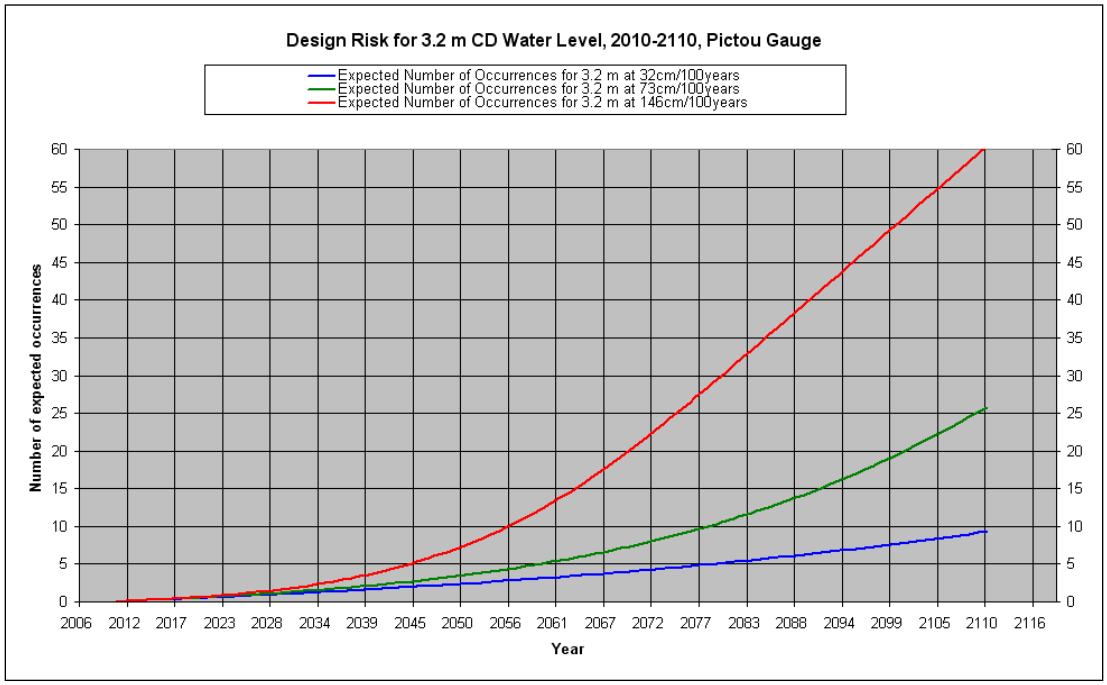

Figure 24 Combined expected number of occurrences of water level 3.2 m CD under different relative sea-level rise conditions for Pictou.

Planners are often interested in knowing “What is the 100 year flood level”? Now with climate change to consider for longer term projects one must consider asking the same question under a certain relative sea-level rise condition. One can fix the probability to a set value such as 99.5% and plot when a given water level is expected to occur. This is known as the “Design Level” and plots water level versus year for a given probability of occurrence. Thus one can be conservative and determine the water level and return period for a 10 % probability of occurrence or can accept more risk and state a 99.5% probability. Variable RSL rates can be used when calculating the design level plots as well. The RSL rates of 32 cm/100 years (current observed rate), 73 cm/100 years (IPCC AR4 highest rate A1FI), and 146 cm/100 years based on thermal expansion of the ocean were used in constructing the graphs (Fig. 25). On the top graph under present RSL conditions, the 100 year flood level at 99% probability is ~3.25 m, however as RSL increases to 74 cm/century this level increases to ~3.30 m and if RSL increases to 146 cm/century it will be ~4.0 m (Fig. 25).

Benchmark storm water levels from tide gauge records were used for study sites in the Town and District of Yarmouth, the District of Lunenburg and the Oxford-Port Howe area (Table 2). However, there is no long term tide gauge record available from CHS in the Upper Bay of Fundy, so calculating the probability of high-water level return periods for the Chignecto Isthmus or Minas Basin is difficult. The famous Saxby Gale of 1869 produced a storm surge that occurred at a large high tide and overtopped the dykes in the Upper Bay of Fundy, resulting in extensive flooding and the loss of property and life. The storm surge was estimated to be 2 m that occurred on a perigean spring tide. The actual water level of the Saxby Gale is not accurately known, so we have used the predicted highest tide plus storm surge based on the closest harbours within the Chignecto Isthmus and Minas Basin study areas (Table 2). The closest tide gauge with a long time series record is at Saint John, New Brunswick which has a very different tidal range

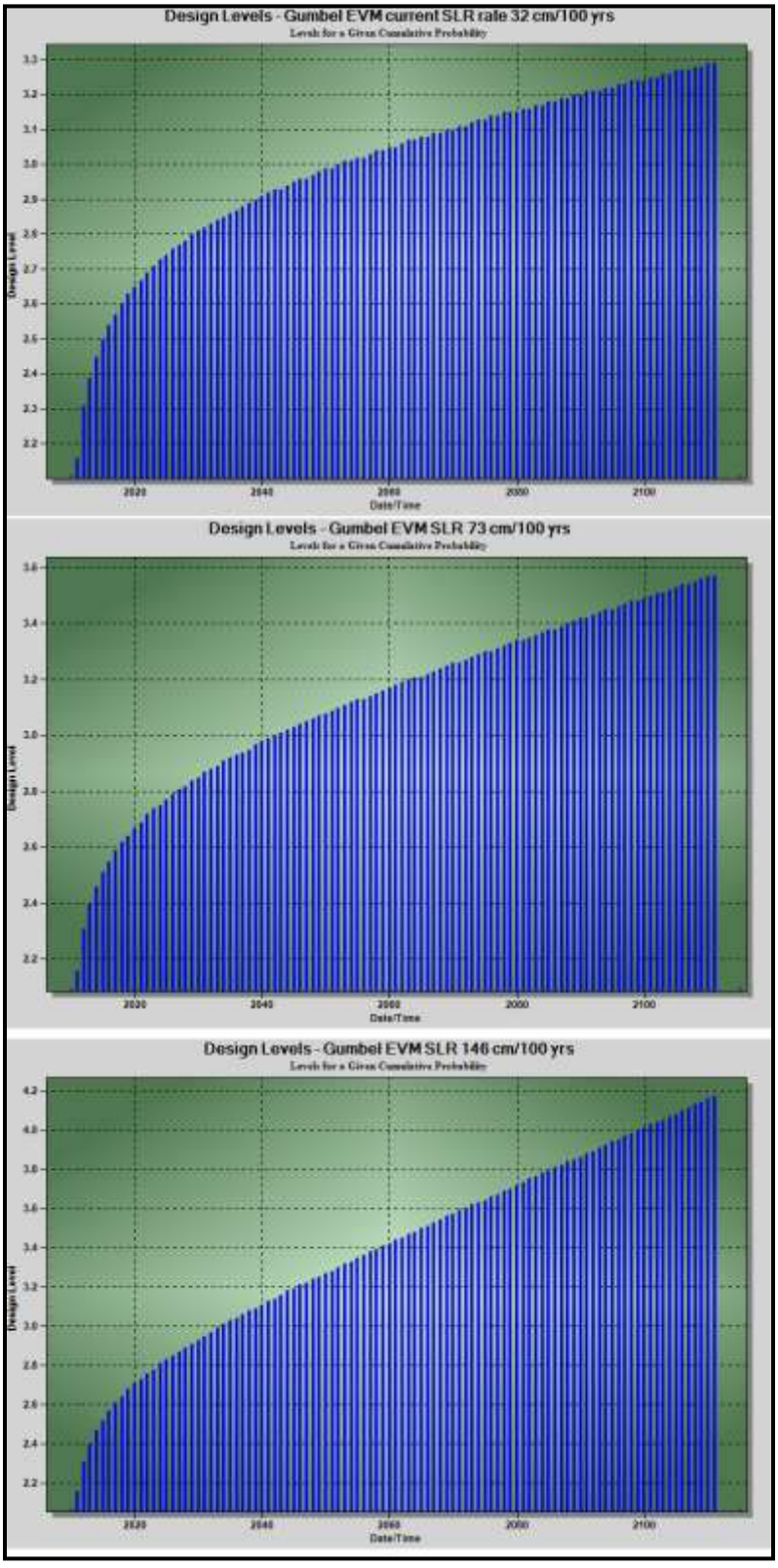

Figure 25 Design level plots (water level on Y-axis and year on X-axis) with different relative sea-level rise conditions. Top 32 cm/100 years, middle 73 cm/100 years, and lower 146 cm/100 years for Pictou. The probability of occurrence of the water levels is 99.5%.

than in the Upper Bay. Storm surge models have been developed for the region and are used for forecasting by Environment Canada. A storm surge model has been also used to hindcast surges using 40 years of wind field data. The results of this model were used to calculate extreme value models for water levels around the region (Bernier 2005; Bernier and Thompson 2006). Daigle (2011) used the results of this analysis to predict the 100 year flood level for Sackville, NB in 2000, 2055, and 2100. These return periods were used for the study sites within the Upper Bay of Fundy where there are no tide gauge records. With either of these methods (modelled hind casts or tide gauge record analysis), the historic Saxby Gale event is not taken into account, and with extreme value models and estimating probabilities, the inclusion of rare extreme events influences the statistics significantly. Thus, the return periods for these study sites should be used with extreme caution.

3. Results

Lidar processing techniques have changed over the years and the data used in this study range from 2003 to 2009 in collection dates. In some locations the study site is comprised of a mosaic of lidar data collected on different dates (Table 1). For example, the lidar processing and classification for the 2003 data covering Kings County (Wolfville) of the Minas Basin study site was carried out by the data provider, Terra Remote Sensing, under contract to AGRG. All other lidar data used for this ACAS study was acquired by AGRG and was generally processed using the same procedures.

The flood inundation maps were constructed from the hydraulically corrected lidar DEMs at 10 cm increments and delivered as GIS layers. This allows planners and other officials to access flood inundation maps for any number of levels as new sea-level rise predictions are made

available in the future. As a result of the flooding at 10 cm increments, animations were constructed for each of the communities and presented at the technology transfer meetings. Two types of animations were built that depicted water levels rising over an aerial photograph or satellite image or possibly the lidar surface model colour shaded relief map in a planimetric view (standard top down map view) or from a perspective view that looks obliquely on the terrain where the photo is draped over the DSM. The water level simulations ranged from 0 m (approximate mean sea-level) to a maximum of 5 m for Oxford-Port Howe and District of Lunenburg areas, and 0-10 m in the Town and District of Yarmouth area and up to 12 m in the Chignecto Isthmus and Minas Basin study sites in the upper Bay of Fundy. The GIS flood inundation maps can be used to examine what is vulnerable to flooding and erosion. The approach we have taken is to use the past benchmark storm events to simulate coastal flooding. In addition to these flood inundation layers we have then projected SLR into the future under different scenarios to show the effects of the benchmark storm 2110.

In terms of the risk of a particular storm event achieving a high water level, we present an assessment of the probability of that water level occurring or the return period in years of a given water level re-occurring. Two approaches have been used in the past for estimating the risk of a given water level occurring; one is to calculate the return period of a given storm surge (ie. Residual water level = observed water level – predicted water level) of occurring, and the second is to calculate the return period of the total water level occurring (surge and tide combined). Other variations on the approaches used to estimate return periods involve analyzing model results or empirical data from tide gauges. In this study we have analyzed the tide gauge water level hourly time series records for the closest harbours within the ACAS study sites. The tide gauges used for the flood risk assessment for each of the communities are listed in Table 4.

Table 4 List of study site communities and tide gauge sites and date of water level records used to calculate return periods of high water levels.

Flood Risk Community Site	Closest Tide Gauge	Years of data
District of Lunenburg	Halifax	1919-2010
Oxford-Port Howe	Pictou	1965-1996 * no longer in operation
Town and District of Yarmouth	Yarmouth	1965-2010
Chignecto Isthmus	Saint John, NB	1941-2010
Minas Basin	Saint John, NB	1941-2010

The results of each ACAS community study site will be presented in the following order: 1) lidar processing and DEM validation, 2) flood inundation mapping, and 3) flood risk in terms of return periods of benchmark storms under current and projected SLR conditions in the future.

3.1.District of Lunenburg

3.1.1. Lidar acquisition, processing and DEM validation of District of Lunenburg

The 2009 lidar acquisition along the coast of Lunenburg County used the Halifax GPS reference station that makes up part of the Canadian Active Control Network. The final lidar surface models are a mosaic of data from 2005 through to 2009 (Table 1) and required a significant amount of processing to ensure the data were all aligned within acceptable tolerances.

The merged lidar surface models were then compared to the validation GPS data that were acquired on July 13th and Dec. 22, 2010. A total of 7,383 GPS check points were used to validate the lidar DEM. The DEM elevation was subtracted from the GPS elevation to calculate the residual or delta Z values. The GPS check points are colour coded by the delta Z value (Fig. 26) and the overall statistics indicate a mean delta Z of -0.01 m and a standard deviation of 0.06 m (Fig. 27).

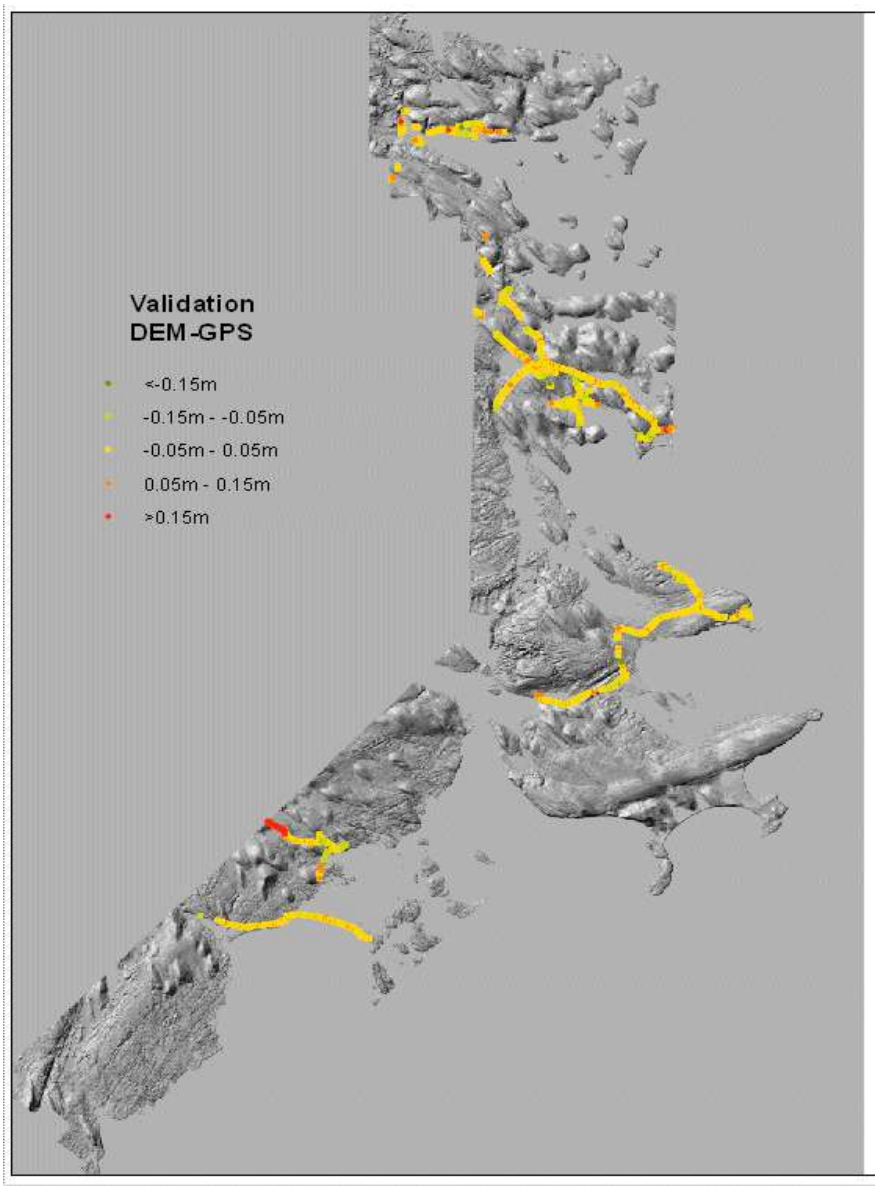

Figure 26 District of Lunenburg lidar DEM validation. GPS check points colour coded by the difference in elevation, DZ, compared to the lidar DEM (DEM-GPS).

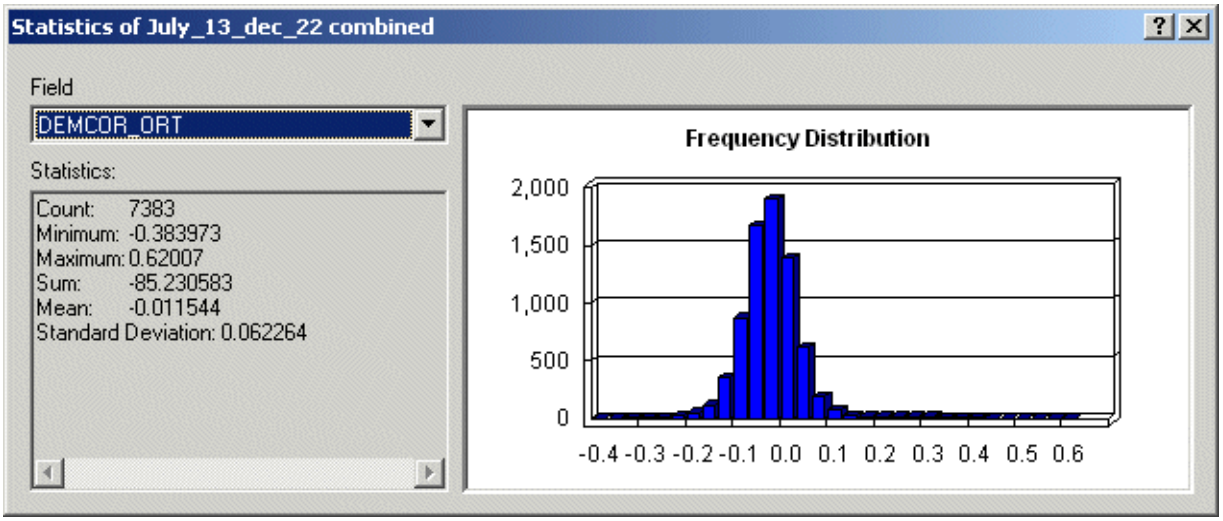

Figure 27 Statistics of the difference in elevation between the lidar DEM and GPS check points. The mean delta Z is -0.01 m with a 0.06 m standard deviation.

3.1.2. Flood Inundation Maps for the District of Lunenburg

For each study site, flood inundation GIS layers were constructed that connected the still water elevation of the ocean with the land based on the lidar DEM surface models. The lidar DEMs have been edited to ensure hydraulic connectivity for culverts and other structures. The NSTDB road network identifies culverts where the road crosses a mapped stream; however there are many more culverts for ephemeral streams. We have interpreted the terrain and land cover and placed culverts across roads that are not mapped, however we know there are many more culverts in use than have been represented in this study. The flood inundation layers have been used to drape over the lidar DSM in order to animate the rise in sea-level from different map and perspective views.

The extent of flooding from a storm similar to Hurricane Juan that occurred in Sept. 2003 was used as the benchmark storm for the District of Lunenburg case study site. The water level observed in Halifax was used for present day flooding and in 100 years under a projected sea-level rise accelerated by climate change (Fig. 28). This perspective view, looking east, clearly shows the coastal areas that are inundated at that level. The colour shaded relief of the DSM is

draped over the DSM, with flood layers derived from the DEM (Fig. 28). The water level observed at Halifax during Hurricane Juan was 2.1 m CGVD28. In figure 28, this elevation (2.1 m) has been used plus an estimated relative SLR of 1.46 m over the next 100 years. The area inundated by such a water level (2.1 + 1.46 = 3.56 m CGVD28) is denoted in the blue colour on figure 28. A significant amount of the town of Lunenburg waterfront is inundated as well the low lying area adjacent to the harbour. As can be observed in figure 28, if a similar storm to hurricane Juan were to occur under the projected RSL conditions in 100 years, the roads and several buildings and properties are affected near the oval track on the outskirts of the urban development. As mentioned, flood layers in 10 cm increments were constructed and are available for each study site to allow planners access to the information as SLR projections change in the future.

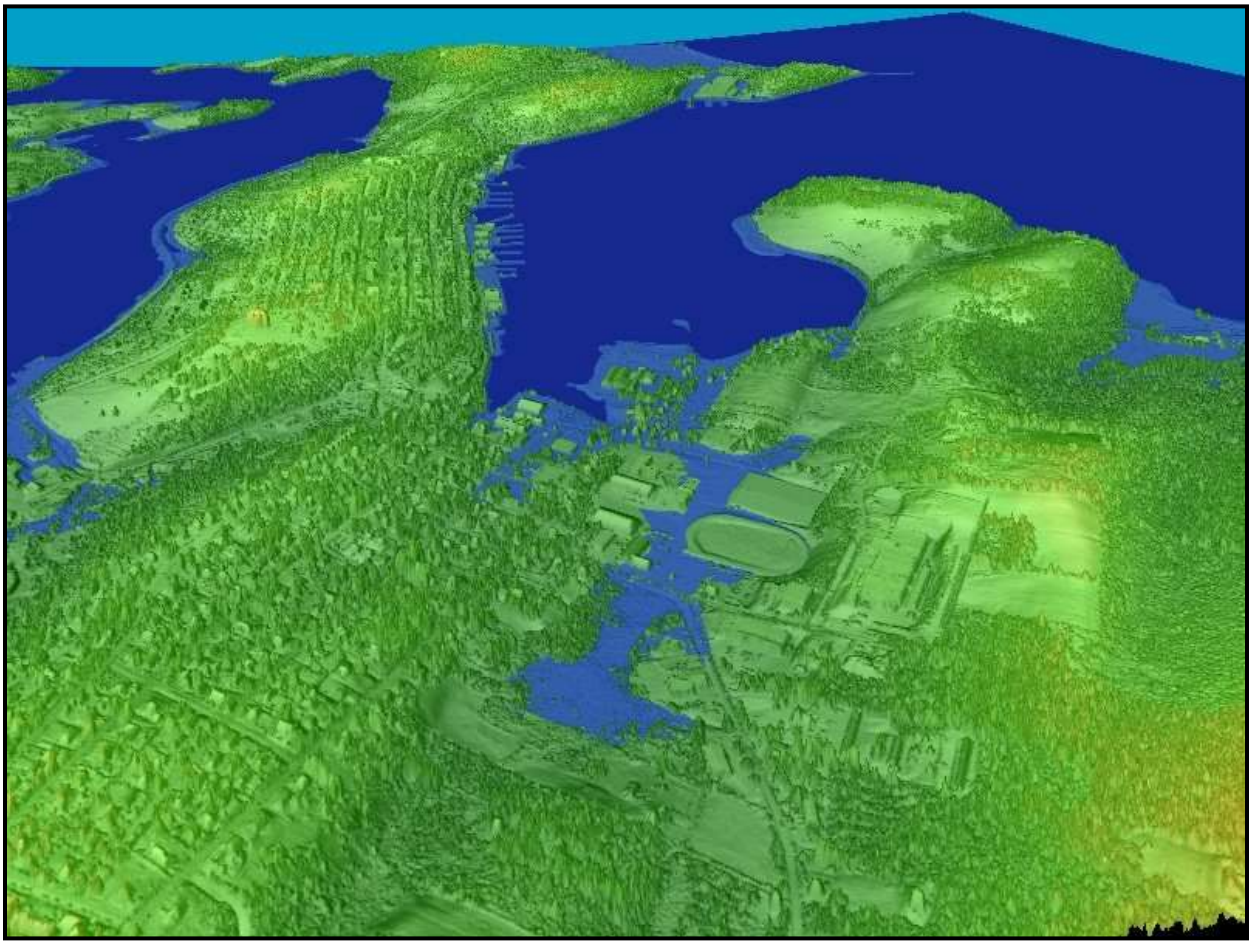

Figure 28 Perspective view of Lunenburg with a sea-level representing Hurricane Juan in the year 2110 with a projected sea-level rise from climate change and crustal subsidence.

The flood layers were also used to construct a series of static maps that represent flood risk from different sea-level rise conditions under different climate change models and projections. The sea-level rise projections are a combination of global mean sea-level rise and crustal subsidence. The flood risk maps are comprised of a past benchmark storm inundation level and that same storm in 100 years under two different sea-level rise estimates. The IPCC A1FI scenario base projection (with subsidence = 73 cm/century), and the Rhamstorf (2007) who related water level to atmospheric temperature (with subsidence = 146 cm/century) (Fig. 29).

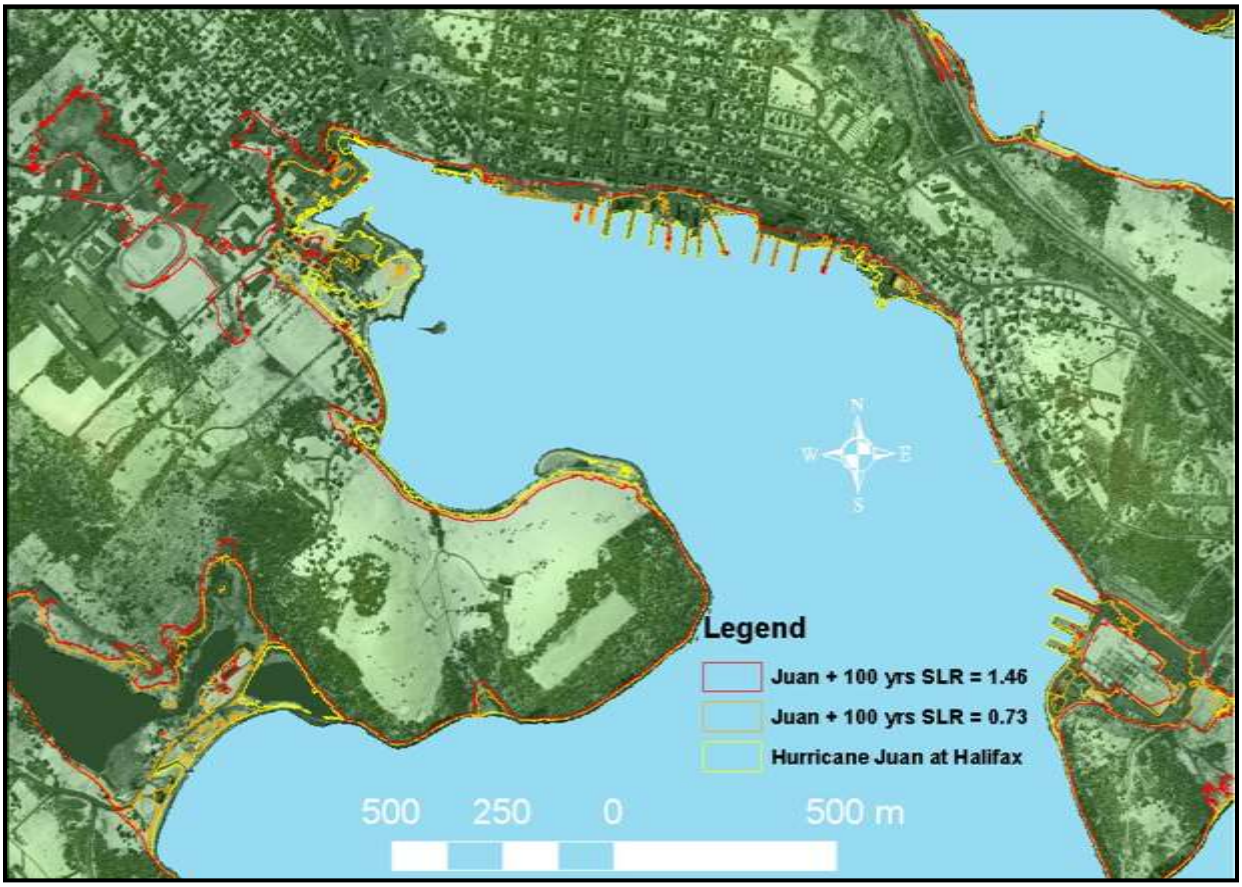

Figure 29 Flood risk from storm surge map of Lunenburg. Lidar intensity map as the background with the water level of Hurricane Juan in Halifax, and that same level in 2110 under different sea-level rise (SLR) rates.

Several areas within the District of Lunenburg show up as being vulnerable to flooding from water levels associated with the storm surge equivalent to what Halifax experienced during Hurricane Juan (Fig. 29). Any lands adjacent to inlets or salt marsh locations are vulnerable to such events. Also some of the thin barrier beaches such as Crescent beach that connect the mainland to seaward land masses are vulnerable to such events.

3.1.3. Flood Risk – Water level return periods and annual probabilities for the District of Lunenburg

Mean sea level has been rising in Halifax at a rate of 32 cm/century and the annual maximum water level has been increasing at a rate of 34 cm/century based on the best fit linear trend line of the tide gauge records (Fig. 30). A Gumbel extreme value model was fitted to the distribution of the annual maximum water levels producing a correlation of 0.98 and a root mean square error (RMS) of 5 cm. Once the model parameters were constructed, the model was used to estimate the return period of any given water level or the probability of a water level occurring. The design level graph was calculated for a probability of occurrence of 95% to determine what water levels are expected over time (Fig. 31). The design level graph provides answers to such questions as “what is the 100 year water level”. Different sea-level rise rates were imposed on the model to determine the return period statistics of different water levels (Fig. 31).

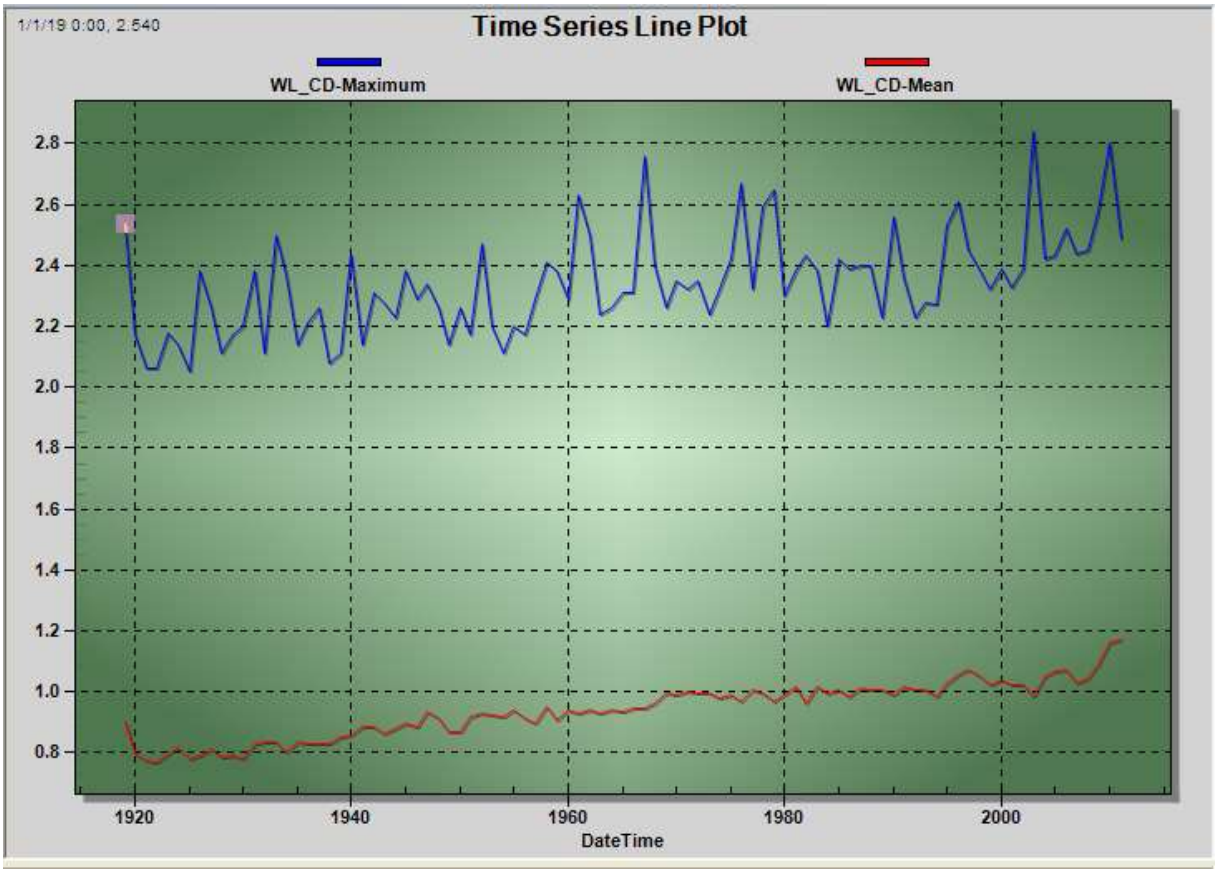

Figure 30 Halifax annual mean (red) and annual maximum (blue) water levels above chart datum for 1919 to 2010.

The one hundred year water level under current sea-level rise conditions is 3.03 m CD and increases to 3.32 if RSL rises at a rate of 0.73 m/century (IPCC AR4) or further increases to 3.94 m CD if RSL rises at a rate of 1.46 m/century (Rhamstorf) (Fig. 31). The expected water levels to be experienced over time at different RSL rates (current 32 cm/century, IPCC 73 cm/century and Rhamstorf 146 cm/century) for the Halifax extreme value Gumbel model are presented in Appendix 7.

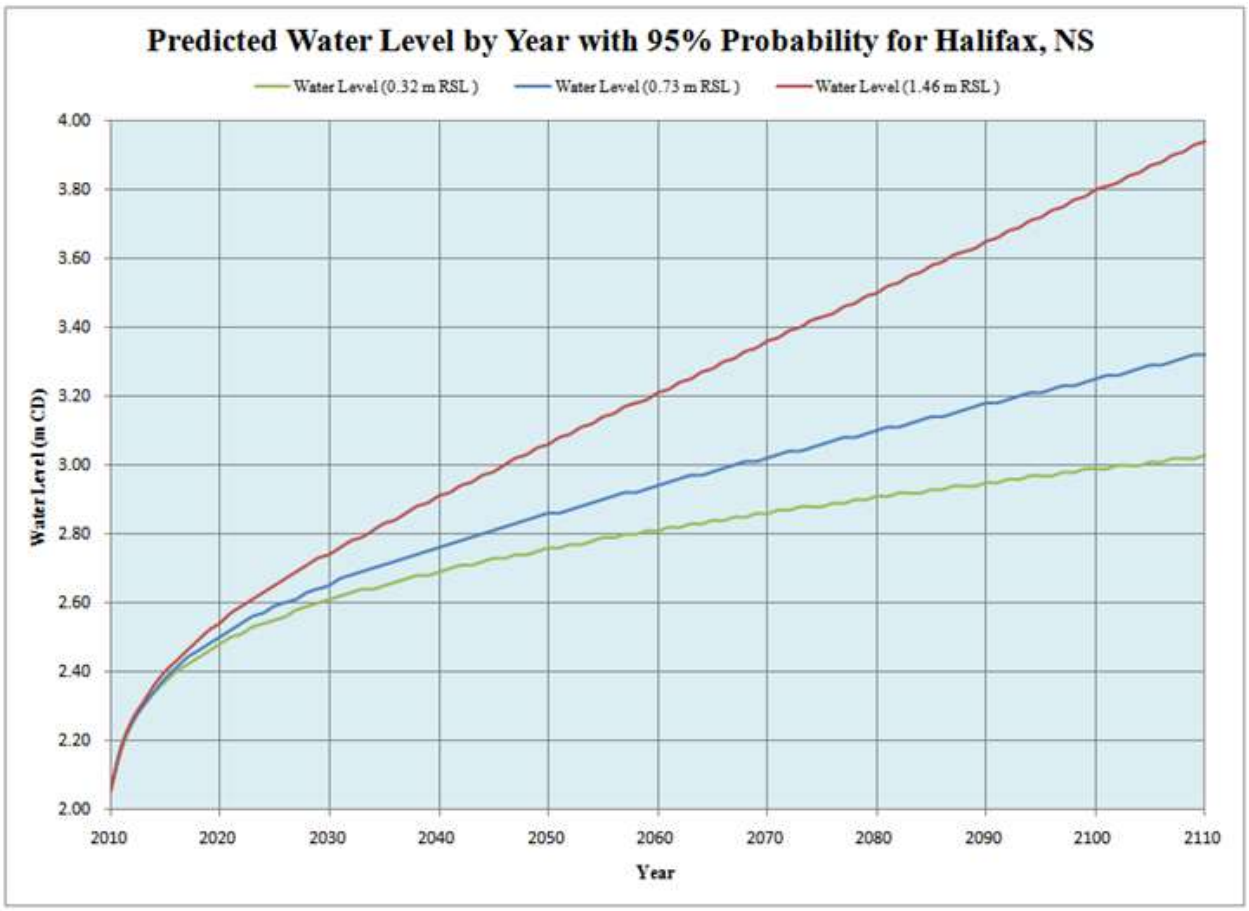

Figure 31 Design level graph for Halifax. Expected water levels to be reached over time with different rates of relative sea-level (RSL) rise (m/century), green – current rate 0.32, blue – 0.73 IPCC, red – 1.46 Rhamstorf.

The one hundred year return period water levels under different RSL conditions have been converted into the CGVD28 vertical datum and used in figure 32. The 100 year flood level under current RSL conditions is 2.2 m which is 10 cm below previous high water level maximum observed during Hurricane Juan in Halifax in Sept. of 2003. If RSL increases to a rate of 0.73 m/century the 100 year water level increases to 2.5 m CGVD28 which further inundates areas (Fig. 32). If RSL increases to a rate of 1.46 m/century the 100 year water level increases to 3.1 m CGVD28 which further inundates areas (Fig. 32).

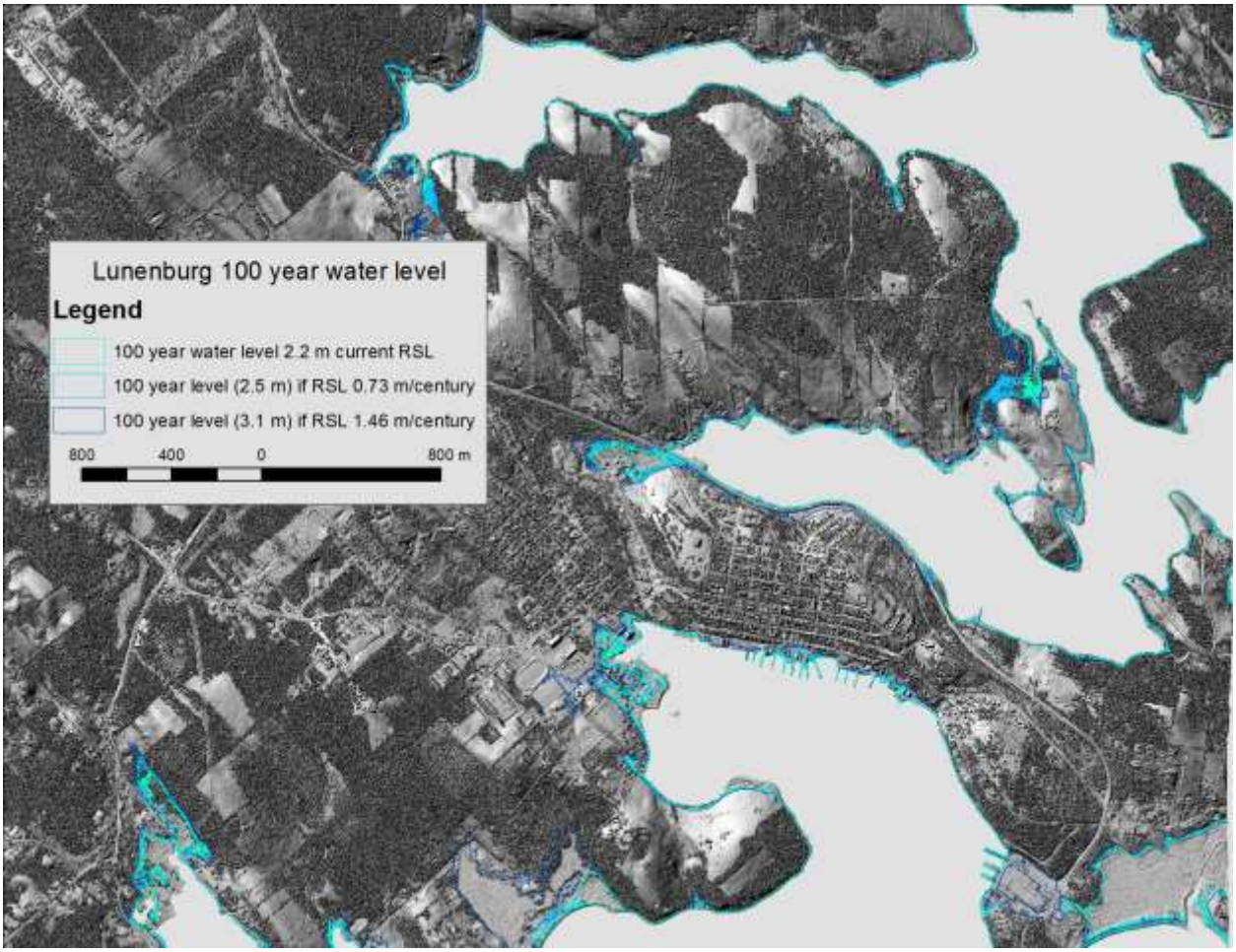

Figure 32 Shaded relief lidar DSM of Lunenburg area with 100 year water level under current RSL conditions and possible RSL conditions with climate change.

3.2.Oxford-Port Howe

3.2.1. Lidar acquisition, processing and DEM validation of the Oxford-Port Howe area

The 2009 lidar acquisition of the Oxford-Port Howe study site was affected by poor weather conditions and it required three flights to finish the survey. The surveys which overlap the existing Oxford lidar DEM were flown with different configurations at different altitudes because of the variable cloud ceiling (Appendix 3). This resulted in problems with horizontal and vertical alignment between the surveys that required extra processing. The merged lidar surface models were compared to the validation GPS checkpoints that were acquired on Oct. 28, 29,

2009 and July 30, 2010 (Fig. 33). The GPS check points are colour coded by the delta Z value (Fig. 33). A total of 889 GPS check points were acquired in Oct. 2009 during the lidar acquisition with overall statistics indicate a mean delta Z of -0.10 m and a standard deviation of 0.13 m and 5801 GPS check points were acquired in July 2010 with overall statistics indicate a mean delta Z of -0.00 m and a standard deviation of 0.13 m (Fig. 34). The 2009 lidar datasets were merged with data covering the town of Oxford acquired by AGRG in May 2006 to form the final lidar surface models.

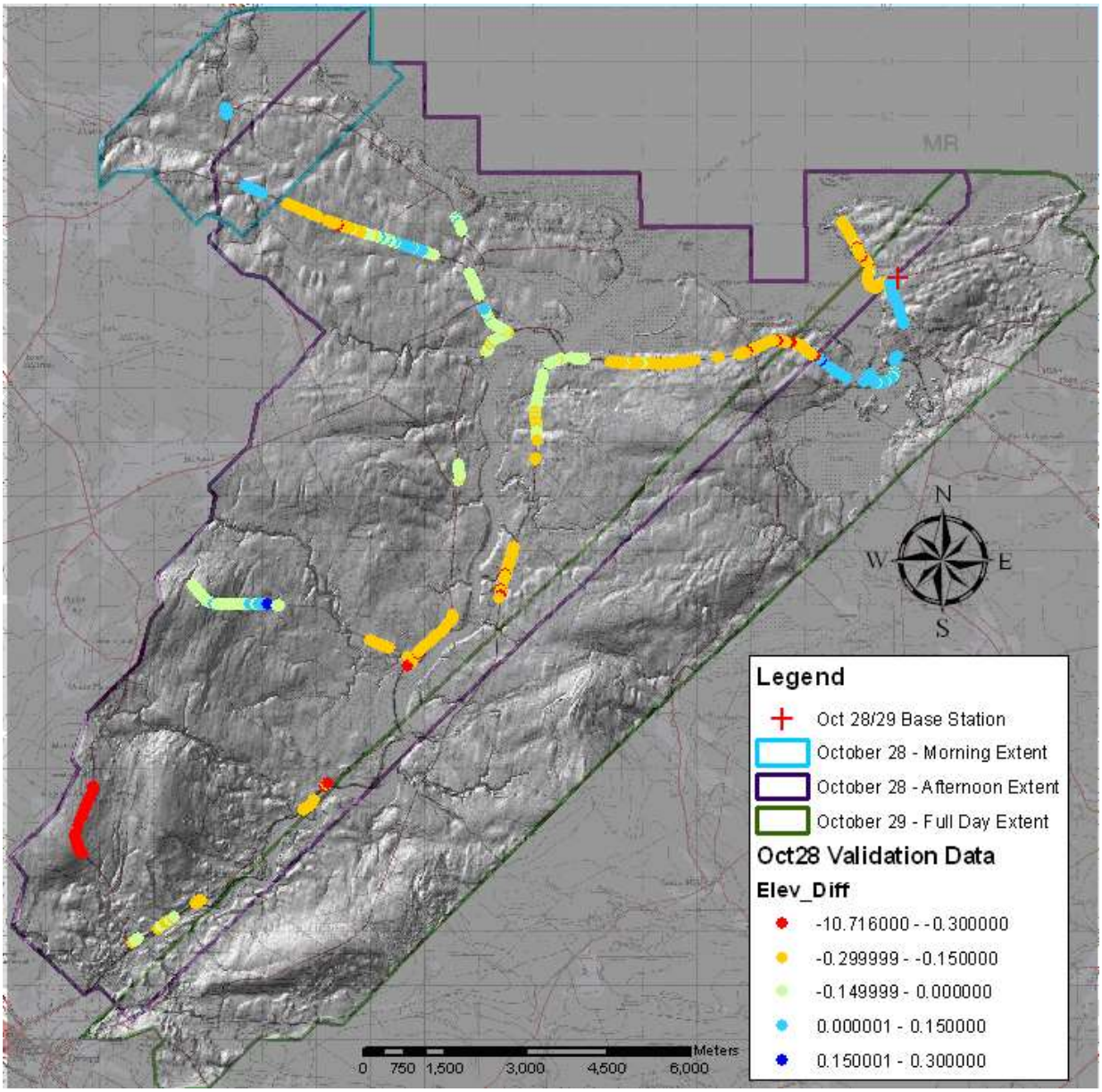

Figure 33 GPS checkpoint elevation differences (DZ) with the lidar DEM for the Oxford-Port Howe area. The GPS check points were collected Oct. 28, 29, 2009 for the river corridor and July 30, 2010 for the coastal area.

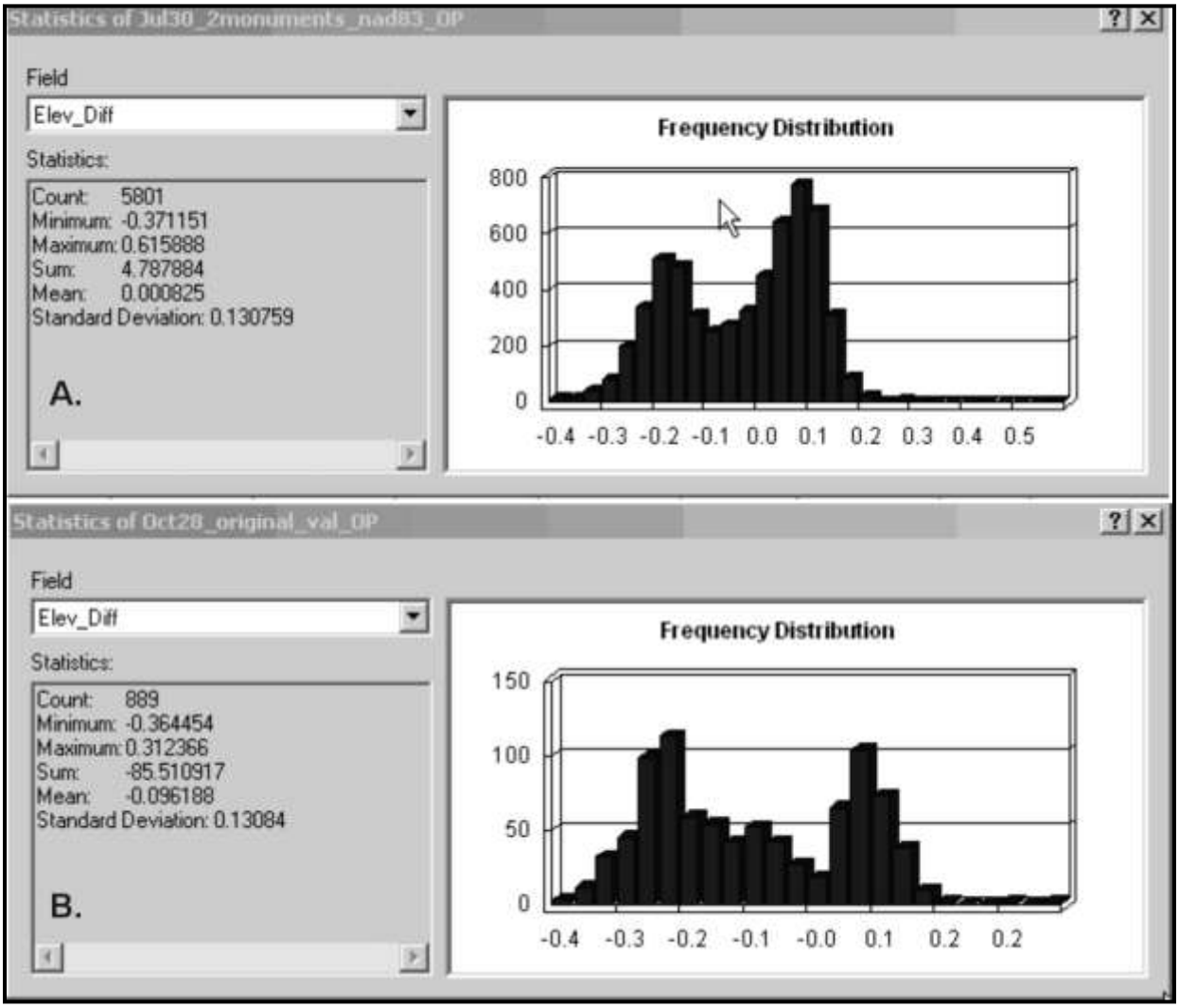

Figure 34 Histograms and statistics of the delta Z between the GPS points & lidar DEM. A) GPS data collected July 30, 2010, the mean difference is 0.00 m with a standard deviation of 0.13 m, B) GPS data collected Oct. 28, 2009, the mean difference is -0.10 m with a standard deviation of 0.13 m.

3.2.2. Flood Inundation Maps for the Oxford-Port Howe area

In the area of Oxford-Port Howe the benchmark storm occurred in Dec. of 1993 and reached a geodetic (CGVD28) elevation of 2.3 m based on the tide gauge that was still in operation at Pictou (Fig. 35). Unfortunately the tide gauge was removed in ca. 1996 and there is no active tide gauge for the north shore of Nova Scotia in the Northumberland Strait.

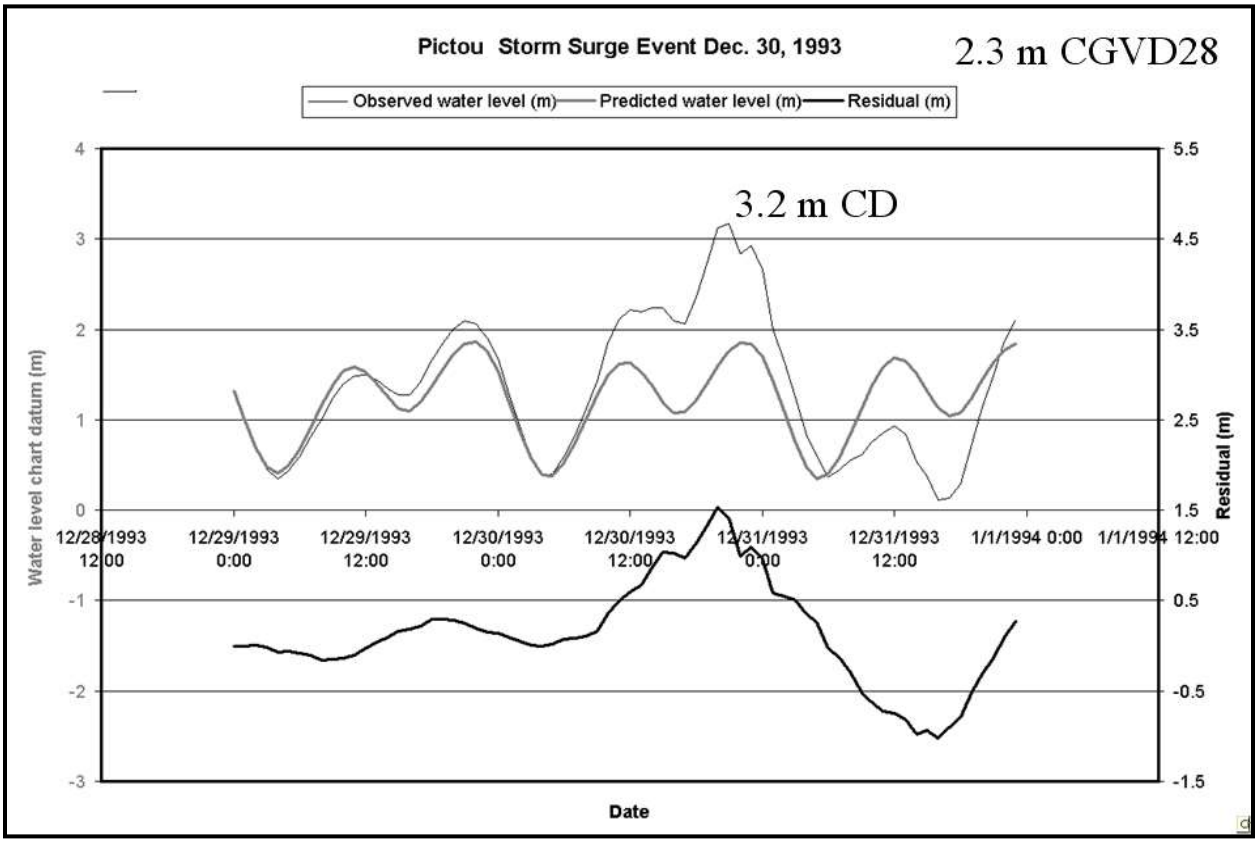

Figure 35 Pictou tide gauge for Dec. 30, 1993 storm surge of 1.5 m. The total water level reached 3.2 m chart datum which translates into 2.3 m CGVD28.

On Dec. 21, 2010 this region was hit by a classic winter Nor' Easter (predominant winds from the northeast) that caused a significant storm surge and associated coastal flooding and erosion (Fig. 36). The Shediac, NB tide gauge recorded a total water level of 2.4 m CGVD28 and a storm surge of at least 1.6 m (CHS, personal communications, Feb. 2011). The entire northern coasts of NS, NB and PEI were severally affected, especial those sections of coastline exposed to the direct impact of the northeast wind.

Figure 36 Waves impacting the coastline west of River Phillip along the Northumberland Strait on Dec. 21, 2010. Source of the photo is the Amherst Daily News.

Researchers from AGRG worked with officials from the Oxford NS Department of Natural Resources regional office to map the high water debris line and used RTK GPS to precisely survey the maximum water elevation of that storm. The total water elevation was estimated to be 2.6 m (CGVD28) based on several locations where wrack lines of debris left behind from the coastal flooding were measured. Coastal flood risk maps have been constructed at different water levels for the lidar coverage (2.4, 2.5, and 2.6 m) and compared, with good agreement, to the wrack lines measured in the field with GPS. An example of these maps shows the mouth of River Phillip with the water level at 0 m (approximately mean sea level) and at the estimated water level of the Dec. 21, 2010, 2.6 m (Fig. 37). Some debris was found as high as 4.5 m which was a result of waves impacting the coastline and projecting the debris landward.

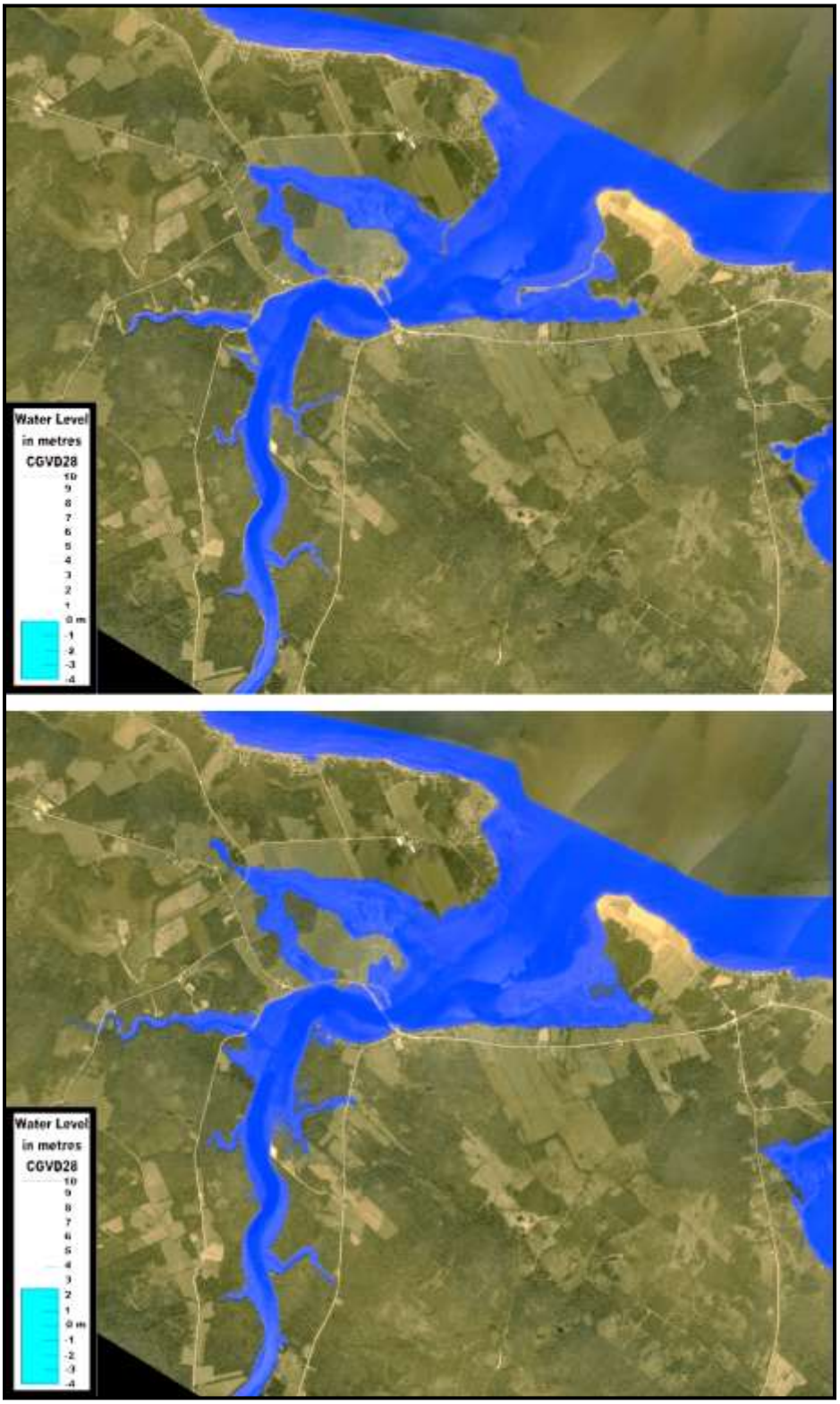

Figure 37 Airphoto (Aug. 2010) of the mouth of the River Phillip estuary with water levels (blue) derived from the lidar DEM. The top map represents a water level of 0 m and the lower map represents the Dec. 21, 2010 storm of 2.6 m CGVD28.

3.2.3. Flood Risk – Water level return periods and annual probabilities for the Oxford-Port Howe area

The Oxford-Port Howe study site on the Northumberland Strait utilized the Pictou tide gauge record that was active from 1965-1996. The Shediac, NB tide gauge was in operation from 1980-1993 and then re-established in 2003, unfortunately missing the significant storm surge of Jan. 21, 2000. The Charlottetown, PEI tide gauge on the opposite side of the strait has a record going back to 1911 with some missing data in the 1920's and a continuous record that started in 1938 to present. However, since it is on the south coast and the wind affects the storm surge water levels differently for the northern NS coast, it was not used. The Pictou record has a longer time series than Shediac and thus was used to estimate return periods of high water events. Mean sea level has been rising in Pictou at a rate of 28 cm/century and the annual maximum water level has been increasing at a rate of 56 cm/century based on the best fit linear trend line of the tide gauge records (Fig. 38).

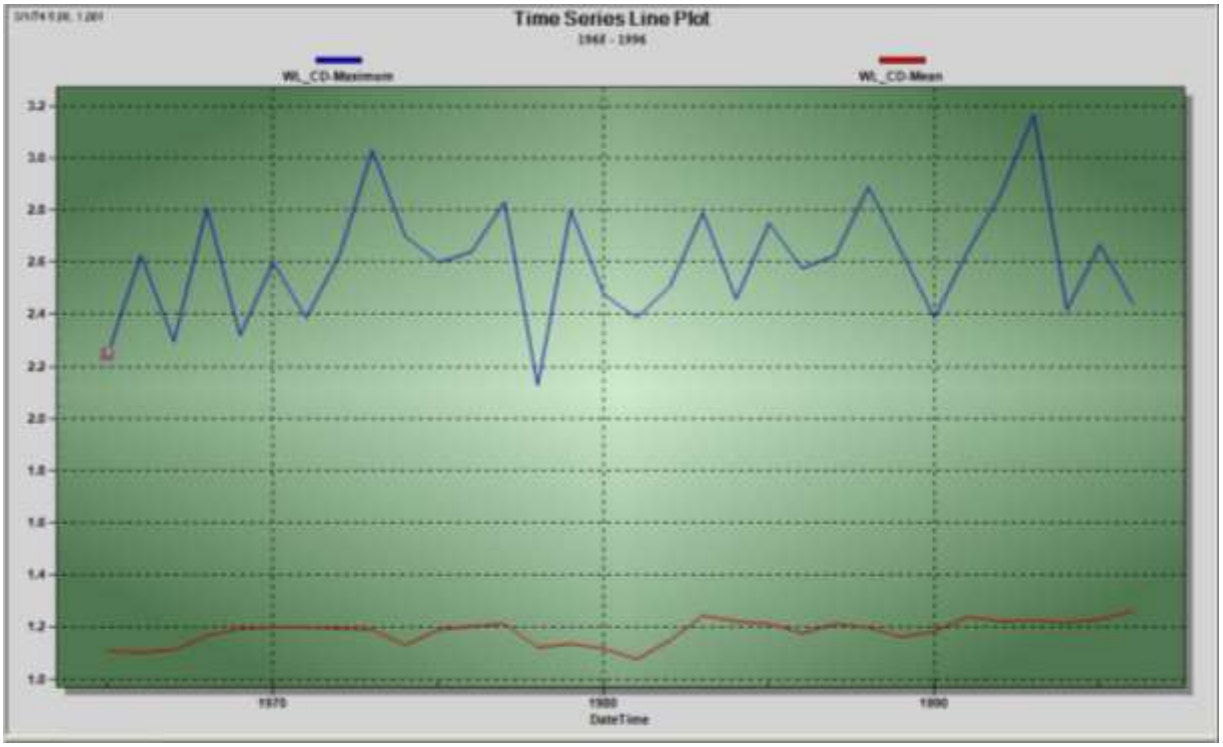

Figure 38 Pictou tide gauge record. Annual mean sea level (CD) from 1965-2010 (red) with annual maximum water levels (CD) (blue).

A Gumbel extreme value model was fitted to the distribution of the annual maximum water levels producing a correlation of 0.99 and a root mean square error (RMS) of 5 cm. The highest water level recorded at the Pictou tide gauge was 3.17 or 3.2 m CD in Dec. 1993 (Figs. 35, 38) and has been used to generate the design risk graphs under different RSL conditions. The design risk, or cumulative probability, of at least one occurrence of a water level of 3.2 m under current RSL conditions of 28 cm/century is expected by 2036, or within 26 years from 2010 (Fig. 39, top).

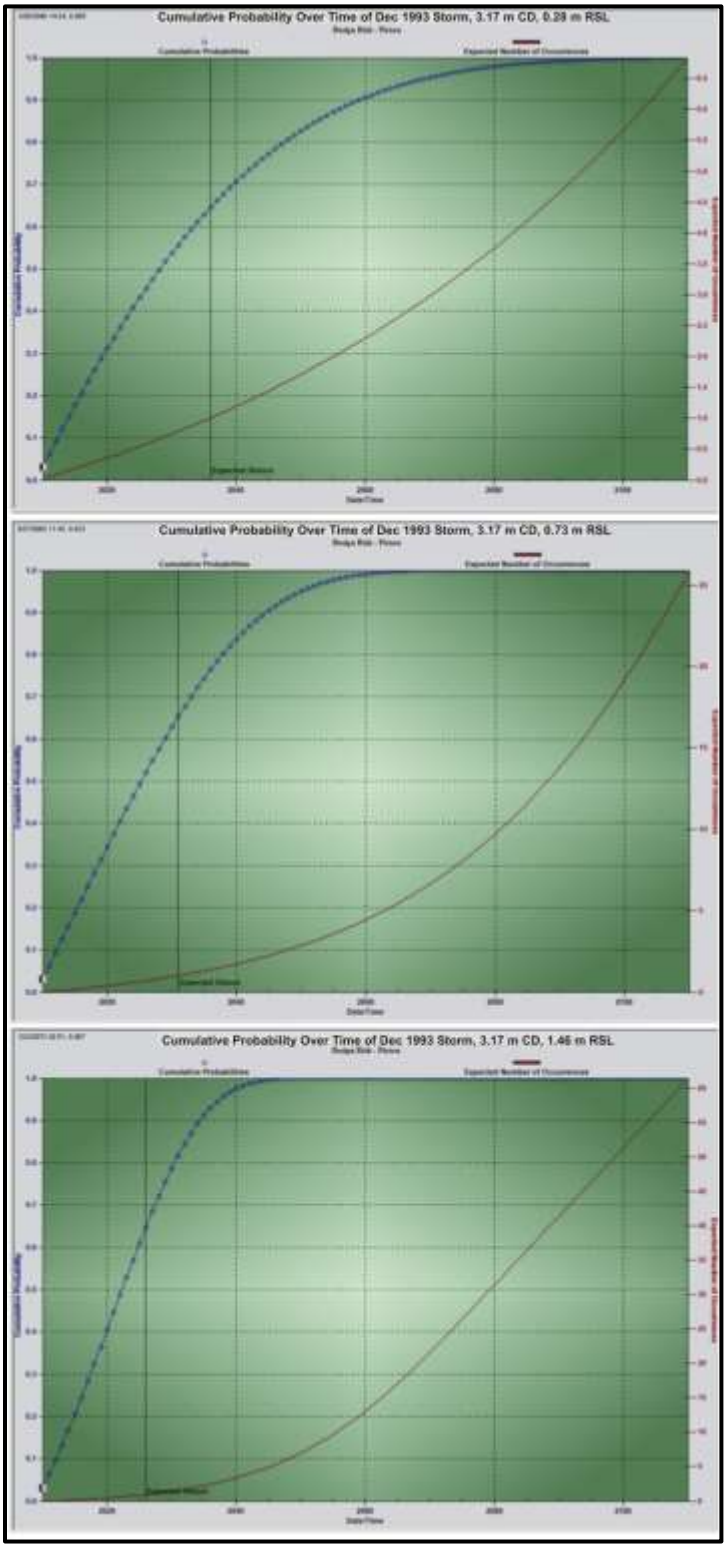

Figure 39 Design risk plot from Pictou extreme value model for the Dec. 1993 storm (3.2 m CD water level) under different RSL conditions. Top plot shows the cumulative probability of that water level being reached and expected number of occurrences under current RSL of 28 cm/century compared to the middle plot of RSL of 73 cm/century and lower plot of RSL at 146 cm/century.

This return period decreases to 21 years or at least one occurrence is expected by 2031 if RSL rises at a rate of 0.73 m/century (IPCC AR4) and further decreases to 16 years or 2026 if RSL rises at a rate of 1.46 m/century (Rhamstorf, 2007) (Fig. 39, middle and lower). The Dec. 21, 2010 storm that impacted much of the northern coast of the Northumberland Strait appears to have slightly exceeded this water level based on GPS field measurements of wrack lines of debris. The design level plot has been constructed from the Pictou EVM for a 95% probability of occurrence to determine the expected water levels at different RSL over time (Fig. 40).

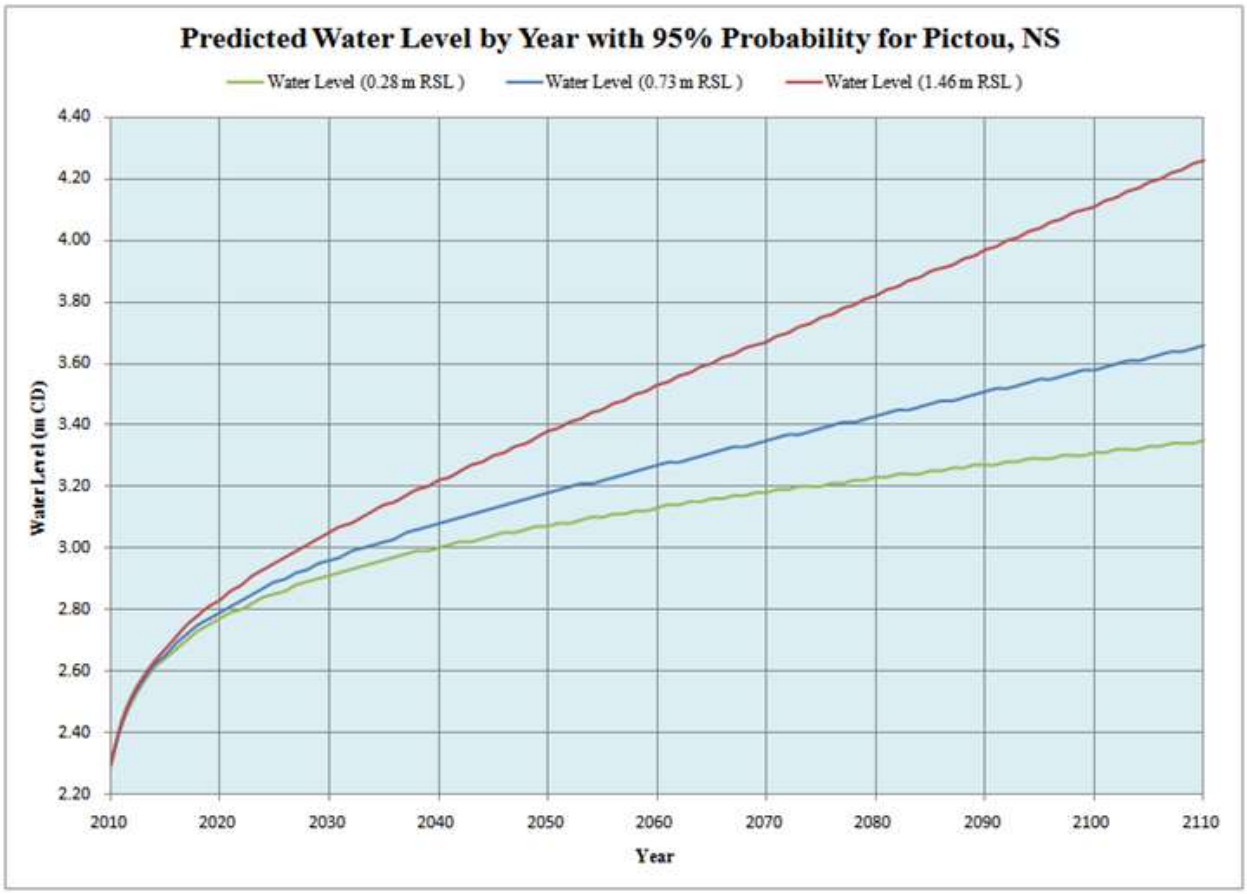

Figure 40 Pictou design level with a 95% probability of occurrence under different RSL conditions. The different RSL correspond to green – current rate 0.28 m/century, blue – 0.73 IPCC, red – 1.46 Rhamstorf.

The one hundred year water level under current sea-level rise conditions is 3.35 m CD and increases to 3.66 m if RSL rises at a rate of 0.73 m/century (IPCC AR4) or further increases to

4.26 m CD if RSL rises at a rate of 1.46 m/century (Rhamstorf) (Fig. 40). The expected water levels to be experienced over time at different RSL rates (current 28 cm/century, IPCC 73 cm/century and Rhamstorf 146 cm/century) for the Pictou extreme value model are presented in Appendix 8. The one hundred year return period water levels under different RSL conditions have been converted into the CGVD28 vertical datum and used in figure 41. The 100 year flood level under current RSL conditions is 2.4 m which is 10 cm below previous high water level maximum observed during the Dec. 1993 storm surge. If RSL increases to a rate of 0.73 m/century the 100 year water level increases to 2.7 m CGVD28 which further inundates areas (Fig. 41). If RSL increases to a rate of 1.46 m/century the 100 year water level increases to 3.3 m CGVD28 which further inundates areas (Fig. 41).

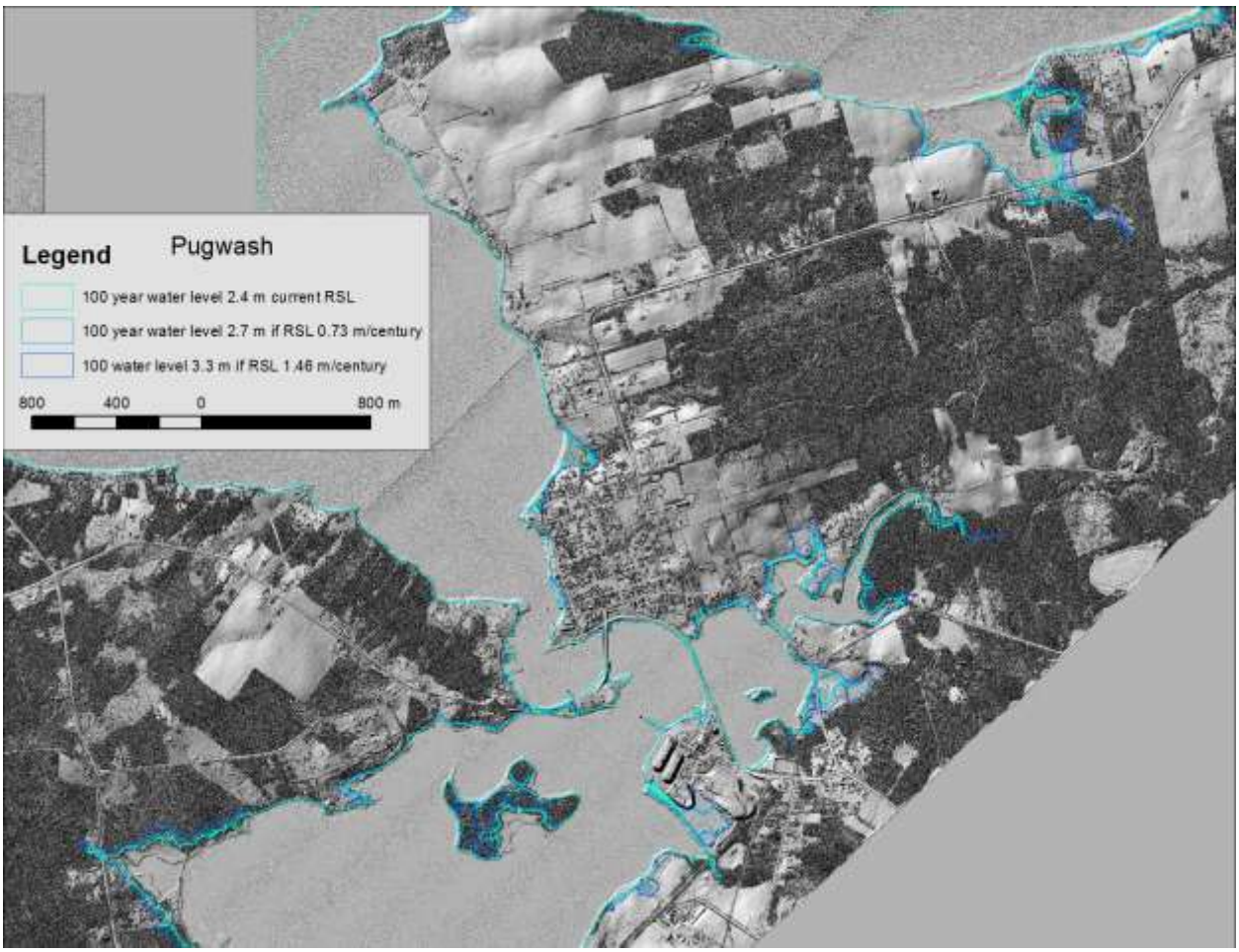

Figure 41 Pugwash shaded relief DSM with 100 year water levels under current RSL and possible future RSL under climate change.

3.3.Town and District of Yarmouth

3.3.1. Lidar acquisition, processing and DEM validation of the Town and District of Yarmouth

The lidar data were acquired for the town and District of Yarmouth study site on Sept. 16, 2008 (Appendix 4). The GPS check points were acquired during the lidar survey utilizing the same base station used by the lidar aircraft. A total of 4088 GPS check points were acquired with overall statistics indicating a mean delta Z of -0.11 m and a standard deviation of 0.06 m (Figs. 42, 43).

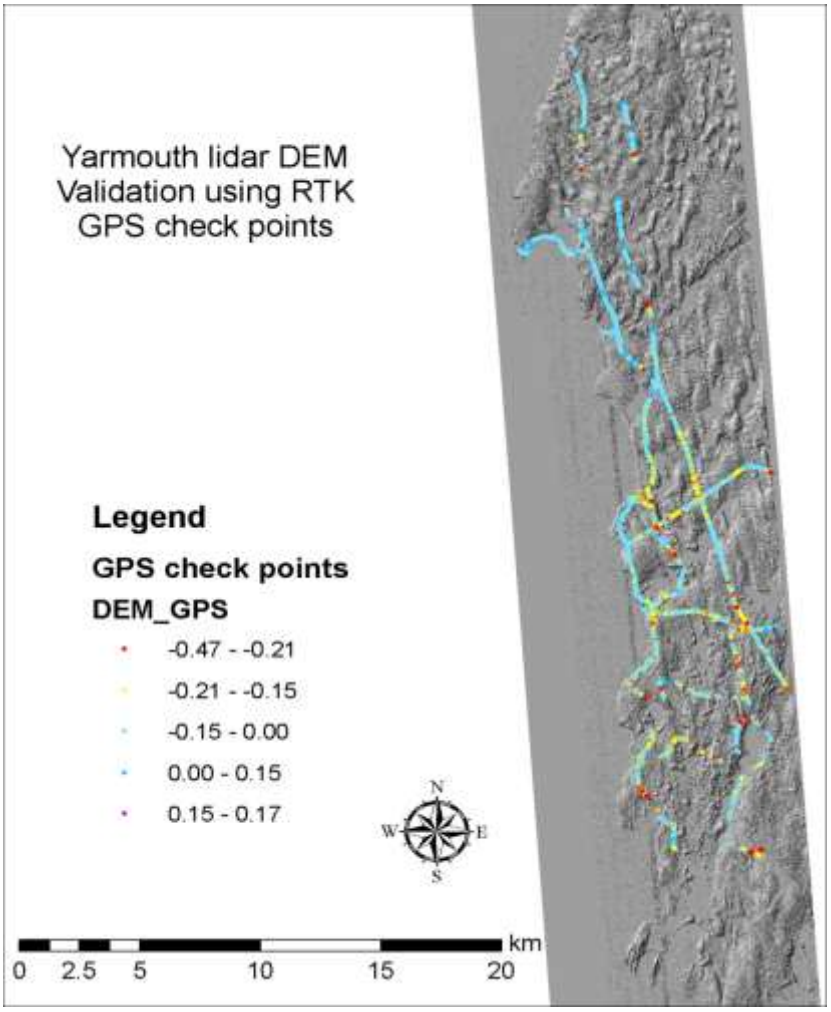

Figure 42 GPS check points colour coded by delta Z (DEM-GPS elevation).

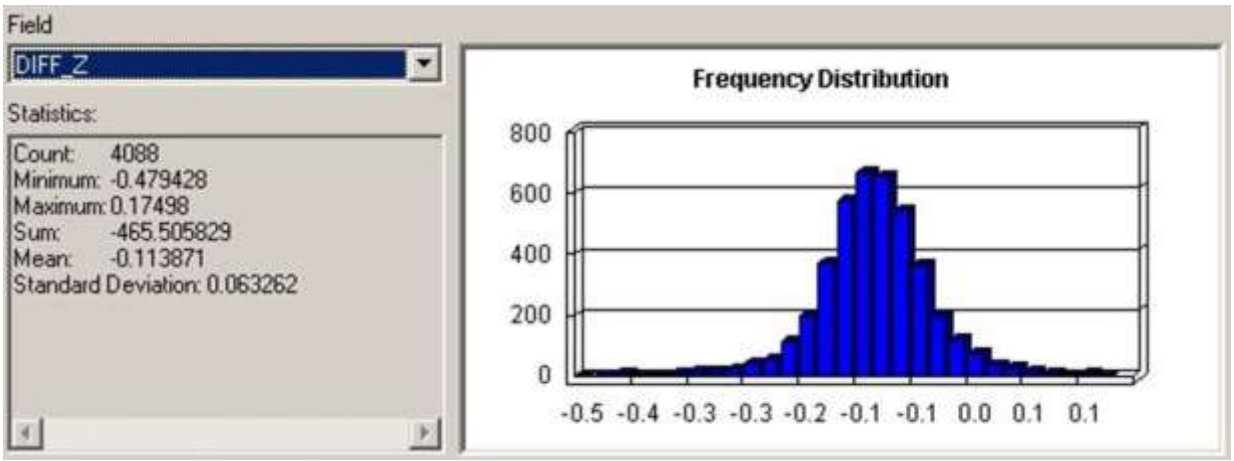

Figure 43 Delta Z distribution of DEM compared to GPS elevations. The DZ mean difference of -0.11 m with a standard deviation of 0.06 m.

3.3.2. Flood Inundation Maps for the Town and District of Yarmouth

In the case of the town and District of Yarmouth, recent digital colour orthophotos are available for the area. We used these photos, where available, for generating the flood risk maps. The benchmark storm used to depict the risk of flooding in Yarmouth was the Groundhog Day Storm of 1976. The storm caused extensive damage around the coast and Annapolis Valley in Feb. 3, 1976. The Yarmouth tide gauge captured the event and recorded the 1.5 m storm surge with a maximum water level of 3.36 m CGVD28 (Fig. 44). The high water wrack line was surveyed in 2010 with RTK GPS and an elevation of 4.81 m (Webster, 2011).

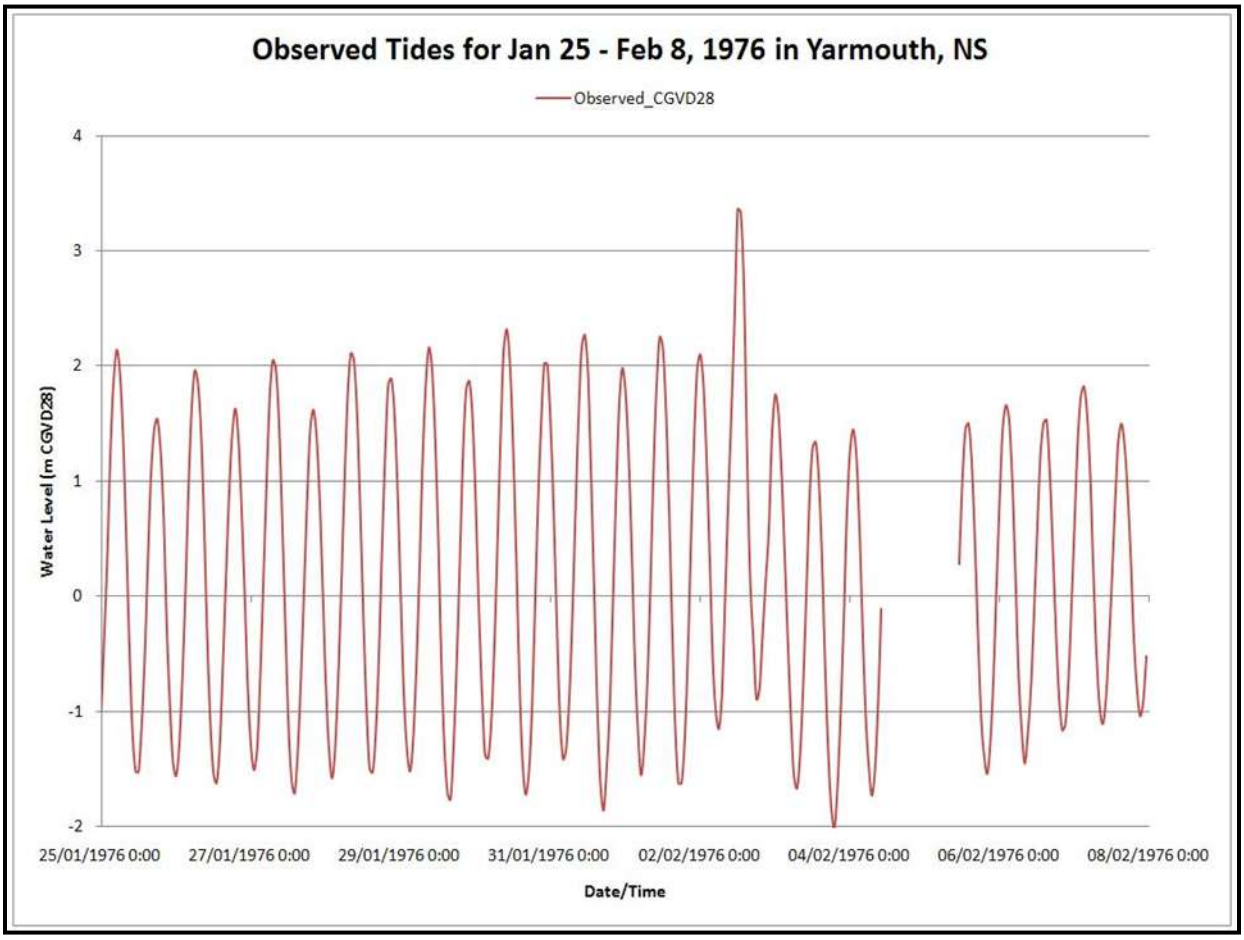

Figure 44 Yarmouth tide gauge record converted to the CGVD28 vertical datum of the Feb. 3 Groundhog Day storm of 1976. The maximum water level was 3.36 m CGVD28.

The Groundhog Day storm water level was projected onto the lidar DEM to generate a flood layer. The water level was scaled from 1976 to 2011 using a relative sea-level rise rate of 70 cm/century for example, as was used in some previous SLR studies for community of Annapolis Royal (Webster et al. 2008; Webster, 2010). The storm was then projected to 2111 under this sea-level rise rate and placed over the orthophoto backdrop for Yarmouth (Fig. 45).

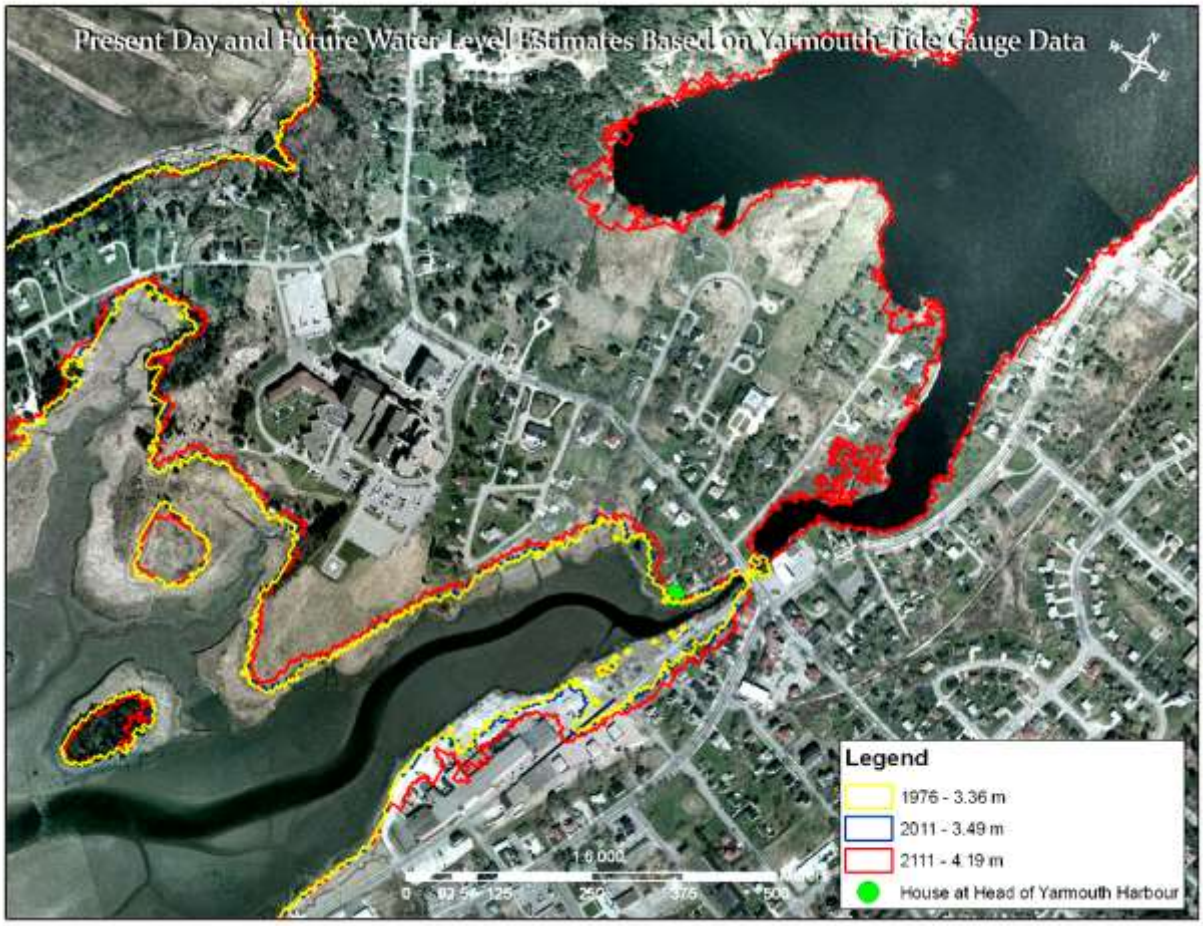

Figure 45 Groundhog Day storm water level of 1976 and the same level projected to today and 2111 based on a relative sea-level rise rate of 70 cm/century.

3.3.3. Flood Risk – Water level return periods and annual probabilities for the Town and District of Yarmouth

The town and District of Yarmouth study site is the best suited of the ACAS communities for this type of risk analysis since the tide gauge has a long record, is still operating, and is located within the study site. The Yarmouth tide gauge has continuous records from 1965 to present (Fig. 46).

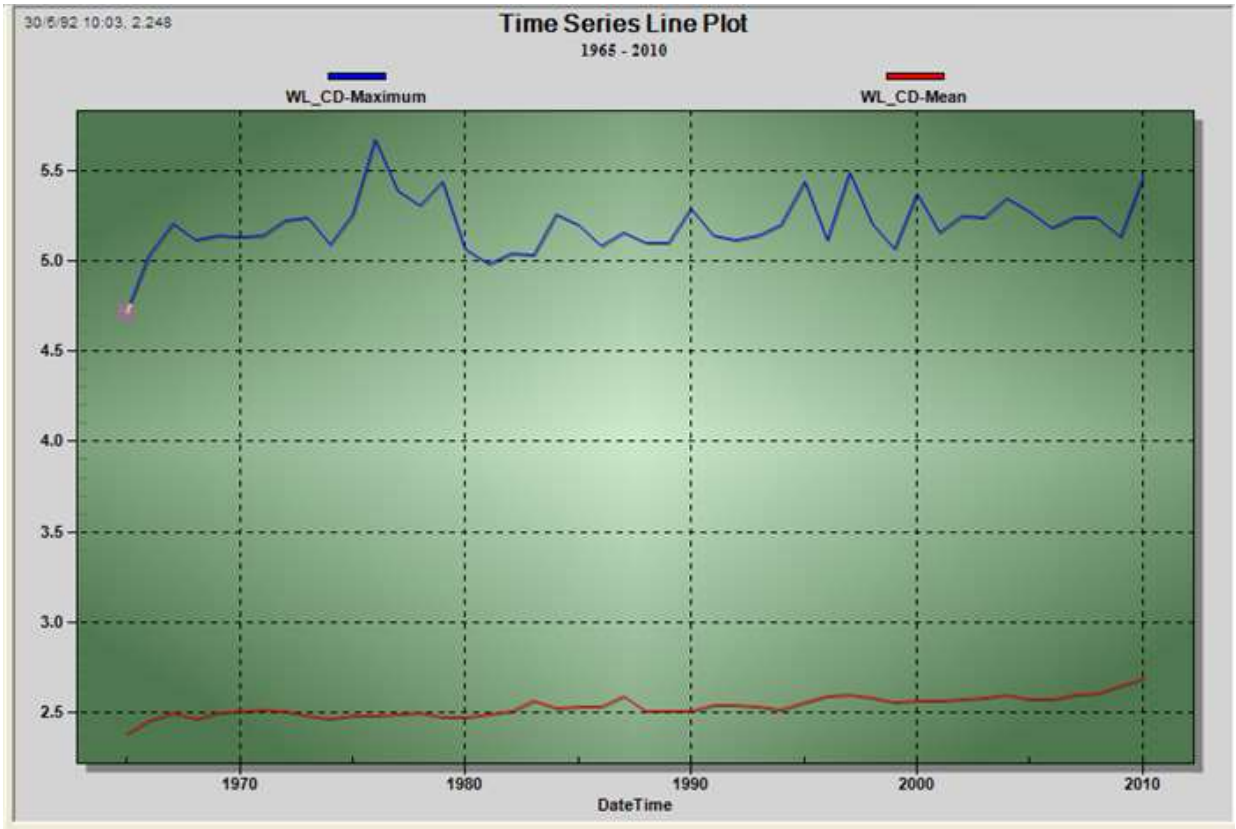

Figure 46 Yarmouth tide gauge record 1965-2010. Annual mean sea-level has been rising at a rate of 35 cm/century (red line) and the maximum annual water level has been rising at a rate of 33 cm/century (blue line).

A Gumbel extreme value model was fitted to the distribution of the annual maximum water levels producing a correlation of 0.96 and a root mean square error (RMS) of 6 cm. The highest water level recorded at the Yarmouth tide gauge is 5.67 m CD in Feb. 1976, the Groundhog Day Storm, (Fig. 46) and has been used to generate the design risk graphs under different RSL

conditions. The design risk, or cumulative probability, of at least one occurrence of a water level of 5.7 m CD under current RSL of 35 cm/century is expected by 2039, or within 29 years from 2010 (Fig. 47, top). This decreases to 23 years or by 2033 if RSL rises at a rate of 0.73 m/century (IPCC AR4) and further decreases to 17 years or by 2027 if RSL rises at a rate of 1.46 m/century (Rhamstorf) (Fig. 47, middle and lower). The design level graph has been constructed from the Yarmouth EVM for a 95% probability of occurrence to determine the expected water levels at different RSL over time (Fig. 48). The one hundred year water level under current sea-level rise conditions is 5.85 m CD and increases to 6.14 if RSL rises at a rate of 0.73 m/century (IPCC AR4) and further increases to 6.77 m CD if RSL rises at a rate of 1.46 m/century (Rhamstorf) (Fig. 48). The expected water levels to be experienced over time at different RSL rates (current 35 cm/century, IPCC 73 cm/century and Rhamstorf 146 cm/century) for the Yarmouth extreme value model are presented in Appendix 9.

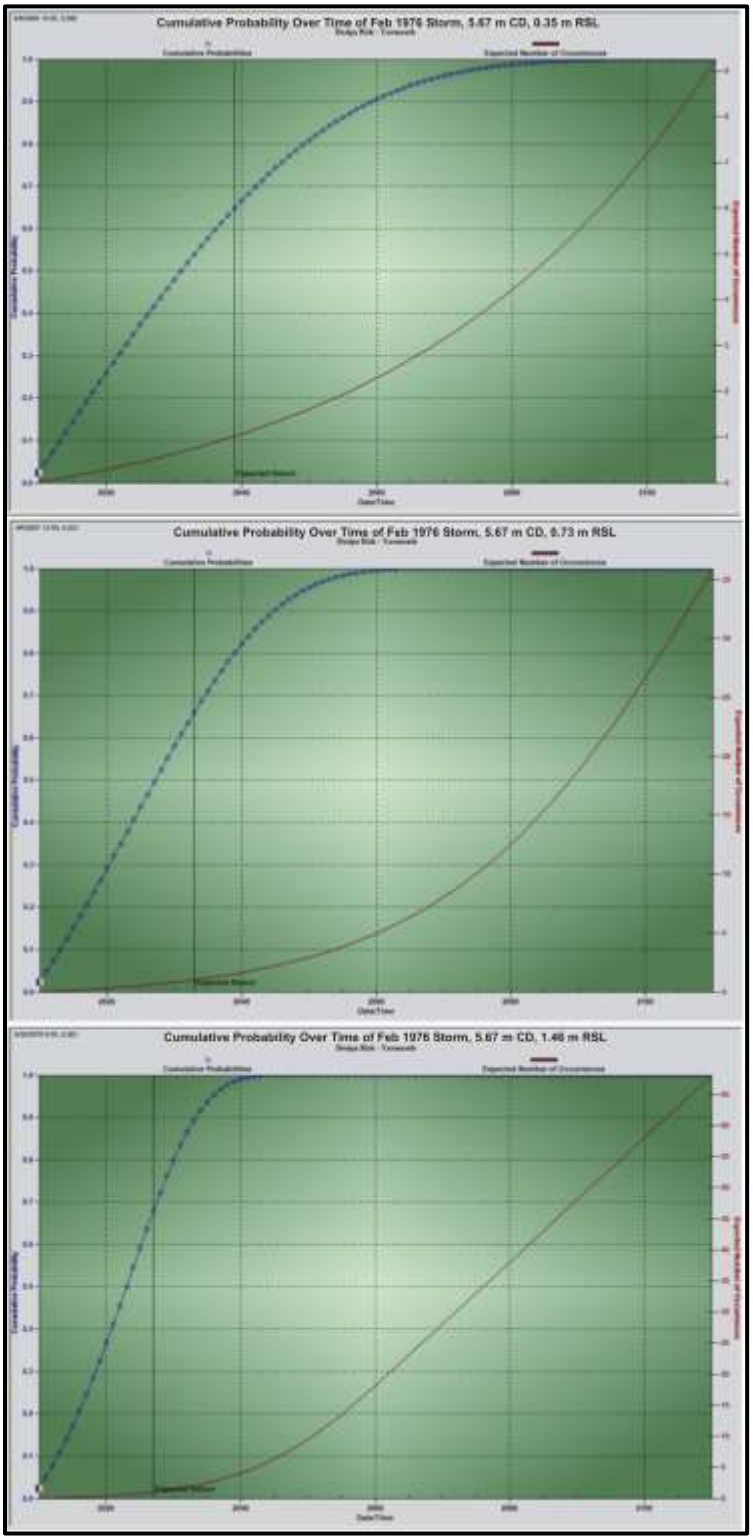

Figure 47 Design risk plot from Yarmouth extreme value model for the Feb. 1976 storm (5.7 m CD water level) under different RSL conditions. Top plot shows the cummulative probability of that water level being reached and expected number of occurrences under current RSL of 35 cm/century compared to the middle plot of RSL of 73 cm/century and lower plot of RSL at 146 cm/century.

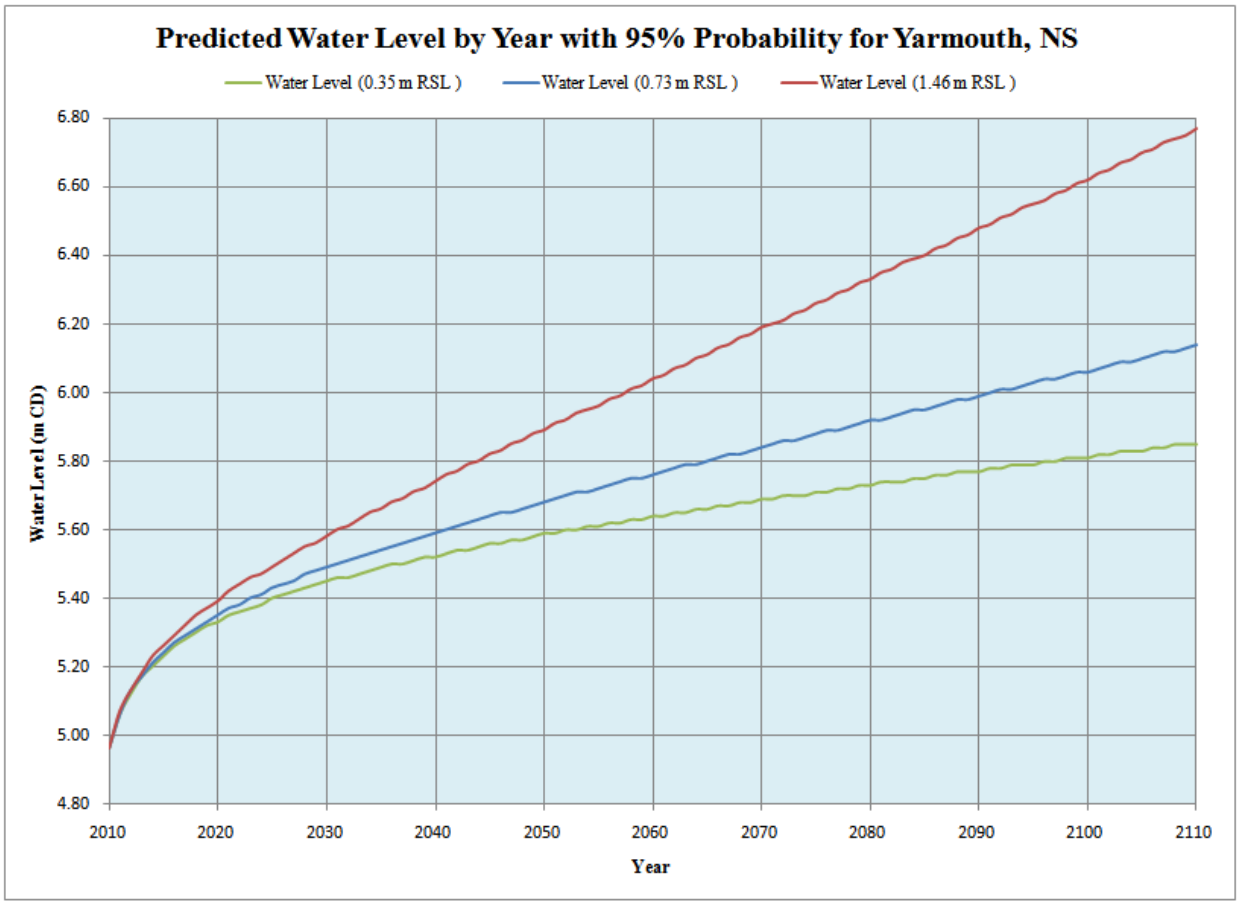

Figure 48 Yarmouth design level with a 95% probability of occurrence under different RSL conditions. The different RSL correspond to green – current rate 0.35 m/century, blue – 0.73 IPCC, red – 1.46 Rhamstorf.

The one hundred year return period water levels under different RSL conditions have been converted into the CGVD28 vertical datum and used in figure 49. The 100 year flood level under current RSL conditions is 3.5 m which is 10 cm below previous high water level maximum observed during the Groundhog Day Storm in Feb. of 1976. If RSL increases to a rate of 0.73 m/century the 100 year water level increases to 3.8 m CGVD28 which further inundates areas (Fig. 48). If RSL increases to a rate of 1.46 m/century the 100 year water level increases to 4.5 m CGVD28 which further inundates areas (Fig. 49).

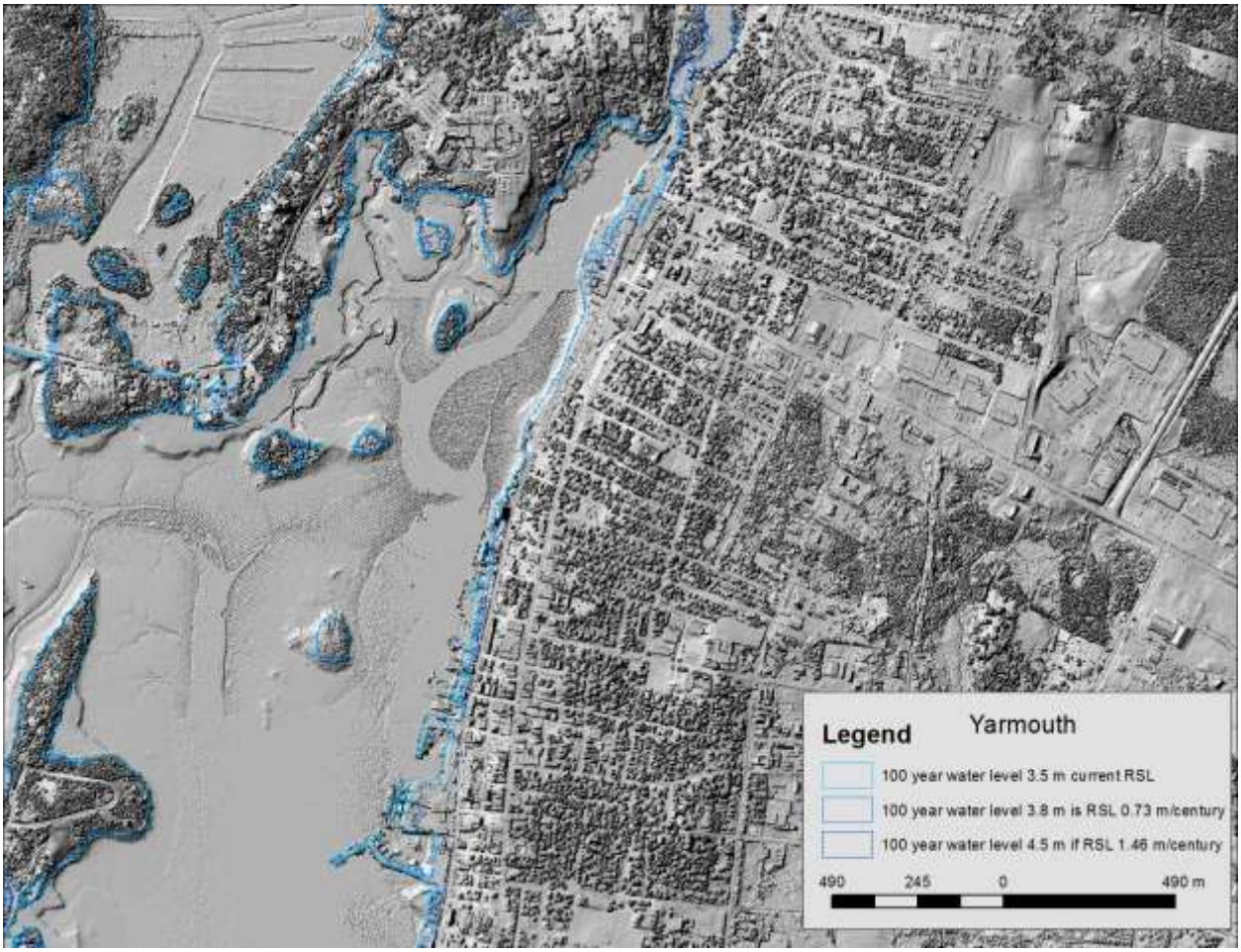

Figure 49 Yarmouth shaded relief lidar DSM with 100 year water level under current RSL conditions and future possible RSL under climate change.

3.4.Chignecto Isthmus

3.4.1. Lidar acquisition, processing and DEM validation of the Chignecto Isthmus area

The lidar data were acquired for the Chignecto Isthmus study site on Oct. 28, 2009 (Appendix 5). The GPS check points were acquired during the lidar survey utilizing the same base station used by the lidar aircraft. The GPS check points are colour coded by the delta Z value (Fig. 50). A total of 2404 GPS check points were acquired with overall statistics indicating a mean delta Z of -0.00 m and a standard deviation of 0.05 m (Fig. 51).

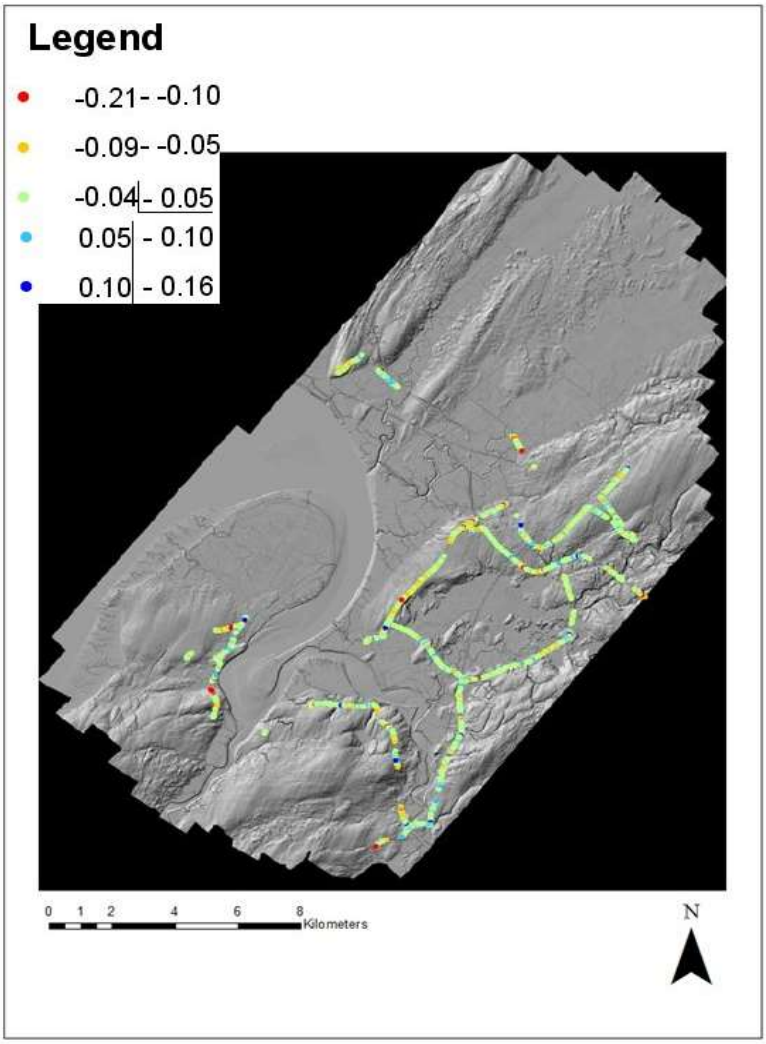

Figure 50 Amherst lidar DEM with GPS check points (Oct. 28, 2009) colour coded by delta Z (DEM-GPS).

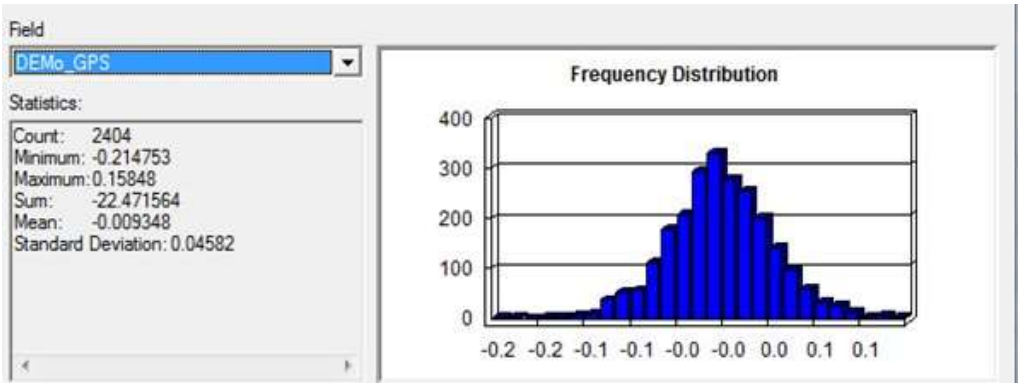

Figure 51 Distribution of GPS check points delta Z. Mean difference -0.00 m with a standard deviation of 0.05 m.

3.4.2. Flood Inundation Maps for the Chignecto Isthmus

Benchmark storm for the upper Bay of Fundy including the Chignecto Isthmus (Amherst-Nappan) consisted of the Saxby Gale of 1869, where a perigean high tide plus a 2 m storm surge water level was used to estimate the water level of this event. In order to estimate the water level for this storm we used the Canadian Hydrographic Service prediction of the Higher High Water Large Tide (HHWLT). The HHWLT water level for the community of Joggins is 13.4 m above chart datum (CD) and is estimated to be at least 1 m higher in the Upper Bay near Amherst (C. O'Reilley, CHS pers. Communication). The offset between chart datum and CGVD28 for Joggins is 6.5 m, therefore HHWLT is estimated to be 7.9 m CGVD28 in the Amherst and Nappan. With a 2 m storm surge on top of HHWLT, as was estimated during the Saxby Gale, all of the dykes are over topped in this area. In the case of the Chignecto Isthmus, the coastline consists of dykes that protect low lying agricultural land. A set of flood layers that represent the dykes overtopping have been constructed. These maps show the water levels up to the top of the dyke, and then the areas higher than the dyke landward with no intermediate water level elevations on the low lying land behind the dykes. To improve upon this method and provide details of the immediate area behind the dykes and there susceptibility to flooding, a set of inundation maps representing a dyke breach (hole in the dyke) were simulated (Fig. 52).

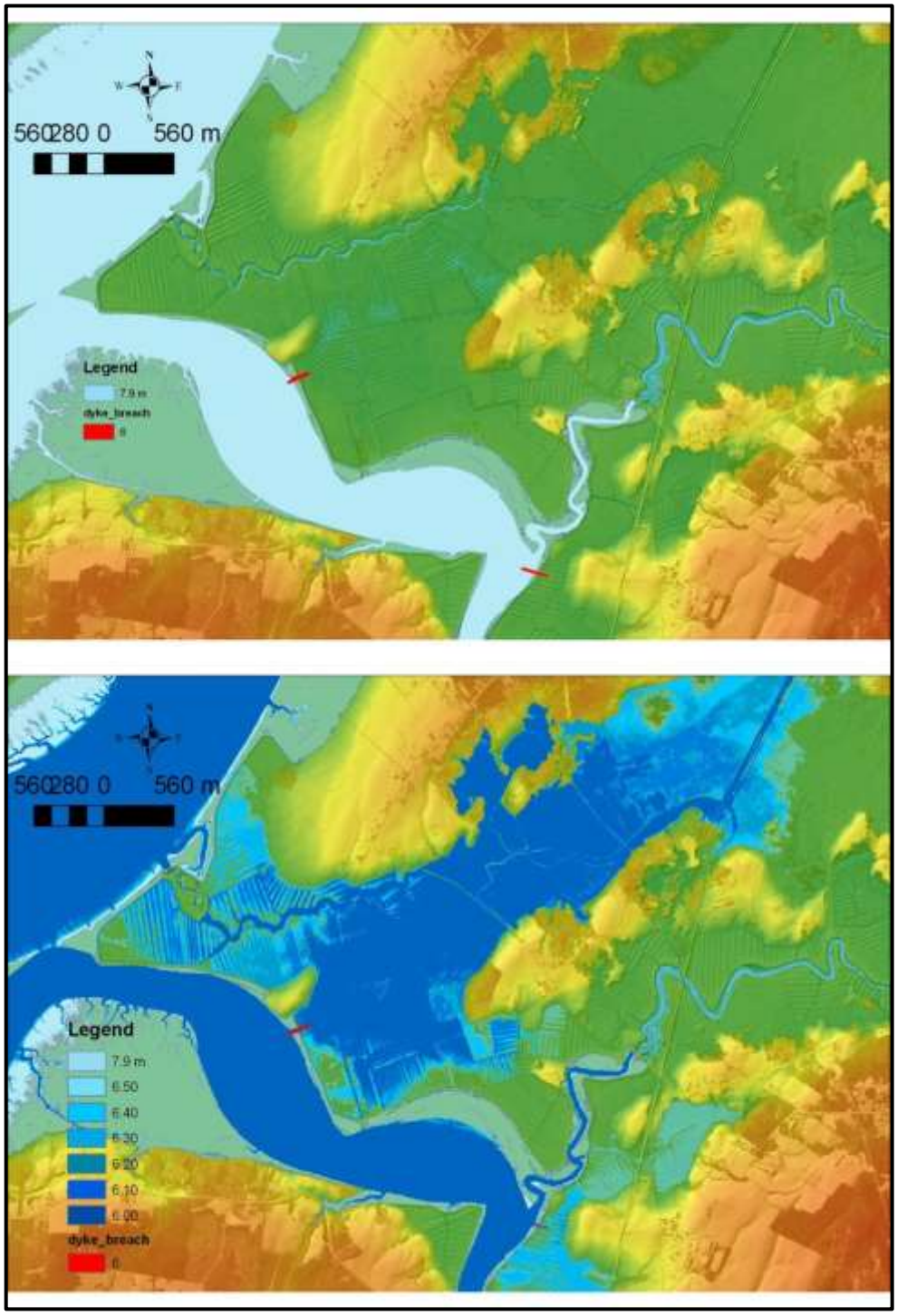

Figure 52 Example of breached dyke flood inundation maps for the Chignecto Isthmus (Nappan area), Upper Bay of Fundy. The top map represents the lidar DSM with the water level to the top of the dyke and breach locations in red.

3.4.3. Flood Risk – Water level return periods and annual probabilities for the Chignecto Isthmus

The calculation of return periods of high water levels is very challenging for the communities in the upper Bay of Fundy at the Chignecto Isthmus and Minas Basin ACAS study sites because there is no tide gauge of significant long record for these areas. The closest tide gauge in the Bay of Fundy is at Saint John, NB which experiences a significantly smaller tidal range than the communities in the upper bay where the water is funnelled up into the estuaries. The tide gauge at Saint John has been operating since 1918, but with data gaps until 1941 when the record becomes continuous. The results of return periods and water levels from Saint John must be used with extreme caution for the study sites in the upper bay. For example, the return period of the Groundhog Day storm may be able to be translated to other areas of the bay, however the water level achieved at Saint John cannot be directly transferred to these areas because of the significant difference in the tidal amplitudes between the sites. However, because there is no other long term time series record of water levels in the Bay of Fundy, the Saint John tide gauge has been processed to give a sense of high water return periods in the bay (Fig. 53).

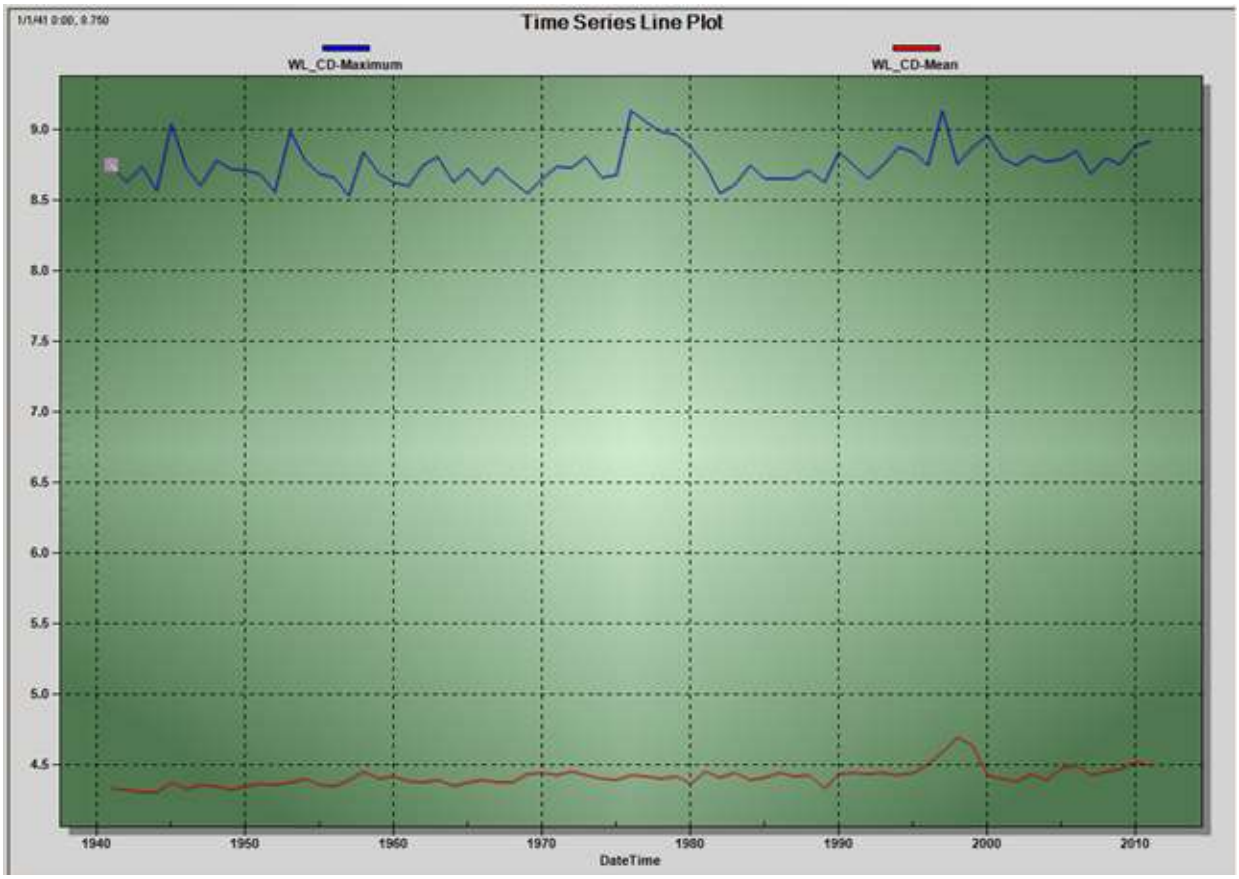

Figure 53 Saint John tide gauge record 1941-2010. Annual mean sea-level has been rising at a rate of 22 cm/century (red line) and the maximum annual water level has been rising at a rate of 19 cm/century (blue line).

A Gumbel extreme value model was fitted to the distribution of the annual maximum water levels producing a correlation of 0.99 and a root mean square error (RMS) of 2 cm. The highest water level recorded at the Saint John tide gauge is 9.14 m CD that occurred twice, once in Feb. 2, 1976, the Groundhog Day Storm, and again in Jan. 1997. The design risk, or cumulative probability, of at least one occurrence of a water level of 9.1 m CD under current RSL of 22 cm/century is expected by 2043, or within 33 years from 2010 (Fig. 54, top).

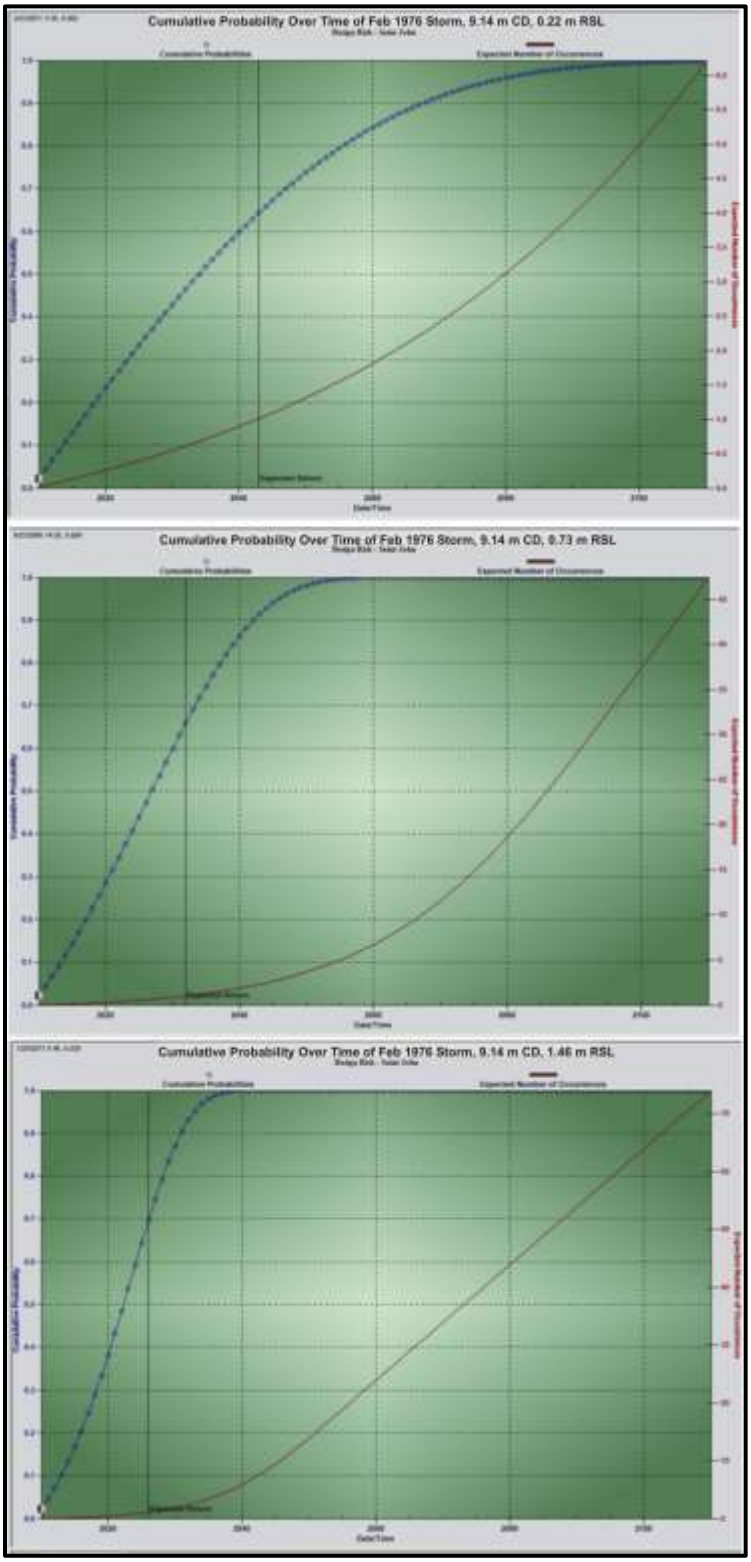

Figure 54 Design risk plot from Saint John extreme value model for the Feb. 1976 and Jan. 1997 storms (9.1 m CD water level) under different RSL conditions. Top plot shows the cummulative probability of that water level being reached and expected number of occurrences under current RSL of 22 cm/century compared to the middle plot of RSL of 73 cm/century and lower plot of RSL at 146 cm/century.

This decreases to 22 years or by 2032 if RSL rises at a rate of 0.73 m/century (IPCC AR4) and further decreases to 16 years or by 2026 if RSL rises at a rate of 1.46 m/century (Rhamstorf) (Fig. 54, middle and lower). The design level plot has been constructed from the Saint John EVM for a 95% probability of occurrence to determine the expected water levels at different RSL over time (Fig. 55). The one hundred year water level under current sea-level rise conditions is 9.24 m CD and increases to 9.63 if RSL rises at a rate of 0.73 m/century (IPCC AR4) or further increases to 10.28 m CD if RSL rises at a rate of 1.46 m/century (Rhamstorf) (Fig. 55). The expected water levels to be experienced over time at different RSL rates (current 22 cm/century, IPCC 73 cm/century and Rhamstorf 146 cm/century) for the Saint John extreme value model are presented in Appendix 10.

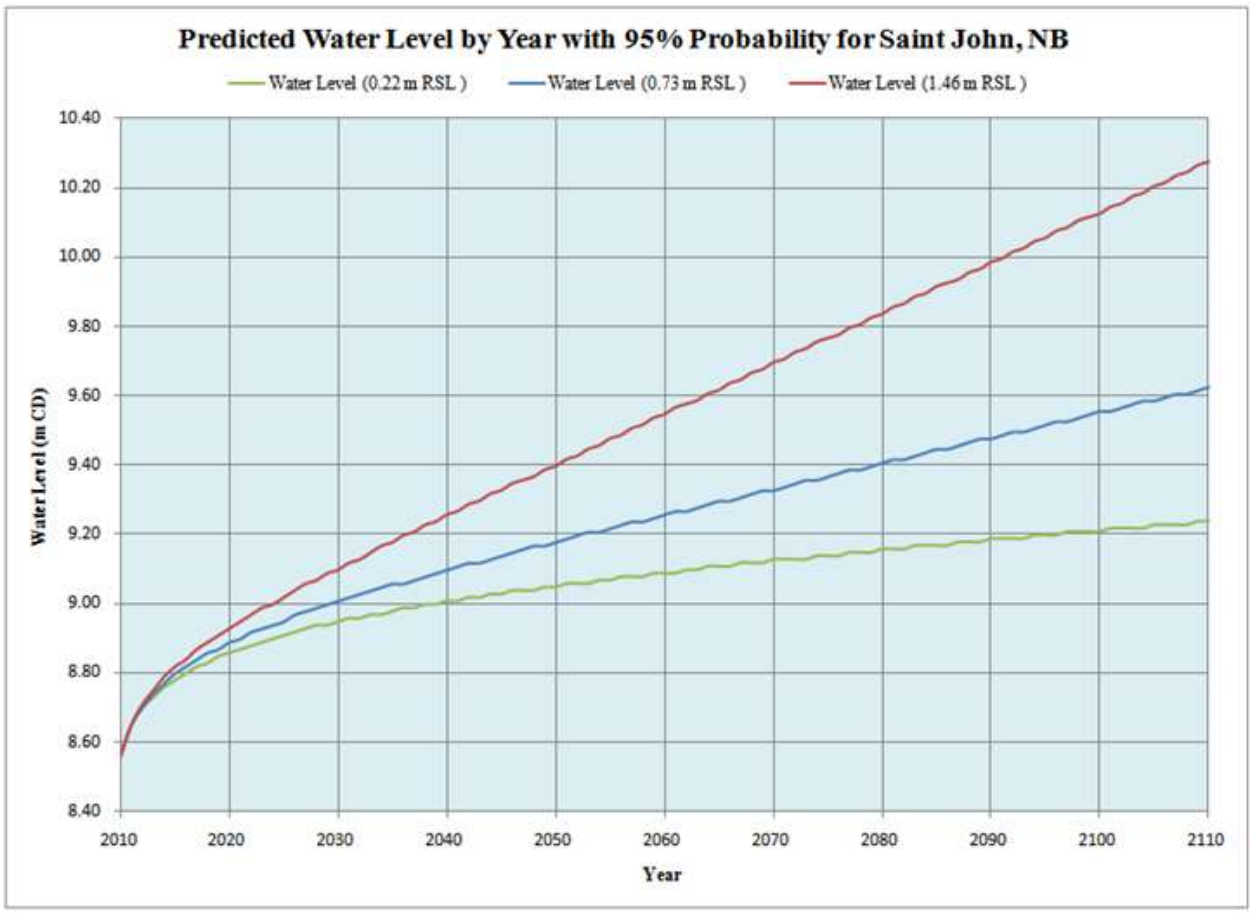

Figure 55 Saint John design level with a 95% probability of occurrence under different RSL conditions. The different RSL correspond to green – current rate 0.22 m/century, blue – 0.73 IPCC, red – 1.46 Rhamstorf.

The tidal amplitude increases by at least 3 m from Saint John to the Chignetco Isthmus Amherst and Minas Basin study areas and one could attempt to translate the return period water levels from Saint John to these sites based on this increased tidal range. However, these predictions would be highly uncertain. We have prepared maps indicating when critical threshold water levels are reached that overtop the protective dykes (Fig. 56).

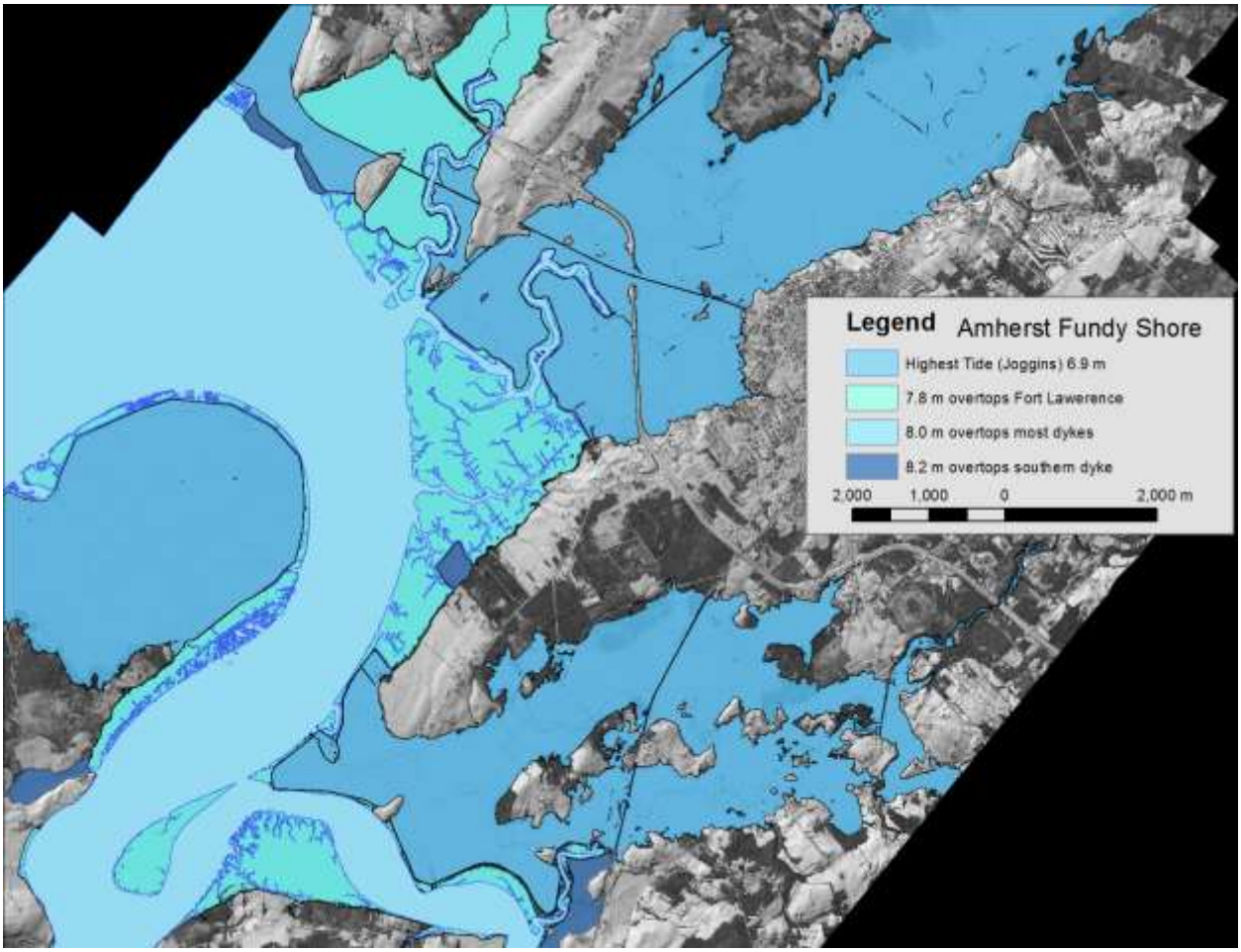

Figure 56 Amherst Fundy shore shaded relief lidar DSM with critical dyke overtopping water levels (CGVD28).

3.5.Minas Basin

3.5.1. Lidar acquisition, processing and DEM validation of the Minas Basin area

The Minas Basin lidar data covering Kings County were acquired in April and May 2003. The GPS check points were acquired in May 2003 and were used to validate the lidar DEM for the entire Kings County area. As a result a total of 39,210 GPS check points were acquired and used for validation (Fig. 57). The mean delta Z is 0.0 m with a standard deviation of 0.21 m for the May 2003 lidar DEM (Fig. 58). The extent of the lidar data from 2003 extends throughout the

eastern end of the Annapolis Valley, from Lawrencetown east to the Gasperaux Estuary and the Guzzle (island off of Grand Pre). The lidar data along the Avon River estuary to Windsor were acquired in April 2007 with the AGRG ALTM 3100 system. GPS check points were acquired along roads, similar to other sites. These data were compared to the lidar DEM and statistics calculated on the differences in elevation (Fig. 59). The April 2009 DEM shows a mean DZ = 0 m and a standard deviation of DZ of 0.10 m (Fig. 59). The three DEM layers (2003 and 2 from 2009 see outlines on Fig. 57) had to be bulk adjusted to match one another and then to the mean of the GPS data. Figure 57 shows the spatial distribution of the differences between the GPS and DEM elevations as depicted by colourized dots of the DZ attribute every 15 cm.

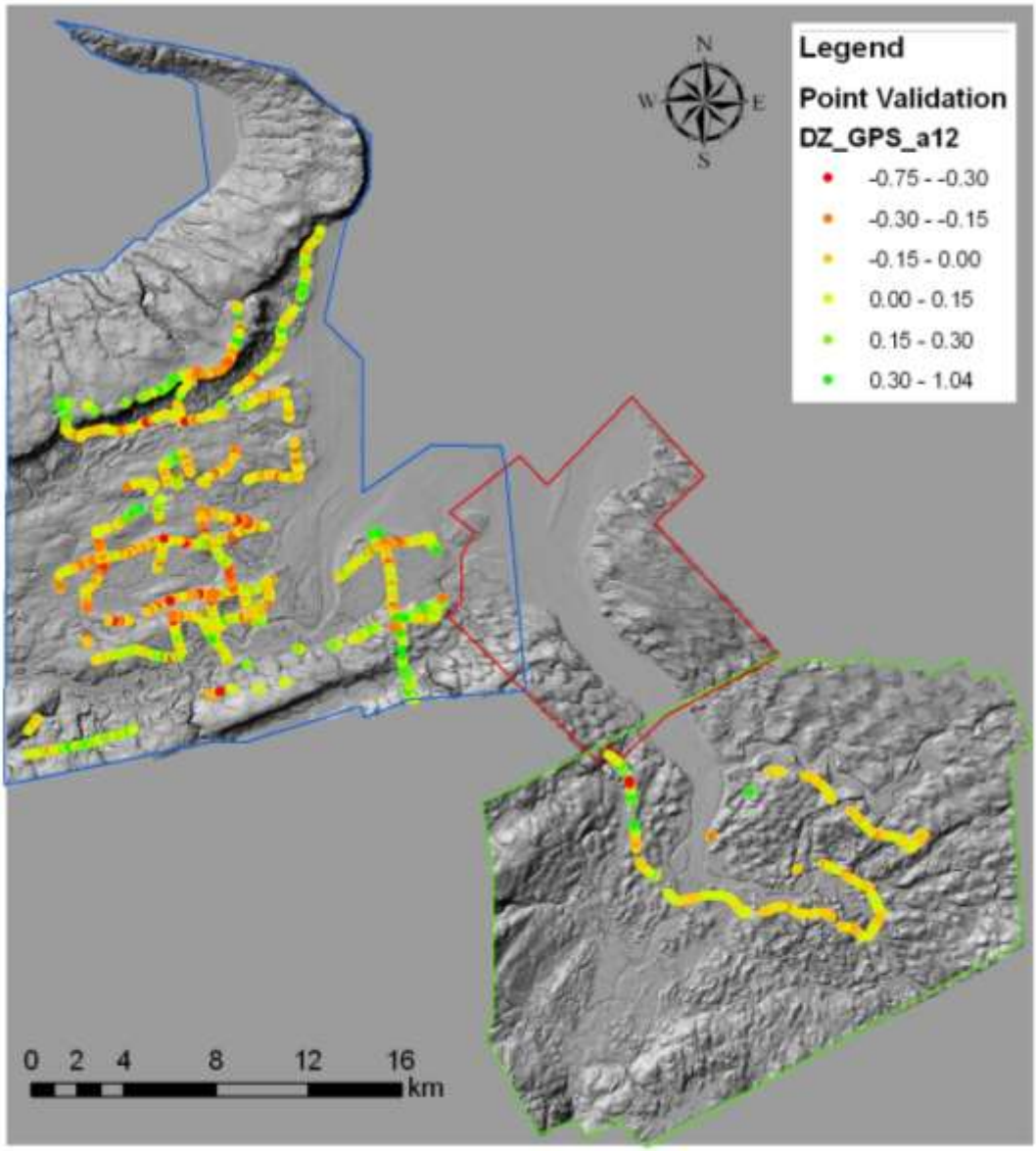

Figure 57 GPS validation of the May 2003 lidar DEM (blue outline) and the April 7, 2009 lidar DEMs (red & green outlines) in the Annapolis Valley & Windsor area. The background map is a shaded relief DEM with GPS check points colour coded by the difference in elevation between GPS and the DEM.

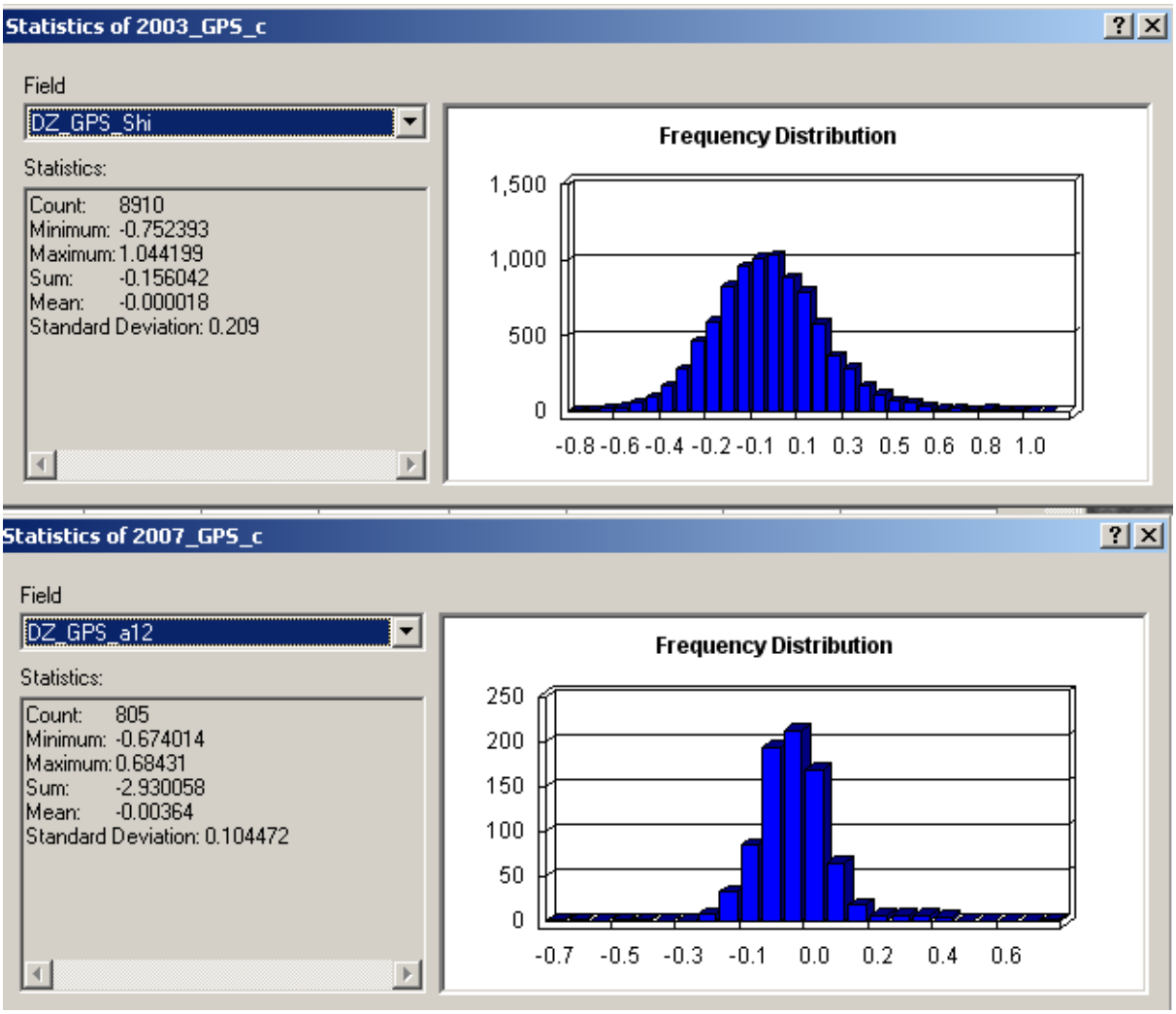

Figure 58 Histograms of the delta Z values which represent the difference between the GPS elevations and the DEM surfaces. The top histogram is the DZ distribution for the May 2003 DEM and the lower graph represents the April 2009 DEM.

The lidar system used to collect the data in 2003 had a limited laser ranging system to one decimeter. As a result of this, in areas of flat terrain, small steps occur in the terrain as a result of the limited ranging precision. The steps are less than 30 cm in relief and do not cause the data to exceed the accuracy specification. This “wood grain” effect is only evident on flat cleared areas (Fig. 59).

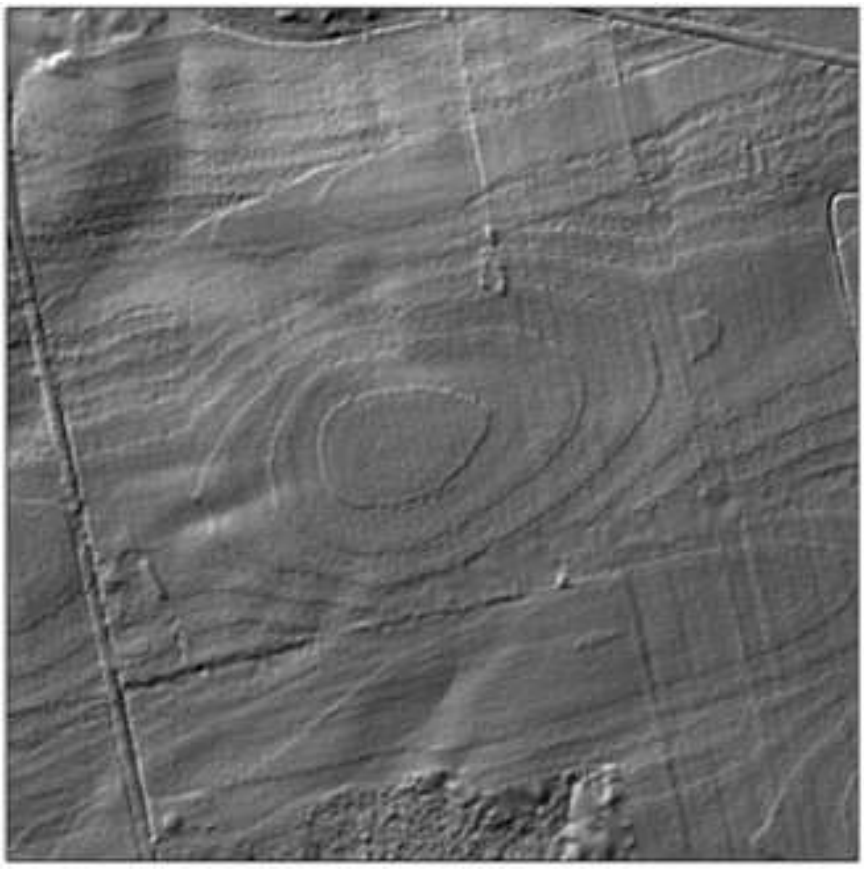

Figure 59 Example of shaded relief DEM from May 2003. Note the ridges or "wood grain" that are evident in the cleared field.

3.5.2. Flood Inundation Maps for the Minas Basin

The HHWLT water level for the community of Hantsport is 15.38 m above chart datum (CD). The offset between chart datum and CGVD28 for Hantsport is 7.23 m, therefore HHWLT is 8.15 m CGVD28. For the community of Blomidon, HHWLT above CD is 13.86 m and no value is reported for the CD-CGVD28 relationship. However, if one assumes the value for Hantsport, the HHWLT at Blomidon becomes 6.63 m CGVD28. These values would be equal to a high perigean spring tide. If we add a 2 storm surge to those levels to simulate the reported conditions during the 1869 Saxby Gale we obtain values of 10.15 m CGVD28 for Hantsport and 8.63 m for Blomidon (Fig. 60).

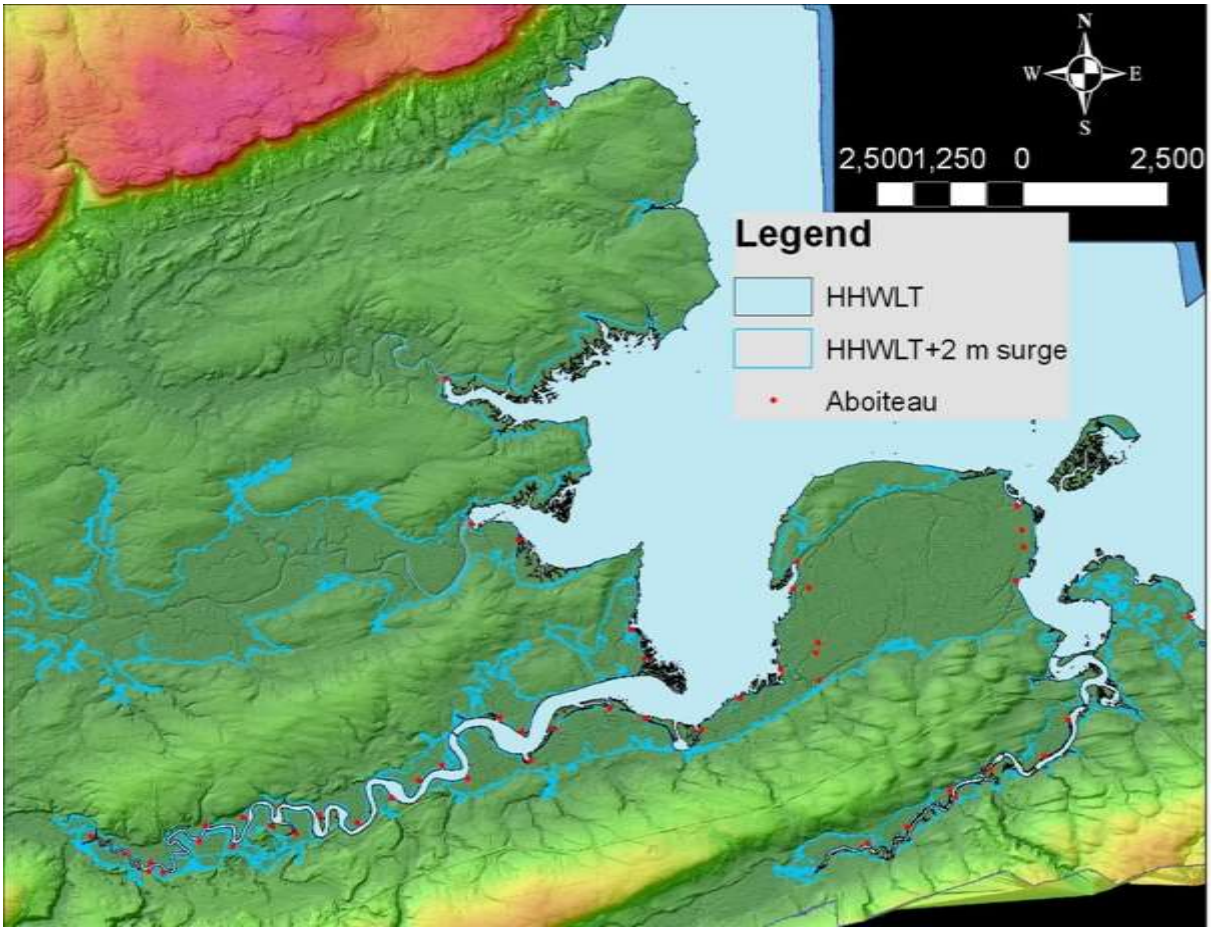

Figure 60 Minas Basin colour shaded relief map with HHWLT in solid light blue and the areas innundated by an additional 2 m storm surge (blue outlines). This is a water level similar to that estimated during the Saxby Gale which occurred in 1869.

If we project this storm into the future assuming a RSL of 1.4 m for the upper Bay of Fundy (Greenburg et al. (in press) then the levels could be as high as 11.6 m CGVD28. Other times in history when the dykes were breached include 1913, 1931, and 1958 (Bleakney, 2009) (Fig. 61).

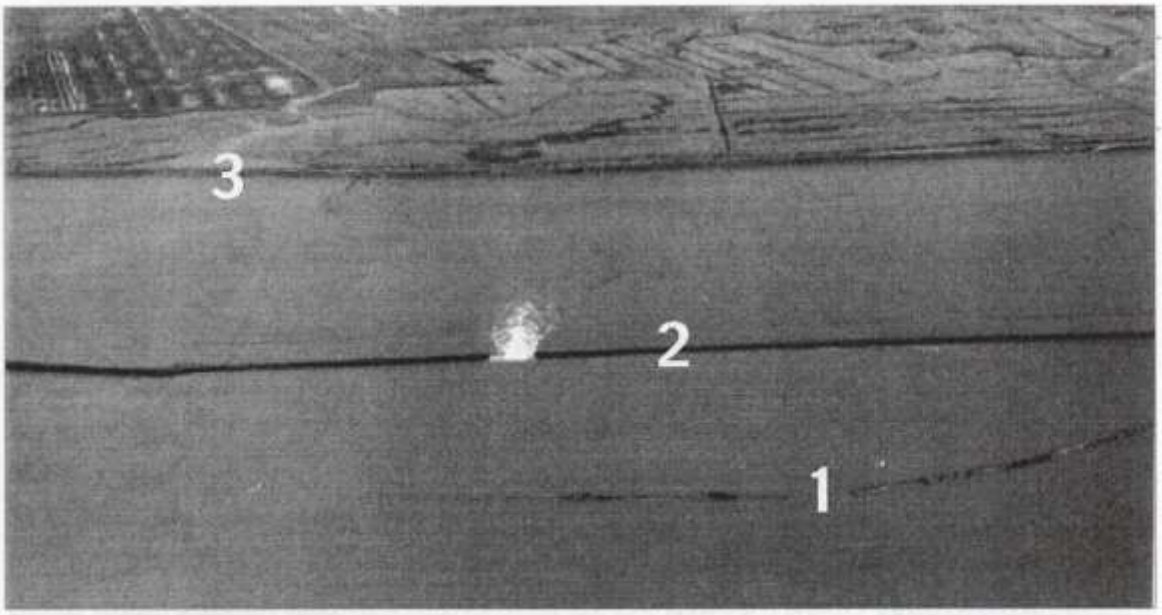

Figure 9.2.4 Aerial view from above the Guzzle channel looking west on 6 April 1958. Dyke 1 is a Planter dyke from 1760–70; the breached Dyke 2, where water is foaming through the gap, was built by Robert Palmeter in 1939–40; and Dyke 3 was the new, larger one constructed in 1950. The entire Grand Pré farmland was threatened by the Seros Cycle extreme tide in 1958. (Nova Scotia Department of Agriculture and Marketing, MMRA photo no. 16-028)

Figure 61 Photo of breached dyke near Grand Pre in 1958 (From Bleakney, S. 2009).

Other notable storms include the Groundhog Day storm of Feb. 3, 1976 and April 6, 1977 when the dyke was breached at Port Williams. As seen in figure 61, storm in 1958 that corresponded with the highest normal tides in the Saros Cycle (the same tidal cycle that is associated with the Saxby Gale) also cause flooding in the Minas Basin area. In the case of the Windsor area the highest predicted tide (using the Hantsport tidal constituents) is 8.15 m. With increased water levels to 8.3 m the dykes are overtopped west of the Windsor causeway (Fig. 62). At 8.4 m the dykes are overtopped west of the causeway and the water can reach the lower sections of the town of Windsor (Fig. 62). At the 9.2 m level water covered Highway 101 at the eastern end of the causeway and overtops the causeway at the 9.6 m (Fig. 62).

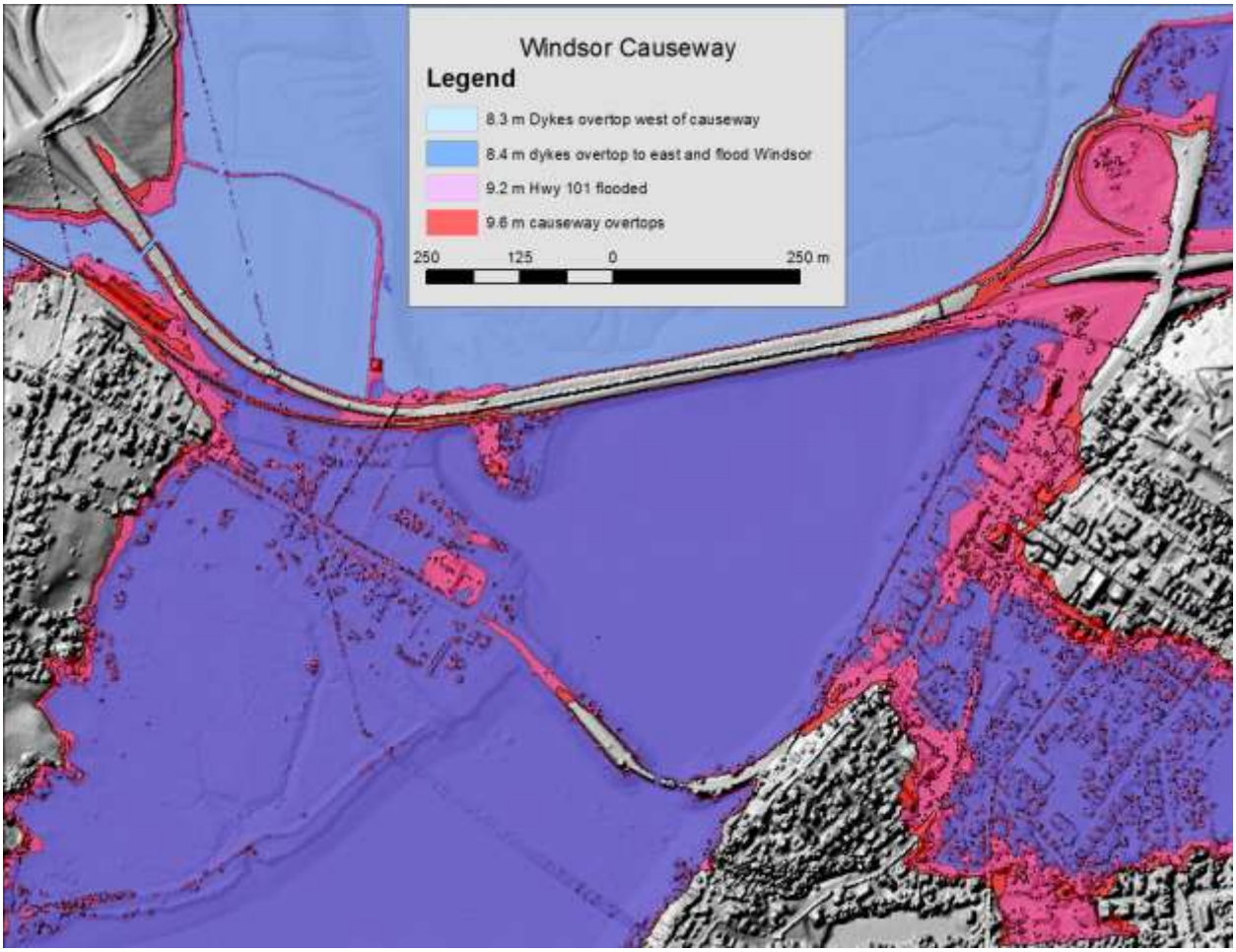

Figure 62 Windsor causeway shaded relief lidar DSM with critical water levels that overtop the dykes and causeway.

3.5.3. Flood Risk – Water level return periods and annual probabilities for the Minas Basin

As mentioned in the previous section, it is very challenging to accurately determine risk of high water levels in the upper Bay of Fundy because there is no long term tide gauge record for this area. The closest long term tide gauge record exists for Saint John, New Brunswick. Although this gauge provides a time series of water level records within the Bay of Fundy, the tidal range is significantly lower in Saint John than in the Minas Basin or Chignecto Isthmus areas. The Saint John tide gauge has been used to examine the return periods of benchmark

storms that affected the communities around the Bay of Fundy, such as the Groundhog Day storm of Feb. 1976. These results were presented in the previous section for the Chignecto Isthmus and are as applicable, given the lack of a more local water level time series record, for the Minas Basin communities. Please refer to section 3.4.3 “Flood Risk – Water level return periods and annual probabilities for the Chignecto Isthmus”.

4. Discussion

Based on previous studies in the Maritime region concerning flood inundation analysis, it has been determined that lidar derived DEM’s are the most suitable sources of information for flood risk mapping. This is primarily due to their spatial resolution (ca. 1 m) and vertical accuracy (ca. 15 cm) as they are accurate enough to represent storm surges of 1-2 m in magnitude and map the long term effects of decimetre to metre ranges of climate change induced sea-level rise. However, it is imperative that detailed ground validation, such as GPS surveys, are carried out to ensure that the lidar data are of adequate accuracy and meets the specifications to ensure reliable results (Webster et al., 2004). The lidar surveys conducted for this project involved correcting misalignments between the laser sensor and navigation sensor (GPS & IMU) as well as some errors associated with the edges of the scan. This is a time consuming process and required specialized software and personnel. The details of some of the corrections applied to ensure a consistent and accurate set of lidar surface models are supplied in the Appendices. Based on independent GPS checkpoints, the lidar surface models, including the DEMs, meet or exceed the specifications for each survey and sensor. Based on this analysis we have confidence in the derived information products from the lidar, such as the flood inundation maps.

Using the still water method to raise the sea-level of the ocean in order to determine areas of inundation landward has proven to be an effective way to model areas at risk of coastal flooding (Webster et al., 2004; Webster, 2010). However, for many areas in Nova Scotia barriers exists, both natural in the case of a dune or gravel beach, and anthropogenic in the case of dykes to protect low lying land. The approach we have employed in this study is to modify the DEM to ensure that hydraulic pathways, such as bridges and culverts, allow connection, where appropriate, of the ocean to the low lying areas landward of the barrier. The NS topographic database has culverts defined within the road layer where the road crosses a mapped stream at the 1:10,000 scale. However, we are aware that many other culverts exist in reality to aid in surface runoff drainage. We have done our best to interpret where theses culverts exists, based on the terrain and landcover. In the case of the dyked areas, we have used information from NS Department of Agriculture to denote one-way culverts, aboiteaux, versus two way culverts. The correctness of the hydraulic pathways of the DEM could be improved or validated against a field survey of existing culverts or other drainage control structures. This type of analysis was beyond the scope of this project, but could be verified by the local municipalities in the future.

It is imperative that the practitioners who use these derived datasets, flood risk layers, understand the relationship between the different vertical datums used along the coast. For example, if there is a warning of a 2 m storm surge for a given community, there are a set of procedures that one should follow in order to determine what the potential water level could be on land and thus which flood inundation layers to examine to determine where the impacted areas will be. The process would involve determining the predicted tide level for the dates and times in question, e.g. when the storm is predicted, adding the storm surge to the predicted tide level. The predicted tide level can be derived from the tide tables or acquired at various internet sites for selected harbours. The water level predicted is based on chart datum, which is typically

an elevation lower than the lowest possible tide. This would be the same datum used for a hydrographic chart showing depths in the offshore. In order to convert the total water level (predicted tide plus storm surge), one must subtract the offset between chart datum (CD) and the datum used on land and for the lidar DEM flood layers which is the Canadian Geodetic Vertical Datum of 1928 (CGVD28). The relationship between CD and CGVD28 for the ACAS communities involved in this project is represented in Table 2. For example if a 2 m storm surge was predicted for Jan 1, 2012 at noon in Yarmouth. The predicted tide at that time is 1.26 m CD, however that does not correspond to high tide, which occurs at 4:00 pm and is predicted to be at 3.64 m CD with the tide being predicted to be even higher the next morning at 5:00 am at 3.79 m CD. These values can be used to then add the 2 m storm surge to determine the total water level expected; 5.64 m CD at 4:00 pm on Jan 1 and 5.79 m at 5:00 am on Jan 2 for example. The CD-CGVD28 relationship for Yarmouth is reported to be 2.31 m by the Canadian Hydrographic Service (CHS). Therefore the expected water level on the land surface at 4:00 on Jan 1 is 3.33 m CGVD28 (5.64 m CD – 2.31 m CD-CGVD28) and 3.48 m at 5:00 am on Jan 2. Thus the appropriate flood risk maps to be consulted correspond to layers “p00330” which corresponds to 330 decimeters or 3.3 m for Jan. 1 at 4:00 pm and “p00350” which corresponds to 350 decimeters or 3.5 m (3.48 m rounded to the nearest decimeter since the lidar is only accurate to 10-15 cm in the vertical) for Jan. 2 at 5:00 pm. One would be wise to plan for water levels that could be higher than these values by up to 1 m in order to consider the effects of wave-run up which will depend on the wind direction and local orientation of the coastline.

The same conversions from CD to CGVD28 must be taken into account when interpreting the return periods of water levels reported here or for the 100 year water level at a 95% probability. This is because these statistics have been derived from the tide gauge records directly where the water levels have been referenced to local chart datum. The Time Series

Modeler (formally Water Modeler) has been tested in a few different cases, and has been demonstrated to be a useful method for providing the risks associated with coastal flooding and storm-surge events (Webster et al. 2008; Webster 2010). The work by Bernier (2005) and Thompson et al. (2009) have been compared for the Pictou tide gauge. Thompson et al. (2009) have calculated the 100 year return period of the total water level for this site to be approximately 2.3 m CD. Using the Time Series Modeler for the Pictou tide gauge we have estimated the 100 year return period total water level to be 3.35 m CD.

Bernier (2005) used the Dalhousie University storm-surge model to reconstruct storm-surges for the last 40 years in order to calculate return periods of water levels and how they might change under climate change scenarios. She plotted the return periods of observed extreme annual water level maxima residuals (observed water level minus predicted) for various locations where tide gauge data exists in the region. The purpose of her study was to test the "skill" of the storm-surge model by comparing model outputs based on atmospheric wind and pressure fields with the observed water level records for several stations (36 sites) around the North Atlantic coast. The tide gauge data are reported hourly based on a 5 minute average to remove surface wave effects (Bernier, 2005). Sea-level residuals were calculated which represent the difference between observed sea level and predicted tide sea level. The Atmospheric Environment Service (AES) of Environment Canada have produced AES40 wind fields for the past 4 decades. The AES40 winds fields have a horizontal resolution of about 0.625^{o} latitude by 0.833^{o} longitude and have been used by Bernier (2005) to infer the air pressure field. The surge model is driven by winds and air pressure every 6 hours. Thus, the surge model output will not generate variability at periods shorter than 12 hours (Bernier, 2005). Therefore, to compare the storm-surge model output and the observed water levels and residuals, variability in the residuals at periods shorter than 12 hours were removed by applying a low-pass filter, effectively removing high-frequency

signals. The examination of large surges was accomplished by extremal analysis of the low-pass filtered residual data. The smoothed residual annual maxima and minima where calculated for each station and return periods where plotted (Bernier, 2005). Based on her analysis, the largest observed magnitude of the annual maximum surge at Saint John, New Brunswick is approximately 0.7 m. This is approximately only about one half of the storm-surge that was recorded during the Groundhog Day storm of 1976 at Saint John. The difference in the annual maximum surge level is a result of the aggregation and smoothing procedures (low-pass filter) that have been applied by Bernier (2005) in order to compare observed water levels with model outputs.

The 40 year hindcast that resulted from running the storm-surge model on the AES40 wind and inferred pressure fields was used to determine the 40 year return period storm-surge water levels throughout the study area domain (Maritime Provinces). Bernier (2005) states that there is a tendency to underestimate the 40 year return levels; however, the estimates are within the 95% confidence intervals of the filtered observed return levels. She also acknowledges that the resolutions of the forcing fields (i.e. AES40 winds and inferred pressure) are too coarse to be able to resolve hurricanes and the method underestimates these events. Thus, the return periods and associated storm-surge water levels reported in Bernier (2005) represent a conservative calculation of past events where the effects of some short lived events such as hurricanes have been filtered out.

This method of estimating the return period for storm surges based on the storm surge model allows predictions to be made in areas that do not have a tide gauge. As part of the ACAS project R. J. Daigle Enviro was contracted to estimate return periods of high water levels for the different study sites. He used the results of the model and analysis by Bernier (2005) to estimate the storm surge residuals for the different regions for return periods of 10, 25, 50 and 100 years.

These storm surge water levels were then added to the highest predicted tide (HHWLT) to determine the total water level expected within these time frames. This approach is quite different than that utilized in this report where the total water level, as measured hourly at the tide gauge locations, was used to determine the statistics. The method employed by R. J. Daigle Enviro is conservative in the estimation of storm surge levels and return periods as a result of the temporal (6 hrs) limitations of the driving forces (wind and atmospheric pressure) of the storm surge model. However, when these storm surge values are applied to the HHWLT, which occurs relatively infrequently within the 18 year tidal cycle, they represent the worst case scenario. It is important for the coastal practitioners to understand the background used in both methods and the associated limitations of each.

The results of this project provided each ACAS community a dataset of coastal GIS layers in the form of detailed lidar derived elevation and surface models, flood inundation layers and a statistical analysis of the nearest tide gauge to determine the risk or probability of a high water level occurring. The occurrence of storms that cause coastal flooding can be quite localized and often are controlled by the local wind direction and orientation of the coastline. In these cases the tide gauge records may not accurately represent such events depending on the distance from the gauge and local geographic considerations. To address this, researchers at AGRG have been working with officials from the Emergency Management Office and the Department of Natural Resource to map the high water elevation of coastal flood events for communities. These elevations can supplement the tide gauge records and can be used in the calculation of return periods. It is important to document such storm events and to quantify the elevation limit of flooding in order to better understand the frequency of such events, therefore increasing our ability to accurately predict their re-occurrence in the future.

Although the flood risk maps derived in this project are highly accurate and detailed, they are static representations of a dynamic phenomenon and do not consider the time it takes for water to move across a surface. These maps are static in nature and are intended for planning purposes and to be used to mitigate and devise adaptation strategies. The maps do not directly address such questions as “if the dyke were to be breached to a depth x, how long would it flood on the high tide?” or “if the dyke were to be breached or overtopped and a significant amount of water were to inundate the area, how long would it take to drain?”. There are so many factors involved in such questions, that even the application of sophisticated hydrodynamic models would be challenged to accurately model all of the scenarios required to have the information at hand to answer such questions. However, in communities where the lidar data exist, they have the dominate information required to begin to address such detailed questions. The bigger challenge will be to determine the other factors that influence the processes such as drainage infrastructure. For example, where and what is the diameter and types of culverts used to drain marshes behind the dykes and at what elevations are the inlet and outlets. Much of these data are not readily available although other ACAS projects are trying to address these issues.

5. Conclusions

This project has achieved the objectives of the ACAS in terms of providing the case study communities with the information and tools required to make informed decisions about the risk from coastal flooding. Flood inundation mapping allows for the observation of areas at risk from coastal flooding associated with storm-surge events and long term sea-level rise and allows for future planning within these sensitive areas. The flood risk maps were generated in such a way that as new sea-level rise projections are proposed, the appropriate water flood level can be

extracted and examined. However, the end user must be aware that in the coastal zone, water levels related to tide prediction and charts are referenced to chart datum, while the land information is referenced to a different datum, CGVD28 that is approximately mean sea-level, typically within a few decimeters. In addition to the flood risk maps and analysis, the municipalities also gain a tremendous asset in the lidar surface models, DSM & DEM. These data will provide benefits to many planning applications in the future besides sea-level rise and storm surge. Other coastal communities where lidar does not exist do not have mapping of the same level of precision and accuracy and as a result will have a higher degree of uncertainty identifying areas vulnerable to present day storms and at risk from sea-level rise and storms in the future.

We have attempted to use benchmark storms for each community to highlight past flooding events. This was done to show decision makers and citizens that these coastal areas are vulnerable to storm surges in the past and presently. This allows people to better understand the potential implications of climate change and sea-level rise in the future. The other benefit of using a past storm event, where possible, is the ability to validate the flood inundation maps. The choice of sea-level rise predictions into the next century is challenging because new information from observations and models are continually being published and refined. Because of the limited certainty in the future climate change, global sea-level rise, and regional crustal subsidence differences, we have provided flood inundation layers every 10 cm up to a maximum level that exceeds realistic predictions for the next century. This will allow each community to access the appropriate flood layer as new RSL predictions become available in the future.

The flood inundation layers have been applied to a hydraulically altered DEM where the pathways, as represented by culverts and bridges, connecting the ocean to inland areas have been applied. This approach works well for most coastal areas within Nova Scotia, where areas

become flooded once the ocean water level reaches a certain height and has connection to the low lying areas. However, we recognize that this method has limitations for coastal areas that are protected by dykes. We have generated a set of flood layers that represent dyke overtopping and highlight the areas at risk of flooding if the ocean water level were to exceed the dyke elevation. These maps do not account for the time that the ocean would be above the dyke elevation or the movement of the water immediately landward of the dyke. As a result of this limitation, we have also implemented a set of flood layers associated with dyke breaching, where we have simulated a break in the dyke and allowed the water to flood immediately behind the dyke. These flood layers show what areas behind the dyke are vulnerable to flooding if a breach were to occur. They do not take into account the time that the water would take to cross the land surface or the time that the ocean would be high enough to flood the breach. However, we believe these are useful static maps for planning and emergency measures organizations to determine what areas would be at risk if such an event were to occur. These flood breach layers have been produced for the study sites in the Chignecto Isthmus (Amherst to Nappan) and the Minas Basin (Wolfville-Windsor) in addition to the dyke overtopping layers.

Other studies being carried out by AGRG as part of the ACAS project involve examining the interaction between ocean storm surge and river runoff, since so many of our communities are located along estuaries. The current limitation of this type of analysis is the lack of data related to the estuary bathymetry and river channel geometry upstream. Bathymetric charts provided by CHS only cover the offshore areas and do not represent the estuarine or near shore coastal areas. As a result, AGRG has been collecting bathymetric information in the River Phillip estuary in the Oxford-Port Howe study site and to a lesser degree in the LaHave estuary in the District of Lunenburg site to assist in the hydrodynamic modeling of storm surge and rainfall runoff. The town of Oxford has experienced flooding conditions that are exasperated by high tide

levels indicating there is a strong interaction, even 18 km from the coast, between the ocean and fresh water runoff at this site.

6. References

Bernier, N.B. (2005) Annual and seasonal extreme sea levels in the Northwest Atlantic: hindcasts over the last 40 years and projections for the next century. PhD thesis, Dalhousie University.

Bernier, N.B., Thompson, K.R. (2006) Predicting the frequency of storm surges and extreme sea levels in the Northwest Atlantic. J Geophys Res 111:10009. doi:10.1029/2005JC003168.

Bleakney, S. (2009). Sods, Soil, and Spades, The Acadians at Grand Pré and Their Dykeland Legacy.

Church, J., & Gregory, J. (2001). Changes in Sea Level. In Climate Change 2001: The Scientific Basis: Contribution of working Group 1 to the Third Assessment Report of the Intergovernmental Panel on Climate Change (pp. 639-692). Cambridge, New York: Cambridge University Press.

Daigle, R. (2011). Sea-Level Rise Estimates for New Brunswick Municipalities. Draft Report.

Flood, M., and Gutelius, B. (1997). Commercial Implications of Topographic Terrain Mapping Using Scanning Airborne Laser RaDAR. Photogrammetric Engineering and Remote Sensing , 4, 327-366.

Forbes, D.L., Manson, G.K., Charles, J., Thompson, K.R., and Taylor, R.B. (2009). Halifax Harbour Extreme Water levels in the Context of Climate Change: Scenarios for a 100-Year Planning Haorizon. Geological Survey of Canada, Open File 6346, 21 p.

Godin G. (1992). Possibility of rapid changes in the tide of the Bay of Fundy, based on a scrutiny of the records from Saint John. Continental Shelf Research**,** 12.

Greenburg, D., Blanchard, W., Smith, B. and Barrow, E. (in review). Climate Change, Mean Sea Level and High Tides in the Bay of Fundy.

IPCC, 2007: Climate Change 2007: The Physical Science Basis. Contribution of Working Group I to the Fourth Assessment Report of the Intergovernmental Panel on Climate Change [Solomon, S., D. Qin, M. Manning, Z. Chen, M. Marquis, K.B. Averyt, M. Tignor and H.L. Miller (eds.)]. Cambridge University Press, Cambridge, United Kingdom and New York, NY, USA, 996 pp.

Levermann, A.; Griesel, A.; Hofmann, M.; Montoya, M.; Rahmstorf, S. (2005). Dynamic sea level changes following changes in the thermohaline circulation. Climate Dynamics, 24, 347-354.

Liu, X. (2008). Airborne Lidar for DEM Generation: Some Critical Issues. Progress in Physical Geography , 32 (1), 31-49.

MacCaulay, P. (2009). Canadian Hydrographic Services (CHS). Personal Communication.

McCulloch, M.M., D.L. Forbes, R.W. Shaw and the CCAF A041 Scientific Team. (2002). *Coastal Impacts of Climate Change and Sea-Level Rise on Prince Edward Island*. Geological Survey of Canada. Open File 4261.

Meehl, G.A., T.F. Stocker, W.D. Collins, P. Friedlingstein, A.T. Gaye, J.M. Gregory, A. Kitoh, R. Knutti, J.M. Murphy, A. Noda, S.C.B. Raper, I.G. Watterson, A.J. Weaver and Z.-C. Zhao, (2007). Global Climate Projections. In: Climate Change 2007: The Physical Science Basis. Contribution of Working Group I to the Fourth Assessment Report of the Intergovernmental Panel on Climate Change [Solomon, S., D. Qin, M. Manning, Z. Chen, M. Marquis, K.B. Averyt, M. Tignor and H.L. Miller (eds.)]. Cambridge University Press, Cambridge, United Kingdom and New York, NY, USA.

Nicol, A. (2006). Planning for coastal Areas in the context of changing climate conditions in Antigonish County. Unpublished report. Independent project PLAN 6000. Dalhousie University, December 2006.

Peltier, W.R. (2004). Global glacial isostasy and the surface of the ice-age earth: The ice-5G (VM2) model and Grace. Annual Review of Earth and Planetary Sciences, *32*, 111–149.

Rhamstorf, S.; Cazenave, A.; Chruch, J.A.; Hansen, J.E.; Keeling, R.F.; Parker, D.E.; Somerville, R.C.J. (2007). Recent climate observations compared to projections. Science, 316, 709.

Rahmstorf, S. (2007). A semiempirical approach to projecting future sea-level rise. Science, 315, 368-370.

Raper, S. C., & Braithwaite, R. J. (2006). Low Sea Level Rise Projections from Mountain Glaciers and Icecaps Under Global Warming. Nature , 439, 311-313.

Shaw, J., Taylor, R., Forbes, D., Ruz, M., & Solomon, S. (1998). Sensitivity of the Coasts of Canada to Sea-level Rise. Geological Survey of Canada (Bulletin 505), Natural Resources Canada , 1-79.

Thompson, K.R., Bernier, N.B. and Chan, P. (2009). Extreme sea levels, coastal flooding and climate change with a focus on Atlantic Canada. Natural Hazards. No. 51, pp. 139-150.

Titus, J. G., Park, R. A., Leatherman, S. P., Weggel, J. R., Greene, M. S., Mausel, P. W., et al. (1991). Greenhouse Effect and Sea Level Rise: The Cost of Holding Back the Sea. Coastal Management , 19, 171-204.

Utting, D. J. and Gallacher, A. F. (2009): Coastal Environment and Erosion in Southwest St. Georges Bay, Antigonish County. In Mineral Resources Branch, Report of Activities 2008; Nova Scotia Department of Natural Resources, Report ME 2009-1, p. 139-149.

Vermeer, M.; Rahmstorf, S. (2009). Global sea level linked to global temperature. Proc. Nat. Acad. Sci. USA, doi: 10.1073/pnas.0907765106.

Webster, T. (2011). Community High Water Storm Surge Mapping Network. Unpublished AGRG report submitted to Nova Scotia Department of Environment.

Webster, Tim. L. (2010). Flood Risk Mapping Using LiDAR for Annapolis Royal, Nova Scotia, Canada. Open Access Remote Sensing ISSN 2072-4292. Vol. 2; doi:10.3390/rs2092060, pp. 2060-2082.

Webster, T., Mosher, R., & Pearson, M. (2008). Water Modeler: A Component of a Coastal Zone Decision Support System to Generate Flood-risk Maps from Storm-surge Events and Sea-level rise. Geomatica, 62 (4), 257-265.

Webster, T. and Stiff, D. (2008). The prediction and mapping of coastal flood risk associated with storm surge events and long-term sea level changes. In Risk Analysis VI Simulations and Hazard Mitigation. WIT Press. Edited by Brebbia, C.A. and Beriatos, E. pp. 129-139.

Webster, T., & Dias, G. (2006). An Automated GIS Procedure for Comparing GPS and Proximal Lidar Elevations. Computers & Geosciences , 32, 713-726.

Webster, T.L, Forbes, MacKinnon, E., and Roberts, D. (2006). Chapter 4.4 Lidar digital elevation models and flood-risk mapping. Environment Canada report: Daigle, R. and Project Research Team. 2006. Impacts of sea level rise and climate change on the coastal zone of southeastern New Brunswick/ Impacts de l'élévation du niveau de la mer et du changement climatique sur la zone côtière du sud-est du Nouveau-Brunswick. Environment Canada, 611 pp. (also on CD-ROM and on-line at http://atlantic-web1.ns.ec.gc.ca/slr/).Webster, T., Forbes, D., MacKinnon, E., & Roberts, D. (2006). Flood-risk Mapping for Storm-surge Events and Sea-level Rise Using Lidar for Southeast New Brunswick. Canadian Journal of Remote Sensing , 32 (2), 194-211.

Webster, T., & Forbes, D. (2005). Using Airborne Lidar to Map Exposure of Coastal Areas in Maritime Canada to Flooding from Storm-surge Events: A Review of Recent Experience. Canadian Coastal Conference (pp. 1-11). Lidar Surveys for Storm-surge FloodingWebster, T.L. (2005). LIDAR validation using GIS: A case study comparison between two LIDAR collection methods. GeoCarto International. Vol. 20, No. 4, pp. 11-19.

Webster, T., Forbes, D., Dickie, S., & Shreenan, R. (2004). Using Topographic Lidar to Map Risk from Storm-surge Events for Charlottetown, Prince Edward Island, Canada. Canadian Journal of Remote Sensing , 30 (1), 64-76.

Webster, T.L, Forbes, D.L, Dickie, S., Colvill, R., and Parkes, G., (2002). Airborne Imaging, Digital Elevation Models and Flood Maps. Supporting Document number 4. In Coastal impacts of Sea-Level Rise on Prince Edward Island. Edited by Forbes D.L. Climate Change Action Fund Project A041. Geological Survey of Canada Open File 4261.

Wehr, A., & Lohr, U. (1999). Airborne Laser Scanning - An Introduction and Overview. Journal of Photogrammetry and Remote Sensing , 54, 68-82.

Appendix 1: GIS Metadata

Metadata description of the final products that have been delivered to the province and municipalities. The general directory structure of the delivered data is as follows:

Animation – Examples of sea-level rise up onto the land based on the lidar surface models.

CSRs – Colour shaded relief maps , these are graphic depictions of the DEM or DSM and are designed to be used for GIS backdrops or visual interpretation, not to be querried for elevation values.

DEM – The Arc grid compatible digital elevation model derived from the lidar, NAD83 zone 20, vertical datum CGVD28 (in some cases this could be stored as a GeoTIF files if larger than 2 GB).

DSM – The Arc grid compatible digital surface model derived from the lidar, NAD83 zone 20, vertical datum CGVD28 (in some cases this could be stored as a GeoTIF files if larger than 2 GB).

Flood_layers – These represent the inundation areas predicted from a storm surge of a given water level elevation (areas are only inundated if they are connected to the ocean). The files are Arc vector shape files with the following naming convection: “n” indicates a negative elevation, this is a result of most of the lidar being flown at low tide and thus elevations below mean sea level. A “p” indicates a positive elevation value. “n001”, the numbers after the “n” or “p” represent decimeters units,

Appendix 2: Lunenburg Co. lidar data processing

Flight Date	*October 4th, 2005*	*August 14th, 2006*	*November 21st, 2007*	*October 27th, 2009*
Sensor Platform	ALTM 3100	ALTM 3100	ALTM 3100	ALTM 3100
Pulse Frequency	50kHz	50kHz	71kHz	70kHz
Scan Frequency	26Hz	30Hz	50Hz	32Hz
Scan Angle	±18º	±19º	±23º	±20º
Approx. Altitude	1800 m	1200 m	600 m	1400 m
Total Points	40,405,712	99,720,398	67,494,248	379,250,147

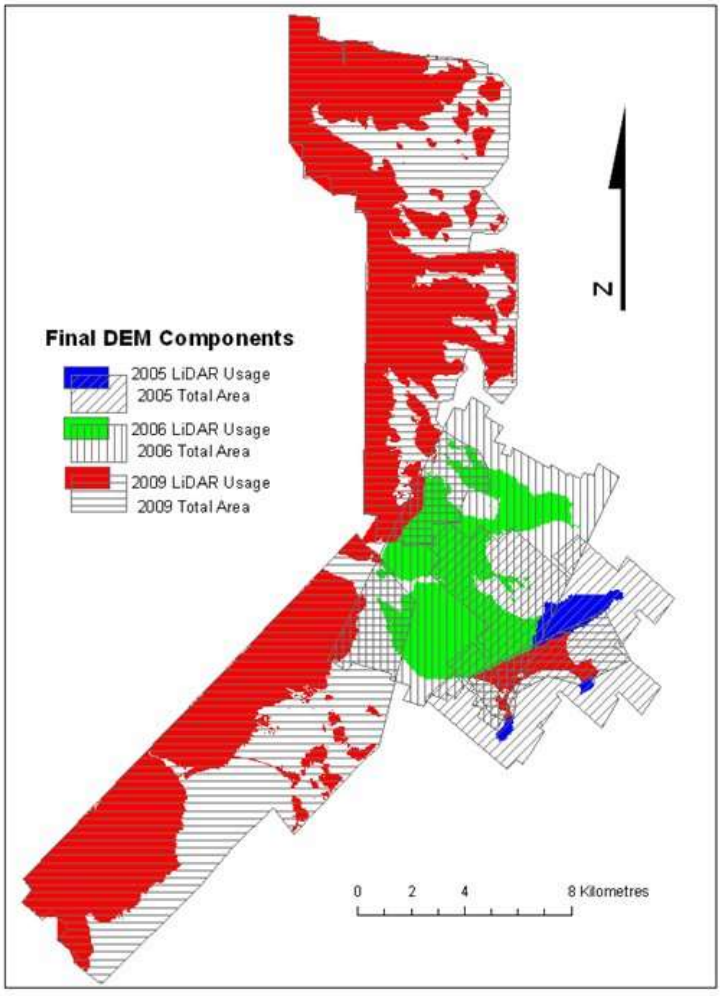

Figure 63 Composite of different lidar datasets used to construct the Lunenburg County lidar surface models.

Appendix 3: River Phillip-Oxford lidar data processing

Flight Date	*October 28th, 2009 Morning*	*October 28th, 2009 Afternoon*	*October 29 th, 2009*	*May 12th, 2006 Town of Oxford*
Sensor Platform	ALTM 3100	ALTM 3100	ALTM 3100	ALTM 3100
Pulse Frequency	45kHz	35kHz	45kHz	70kHz
Scan Angle	±18º	±19º	±23º	±20º
Approx. Altitude	850 m	1300 m	800 m	1400 m

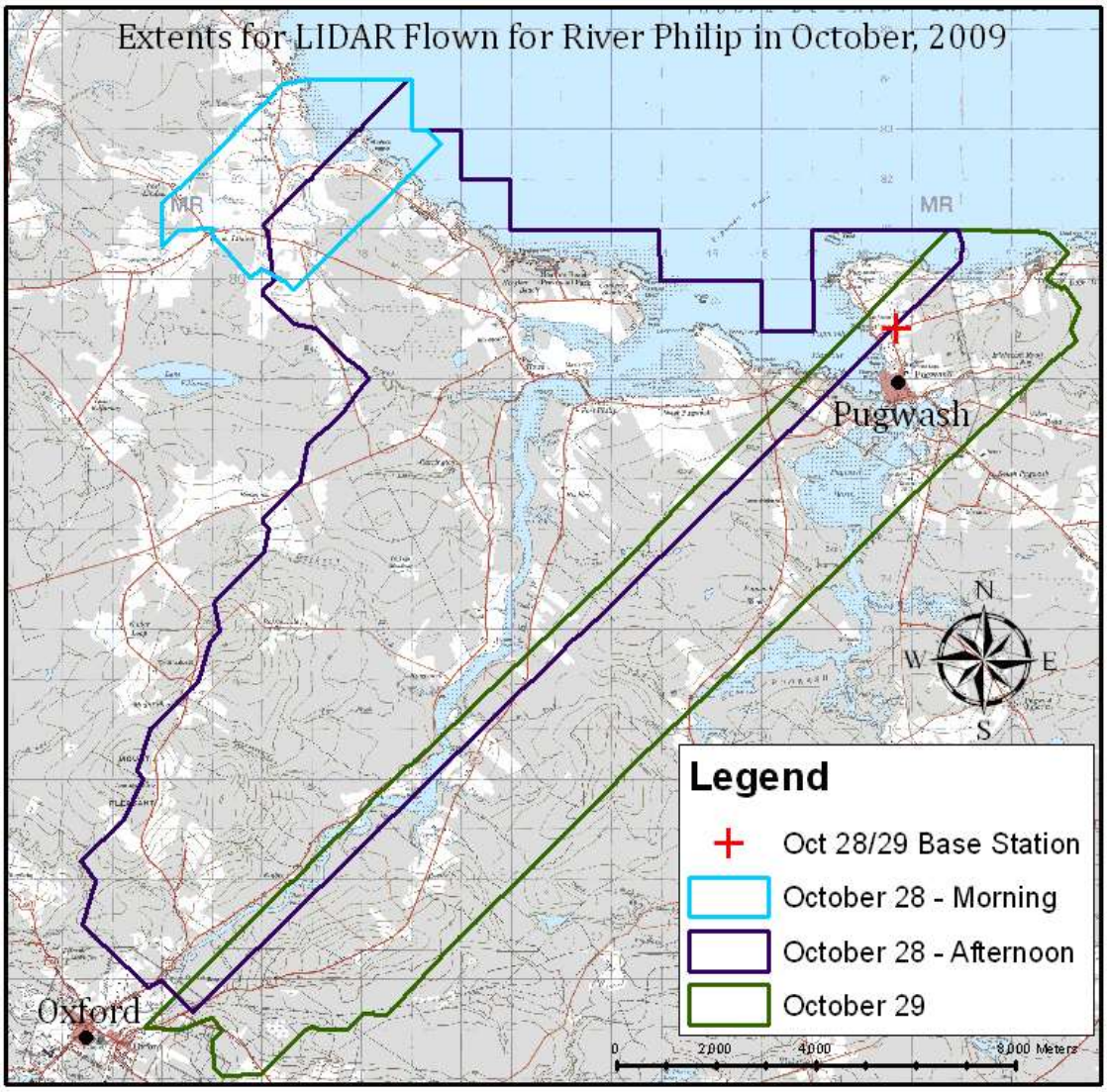

Figure 64 Different lidar surveys to acquire the River Phillip study site. The lidar covering the town of Oxford was acquired in May 2006 and was also added to the composite.

Project	FindMatch Process	Results	Actions
301	heading error (applied)	previously known	applied 0.1809, saved
	whole roll	+0.0009	corrections saved
	individual roll	5 +0.0024 3 +0.0039 4 +0.0024 1 +0.0122 2 -0.0005 6 +0.0083 7 -0.0011 8 +0.0036 9 +0.0017	all corrections saved
	Scale	0.00005	corrections discarded
301b	heading error (applied)	previously known	applied 0.1809, saved
	whole roll	no improvement	n/a
	individual roll	no improvement	n/a
	Scale	-0.00031	corrections saved
302	heading error (applied)	previously known	applied 0.1809, saved
	whole roll	no improvement	n/a
	individual roll	no improvement	n/a
	Scale	no improvement	n/a
	individual z-shift	34 -0.026 35 -0.025 37 +0.006 41 +0.006 36 +0.020 33 -0.042 39 +0.007 30 +0.030 38 -0.002	all corrections saved
		42 +0.027	

Appendix 4: Yarmouth lidar data processing

Flight Date	*September 16th, 2008*
Sensor Platform	ALTM 3100
Pulse Frequency	70kHz
Scan Frequency	26Hz
Scan Angle	±32º
Approx. Altitude	1300 m

Appendix 5: Amherst Fundy lidar data processing

Flight Date	*October 28th, 2009*
Sensor Platform	ALTM 3100
Pulse Frequency	70kHz
Scan Frequency	30Hz
Scan Angle	±20º
Approx. Altitude	1600 m
Total Points	684,102,859

Classification	*Destination*	*Parameter*	*Description*
By Class	Any to 1		
Isolated Points	1 to 7	If fewer than 1 Isolated points Within 9.00	
Low Points	1 to 12	Search Single Points Low points More than 3.00 Within 6.00	
Low Points	1 to 13	Search Groups of points Low points Max Count 4 More than 3.00 Within 6.00	
Ground	1 to 2	Select Aerial low + ground points Ground Max building size 60.00 Terrain angle 88.00 Iteration angle (IA) 7.00 Iteration distance 1.40 Reduce IA when edge length < 3.0 Stop triangulation when edge length N/A	
Below Ground	1 to 14	Limit 8.0 Below ground Z tolerance 0.30	
By Height from Ground	Any to 10	Ground class 2 Max triangle .0100 Min height m 40.00 Max height m 4000.00	

FL	*Z Shift*	*R Shift*
1	0.36716607	-0.00000018
2	0.36288004	0.00047646
3	0.37542255	-0.00021489
4	0.39061543	0.00225249
5	0.38642824	0.00010869
6	0.37044741	0.00005456
7	0.39163934	0.00040621
8	0.37435367	0.00003325
9	0.38518034	0.00014482
10	0.37626071	0.00012780
11	0.38775208	0.00008893
12	0.37214016	-0.00003350
13	0.38928782	0.00014619
14	0.36897216	-0.00010547
15	0.38577130	0.00002549
16	0.38449577	-0.00015485
17	0.37379700	0.00007012
18	0.38636732	-0.00041161
19	0.37438823	0.00011478
20	0.38041855	-0.00004442
21	0.38570851	0.00003932
22	0.38038912	-0.00002789
23	0.36662428	0.00002779
24	0.37685404	-0.00001335

Appendix 6: Windsor-Wolfville lidar data processing

Flight Date	*October 28th, 2009*
Sensor Platform	ALTM 3100
Pulse Frequency	70kHz
Scan Frequency	30Hz
Scan Angle	±20º
Approx. Altitude	1600 m
Total Points	684,102,859

Flight Date	*April 30th and May 21st, 2003*
Sensor Platform	Mark 1
Pulse Frequency	10kHz
Scan Frequency	15Hz
Scan Angle	±25º
Approx. Altitude	600 m

Appendix 7: Halifax expected water level (CD) using the Gumbel EVM under different RSL conditions. ACAS community of the District of Lunenburg (CGVD28-CD Halifax = 0.8 m).

Year	Water Level (0.32 m RSL)	Water Level (0.73 m RSL)	Water Level (1.46 m RSL)
2010	2.05	2.05	2.05
2011	2.17	2.18	2.18
2012	2.25	2.25	2.26
2013	2.30	2.30	2.31
2014	2.34	2.34	2.36
2015	2.37	2.38	2.40
2016	2.40	2.41	2.43
2017	2.42	2.44	2.46
2018	2.44	2.46	2.49
2019	2.46	2.48	2.52
2020	2.48	2.50	2.54
2021	2.50	2.52	2.57
2022	2.51	2.54	2.59
2023	2.53	2.56	2.61
2024	2.54	2.57	2.63
2025	2.55	2.59	2.65
2026	2.56	2.60	2.67
2027	2.58	2.61	2.69
2028	2.59	2.63	2.71
2029	2.60	2.64	2.73
2030	2.61	2.65	2.74
2031	2.62	2.67	2.76
2032	2.63	2.68	2.78
2033	2.64	2.69	2.79
2034	2.64	2.70	2.81
2035	2.65	2.71	2.83
2036	2.66	2.72	2.84
2037	2.67	2.73	2.86
2038	2.68	2.74	2.88
2039	2.68	2.75	2.89
2040	2.69	2.76	2.91
2041	2.70	2.77	2.92
2042	2.71	2.78	2.94
2043	2.71	2.79	2.95
2044	2.72	2.80	2.97
2045	2.73	2.81	2.98
2046	2.73	2.82	3.00
2047	2.74	2.83	3.02
2048	2.74	2.84	3.03
2049	2.75	2.85	3.05
2050	2.76	2.86	3.06
2051	2.76	2.86	3.08
2052	2.77	2.87	3.09
2053	2.77	2.88	3.11
2054	2.78	2.89	3.12
2055	2.79	2.90	3.14
2056	2.79	2.91	3.15
2057	2.80	2.92	3.17

2058	2.80	2.92	3.18
2059	2.81	2.93	3.19
2060	2.81	2.94	3.21
2061	2.82	2.95	3.22
2062	2.82	2.96	3.24
2063	2.83	2.97	3.25
2064	2.83	2.97	3.27
2065	2.84	2.98	3.28
2066	2.84	2.99	3.30
2067	2.85	3.00	3.31
2068	2.85	3.01	3.33
2069	2.86	3.01	3.34
2070	2.86	3.02	3.36
2071	2.87	3.03	3.37
2072	2.87	3.04	3.39
2073	2.88	3.04	3.40
2074	2.88	3.05	3.42
2075	2.88	3.06	3.43
2076	2.89	3.07	3.44
2077	2.89	3.08	3.46
2078	2.90	3.08	3.47
2079	2.90	3.09	3.49
2080	2.91	3.10	3.50
2081	2.91	3.11	3.52
2082	2.92	3.11	3.53
2083	2.92	3.12	3.55
2084	2.92	3.13	3.56
2085	2.93	3.14	3.58
2086	2.93	3.14	3.59
2087	2.94	3.15	3.61
2088	2.94	3.16	3.62
2089	2.94	3.17	3.63
2090	2.95	3.18	3.65
2091	2.95	3.18	3.66
2092	2.96	3.19	3.68
2093	2.96	3.20	3.69
2094	2.97	3.21	3.71
2095	2.97	3.21	3.72
2096	2.97	3.22	3.74
2097	2.98	3.23	3.75
2098	2.98	3.23	3.77
2099	2.99	3.24	3.78
2100	2.99	3.25	3.80
2101	2.99	3.26	3.81
2102	3.00	3.26	3.82
2103	3.00	3.27	3.84
2104	3.00	3.28	3.85
2105	3.01	3.29	3.87
2106	3.01	3.29	3.88
2107	3.02	3.30	3.90
2108	3.02	3.31	3.91
2109	3.02	3.32	3.93
2110	3.03	3.32	3.94

Appendix 8: Pictou expected water level (CD) using the Gumbel EVM under different RSL conditions. ACAS community of Oxford-Port Howe. (CGVD28-CD Pictou = 0.92 m).

Year	Water Level (0.32 m RSL)	Water Level (0.73 m RSL)	Water Level (1.46 m RSL)
2010	2.29	2.29	2.29
2011	2.42	2.42	2.43
2012	2.50	2.51	2.52
2013	2.56	2.57	2.58
2014	2.61	2.62	2.63
2015	2.64	2.65	2.67
2016	2.67	2.69	2.71
2017	2.70	2.72	2.75
2018	2.73	2.75	2.78
2019	2.75	2.77	2.81
2020	2.77	2.79	2.83
2021	2.79	2.81	2.86
2022	2.80	2.83	2.88
2023	2.82	2.85	2.91
2024	2.84	2.87	2.93
2025	2.85	2.89	2.95
2026	2.86	2.90	2.97
2027	2.88	2.92	2.99
2028	2.89	2.93	3.01
2029	2.90	2.95	3.03
2030	2.91	2.96	3.05
2031	2.92	2.97	3.07
2032	2.93	2.99	3.08
2033	2.94	3.00	3.10
2034	2.95	3.01	3.12
2035	2.96	3.02	3.14
2036	2.97	3.03	3.15
2037	2.98	3.05	3.17
2038	2.99	3.06	3.19
2039	2.99	3.07	3.20
2040	3.00	3.08	3.22
2041	3.01	3.09	3.23
2042	3.02	3.10	3.25
2043	3.02	3.11	3.27
2044	3.03	3.12	3.28
2045	3.04	3.13	3.30
2046	3.05	3.14	3.31
2047	3.05	3.15	3.33
2048	3.06	3.16	3.34
2049	3.07	3.17	3.36
2050	3.07	3.18	3.38
2051	3.08	3.19	3.39
2052	3.08	3.20	3.41
2053	3.09	3.21	3.42
2054	3.10	3.21	3.44
2055	3.10	3.22	3.45
2056	3.11	3.23	3.47

2057	3.11	3.24	3.48
2058	3.12	3.25	3.50
2059	3.12	3.26	3.51
2060	3.13	3.27	3.53
2061	3.14	3.28	3.54
2062	3.14	3.28	3.56
2063	3.15	3.29	3.57
2064	3.15	3.30	3.59
2065	3.16	3.31	3.60
2066	3.16	3.32	3.62
2067	3.17	3.33	3.63
2068	3.17	3.33	3.65
2069	3.18	3.34	3.66
2070	3.18	3.35	3.67
2071	3.19	3.36	3.69
2072	3.19	3.37	3.70
2073	3.20	3.37	3.72
2074	3.20	3.38	3.73
2075	3.20	3.39	3.75
2076	3.21	3.40	3.76
2077	3.21	3.41	3.78
2078	3.22	3.41	3.79
2079	3.22	3.42	3.81
2080	3.23	3.43	3.82
2081	3.23	3.44	3.84
2082	3.24	3.45	3.85
2083	3.24	3.45	3.87
2084	3.24	3.46	3.88
2085	3.25	3.47	3.90
2086	3.25	3.48	3.91
2087	3.26	3.48	3.92
2088	3.26	3.49	3.94
2089	3.27	3.50	3.95
2090	3.27	3.51	3.97
2091	3.27	3.52	3.98
2092	3.28	3.52	4.00
2093	3.28	3.53	4.01
2094	3.29	3.54	4.03
2095	3.29	3.55	4.04
2096	3.29	3.55	4.06
2097	3.30	3.56	4.07
2098	3.30	3.57	4.09
2099	3.30	3.58	4.10
2100	3.31	3.58	4.11
2101	3.31	3.59	4.13
2102	3.32	3.60	4.14
2103	3.32	3.61	4.16
2104	3.32	3.61	4.17
2105	3.33	3.62	4.19
2106	3.33	3.63	4.20
2107	3.34	3.64	4.22
2108	3.34	3.64	4.23
2109	3.34	3.65	4.25
2110	3.35	3.66	4.26

Appendix 9: Yarmouth expected water level (CD) using the Gumbel EVM under different RSL conditions. ACAS communities of the town and district of Yarmouth (CGVD28-CD Halifax = 2.31 m).

Year	Water Level (0.32 m RSL)	Water Level (0.73 m RSL)	Water Level (1.46 m RSL)
2010	4.96	4.96	4.96
2011	5.06	5.06	5.07
2012	5.12	5.13	5.13
2013	5.17	5.17	5.18
2014	5.20	5.21	5.23
2015	5.23	5.24	5.26
2016	5.26	5.27	5.29
2017	5.28	5.29	5.32
2018	5.30	5.31	5.35
2019	5.32	5.33	5.37
2020	5.33	5.35	5.39
2021	5.35	5.37	5.42
2022	5.36	5.38	5.44
2023	5.37	5.40	5.46
2024	5.38	5.41	5.47
2025	5.40	5.43	5.49
2026	5.41	5.44	5.51
2027	5.42	5.45	5.53
2028	5.43	5.47	5.55
2029	5.44	5.48	5.56
2030	5.45	5.49	5.58
2031	5.46	5.50	5.60
2032	5.46	5.51	5.61
2033	5.47	5.52	5.63
2034	5.48	5.53	5.65
2035	5.49	5.54	5.66
2036	5.50	5.55	5.68
2037	5.50	5.56	5.69
2038	5.51	5.57	5.71
2039	5.52	5.58	5.72
2040	5.52	5.59	5.74
2041	5.53	5.60	5.76
2042	5.54	5.61	5.77
2043	5.54	5.62	5.79
2044	5.55	5.63	5.80
2045	5.56	5.64	5.82
2046	5.56	5.65	5.83
2047	5.57	5.65	5.85
2048	5.57	5.66	5.86
2049	5.58	5.67	5.88
2050	5.59	5.68	5.89
2051	5.59	5.69	5.91
2052	5.60	5.70	5.92
2053	5.60	5.71	5.94
2054	5.61	5.71	5.95
2055	5.61	5.72	5.96
2056	5.62	5.73	5.98
2057	5.62	5.74	5.99
2058	5.63	5.75	6.01

2059	5.63	5.75	6.02
2060	5.64	5.76	6.04
2061	5.64	5.77	6.05
2062	5.65	5.78	6.07
2063	5.65	5.79	6.08
2064	5.66	5.79	6.10
2065	5.66	5.80	6.11
2066	5.67	5.81	6.13
2067	5.67	5.82	6.14
2068	5.68	5.82	6.16
2069	5.68	5.83	6.17
2070	5.69	5.84	6.19
2071	5.69	5.85	6.20
2072	5.70	5.86	6.21
2073	5.70	5.86	6.23
2074	5.70	5.87	6.24
2075	5.71	5.88	6.26
2076	5.71	5.89	6.27
2077	5.72	5.89	6.29
2078	5.72	5.90	6.30
2079	5.73	5.91	6.32
2080	5.73	5.92	6.33
2081	5.74	5.92	6.35
2082	5.74	5.93	6.36
2083	5.74	5.94	6.38
2084	5.75	5.95	6.39
2085	5.75	5.95	6.40
2086	5.76	5.96	6.42
2087	5.76	5.97	6.43
2088	5.77	5.98	6.45
2089	5.77	5.98	6.46
2090	5.77	5.99	6.48
2091	5.78	6.00	6.49
2092	5.78	6.01	6.51
2093	5.79	6.01	6.52
2094	5.79	6.02	6.54
2095	5.79	6.03	6.55
2096	5.80	6.04	6.56
2097	5.80	6.04	6.58
2098	5.81	6.05	6.59
2099	5.81	6.06	6.61
2100	5.81	6.06	6.62
2101	5.82	6.07	6.64
2102	5.82	6.08	6.65
2103	5.83	6.09	6.67
2104	5.83	6.09	6.68
2105	5.83	6.10	6.70
2106	5.84	6.11	6.71
2107	5.84	6.12	6.73
2108	5.85	6.12	6.74
2109	5.85	6.13	6.75
2110	5.85	6.14	6.77

Appendix 10: Saint John expected water level (CD) using the Gumbel EVM under different RSL conditions. ACAS communities of the Chignecto Isthmus and the Minas Basin (CGVD28-CD Saint John = 4.19 m).

Year	Water Level (0.22 m RSL)	Water Level (0.73 m RSL)	Water Level (1.46 m RSL)
2010	8.56	8.56	8.56
2011	8.65	8.65	8.65
2012	8.70	8.70	8.71
2013	8.73	8.74	8.75
2014	8.76	8.77	8.79
2015	8.78	8.80	8.82
2016	8.80	8.82	8.84
2017	8.82	8.84	8.87
2018	8.83	8.86	8.89
2019	8.85	8.87	8.91
2020	8.86	8.89	8.93
2021	8.87	8.90	8.95
2022	8.88	8.92	8.97
2023	8.89	8.93	8.99
2024	8.90	8.94	9.00
2025	8.91	8.95	9.02
2026	8.92	8.97	9.04
2027	8.93	8.98	9.06
2028	8.94	8.99	9.07
2029	8.94	9.00	9.09
2030	8.95	9.01	9.10
2031	8.96	9.02	9.12
2032	8.96	9.03	9.13
2033	8.97	9.04	9.15
2034	8.97	9.05	9.17
2035	8.98	9.06	9.18
2036	8.99	9.06	9.20
2037	8.99	9.07	9.21
2038	9.00	9.08	9.23
2039	9.00	9.09	9.24
2040	9.01	9.10	9.26
2041	9.01	9.11	9.27
2042	9.02	9.12	9.29
2043	9.02	9.12	9.30
2044	9.03	9.13	9.32
2045	9.03	9.14	9.33
2046	9.04	9.15	9.35
2047	9.04	9.16	9.36
2048	9.04	9.17	9.37
2049	9.05	9.17	9.39
2050	9.05	9.18	9.40
2051	9.06	9.19	9.42
2052	9.06	9.20	9.43
2053	9.06	9.21	9.45
2054	9.07	9.21	9.46
2055	9.07	9.22	9.48
2056	9.08	9.23	9.49
2057	9.08	9.24	9.51
2058	9.08	9.24	9.52

2059	9.09	9.25	9.54
2060	9.09	9.26	9.55
2061	9.09	9.27	9.57
2062	9.10	9.27	9.58
2063	9.10	9.28	9.59
2064	9.11	9.29	9.61
2065	9.11	9.30	9.62
2066	9.11	9.30	9.64
2067	9.12	9.31	9.65
2068	9.12	9.32	9.67
2069	9.12	9.33	9.68
2070	9.13	9.33	9.70
2071	9.13	9.34	9.71
2072	9.13	9.35	9.73
2073	9.13	9.36	9.74
2074	9.14	9.36	9.76
2075	9.14	9.37	9.77
2076	9.14	9.38	9.78
2077	9.15	9.39	9.80
2078	9.15	9.39	9.81
2079	9.15	9.40	9.83
2080	9.16	9.41	9.84
2081	9.16	9.42	9.86
2082	9.16	9.42	9.87
2083	9.17	9.43	9.89
2084	9.17	9.44	9.90
2085	9.17	9.45	9.92
2086	9.17	9.45	9.93
2087	9.18	9.46	9.94
2088	9.18	9.47	9.96
2089	9.18	9.48	9.97
2090	9.19	9.48	9.99
2091	9.19	9.49	10.00
2092	9.19	9.50	10.02
2093	9.19	9.50	10.03
2094	9.20	9.51	10.05
2095	9.20	9.52	10.06
2096	9.20	9.53	10.08
2097	9.21	9.53	10.09
2098	9.21	9.54	10.11
2099	9.21	9.55	10.12
2100	9.21	9.56	10.13
2101	9.22	9.56	10.15
2102	9.22	9.57	10.16
2103	9.22	9.58	10.18
2104	9.22	9.59	10.19
2105	9.23	9.59	10.21
2106	9.23	9.60	10.22
2107	9.23	9.61	10.24
2108	9.23	9.61	10.25
2109	9.24	9.62	10.27
2110	9.24	9.63	10.28